

**INVESTIGATION OF EFFECTIVENESS OF VARIOUS CORROSION
PROTECTION METHODS BY ULTRASONIC GUIDED WAVES AND
ACOUSTIC EMISSION TECHNIQUES**

A dissertation submitted

In partial fulfillment of the requirements

For the degree of

MASTERS OF ENGINEERING

IN

STRUCTURAL ENGINEERING

SUBMITTED BY

PRINCE

(ROLL NO. 801524020)

UNDER THE GUIDANCE OF

Dr. SHRUTI SHARMA

Associate professor

Civil Engineering Department



THAPAR UNIVERSITY, PATIALA 147004

JULY 2017

DECLARATION

I, hereby declare that the thesis “Investigation of Effectiveness of various Corrosion Protection Methods by Ultrasonic Guided Waves and Acoustic Emission Techniques” which is submitted in partial fulfillment of the requirement for the award of the degree of **Master of Engineering in Structural Engineering** in the Department of Civil Engineering (CED), Thapar University, Patiala, is an authentic record of my own independent and original research work carried out by me under the supervision and guidance of **Dr. Shruti Sharma**, Associate Professor, Department of Civil Engineering, Thapar University, Patiala.

The matter embodied in this thesis has not been submitted in part or fully to any other university or institute for the award of any degree.

Date: 21 / 7 / 2017


Prince

Roll No. 801524020

This is to certify that the above declaration made by the student concerned is correct to the best of my knowledge and belief.


Dr. Shruti Sharma

Associate Professor

Department of Civil Engineering

Thapar University, Patiala

ACKNOWLEDGEMENTS

Time has given me the appreciated chance to offer my eager thanks to my guide Dr. Shruti Sharma, Associate Professor, CED, Thapar University, Patiala, who inspired me to complete my research work under her capable direction. I may ever stay obliged to her for her watchful course, helpful input, clear considering, unmistakable intrigue, rigid support and tolerance from the initial starting point of this thesis work to its summit.

The absolute advantage of my close friends and accomplice is truly regarded. Phenomenal appreciation goes to Sh. Ram Simran and other research office members, who helped me in my test work. Moreover I want to thank all the staff individuals from Civil Engineering Department for their full cooperation and help offered by them. I also need to thank Mr. Ashutosh Sharma for making it possible to carry out acoustic emission and ultrasonic testing efficiently.

Finally, I offer my most significant thanks and love to my family without whom I am nothing, for providing the endless help, understanding me and giving me constant support whenever needed throughout my thesis work. Above all, I thank God for his blessing and giving me the strength and power to make this happen.

Prince

ABSTRACT

Corrosion of reinforcement in RC structures is like a ‘Cancer’ which spreads, if not intervened at the right time. It is one of the major challenges faced by structural engineers. World-wide, billions of dollar are wasted on structural maintenance because of undetected corrosion. It results in the cracking and spalling of concrete and loss of cross-section in the form of pitting in reinforcement and can ultimately lead to catastrophic failure of structures. Therefore, non-destructive monitoring of corrosion in reinforcement is very essential. In this research, monitoring of corrosion in RC structures using a combination of elastic wave techniques of Acoustic Emission and Ultrasonic Guided Wave is employed. The efficacy of corrosion impediment by various corrosion prevention methods using epoxy and paint coating on rebar and corrosion inhibitor admixed with concrete is evaluated. Four concrete beam specimens of dimensions 150mm X 150mm X 700mm with MS bar of 1m length and 25mm diameter in the center of cross-section were cast. 1st beam specimen was control specimen, 2nd beam specimen had steel bar coated with epoxy layer, 3rd beam specimen had a steel bar coated with paint and 4th beam specimen was prepared using corrosion inhibitor as an admixture in concrete. All the beam specimens were subjected to accelerated corrosion exposure for 30 days. Ultrasonic monitoring was done after every 24 hours for the entire duration of corrosion exposure. A low frequency mode L(0,1) at 0.1MHz and a high frequency mode L(0,7) at 1MHz were used for Ultrasonic Guided Waves measurements. For Acoustic Emission monitoring 4 AE sensors were mounted on the surface of concrete which collected AE activity during the entire duration of the corrosion exposure. It was found that both the techniques are effective to different extents in picking up corrosion effects in steel and concrete. It was also reported that the specimens treated with epoxy and paint did not undergo any corrosion activity picked up by both UGW and AE even under the accelerated corrosion conditions. The specimen treated with corrosion inhibitor showed a delay in delamination and pitting in comparison to control beam which was easily picked up by the change in signals obtained using UGW monitoring and a delay in the corrosion onset and cracking was also picked up by AE monitoring.

INDEX

	Page no.
CERTIFICATE	i
ACKNOWLEDGEMENT	ii
ABSTRACT	iii
CONTENTS	iv
LIST OF FIGURES	vii
LIST OF TABLES	xii
CHAPTER 1 INTRODUCTION	(1-21)
1.1 Motivation and Background	1
1.2 General	2
1.3 Mechanism of Corrosion	3
1.4 Factors affecting the corrosion	5
1.4.1 Internal Factors	5
1.4.2 External Factors	6
1.5 Corrosion protection measures	6
1.5.1 Corrosion inhibitor	7
1.5.1.1 Classification of corrosion inhibitors	7
1.5.1.2 Mechanism of some commonly used commercially available inhibitors	9
1.5.2 Epoxy Coating	10
1.5.3 Paints	11
1.6 Monitoring of corrosion in RC structures	11
1.7 Ultrasonic Guided Waves Approach	12
1.8 Acoustic Emission	18
1.9 Closing Remarks	21
CHAPTER 2 REVIEW OF LITERATURE	(22-44)

2.1 Ultrasonic Guided Waves for corrosion monitoring	22
2.2 Acoustic Emission for corrosion monitoring	31
2.3 Use of corrosion inhibitor for protection of steel in concrete	38
2.4 Closing Remarks	44

CHAPTER 3 EXPERIMENTAL PROGRAM AND METHODOLOGY (45-64)

3.1 General	45
3.2 Test program	45
3.3 Materials used	48
3.4 Preparation of test specimens	54
3.4.1 Preparation and preconditioning of the reinforcing steel bars	54
3.4.2 Casting of RC beams	54
3.4.3 Inducing corrosion in concrete	55
3.4.4 Corrosion testing	56
3.5 Ultrasonic Guided Waves Investigation	56
3.5.1 Specimen and setup details	56
3.5.2 Selection of excitation mode and frequencies	58
3.6 Acoustic Emission Monitoring	59
3.7 Closing Remarks	64

CHAPTER 4 RESULTS AND DISCUSSION (65-94)

4.1 General	65
4.2 Visual inspection	65
4.3 Cell current	69
4.4 Ultrasonic Guided Wave Monitoring	71
4.4.1 Surface Seeking Mode	71
4.4.2 Core Seeking Mode	76
4.5 Acoustic Emission Testing results	82
4.5.1 Cumulative AE hits	83

4.5.2 Amplitude of AE hits	87
4.5.3 Cumulative AE signal strength	91
CHAPTER 5 CONCLUSIONS AND FUTURE SCOPE	(95-96)
5.1 Conclusions	95
5.2 Future Scope of Work	96
CHAPTER 6 REFERENCES	(97-100)

LIST OF FIGURES

Figure No.	Title	Page No.
1.1	Corrosion of reinforcing bar in concrete as an electrochemical process	4
1.2	Steel bar coated with epoxy	11
1.3	Body and surface wave generated with the help of ultrasonic source	14
1.4	Guided wave propagation through a structure	14
1.5	Propagation of waves when material's thickness \gg wavelength	15
1.6	Different kind of guided waves	16
1.7	Pulse transmission method	17
1.8	Test setup for the pulse echo method	18
1.9	Schematic representation of AE Monitoring Process	19
1.10	Schematic diagram showing some parameters of AE waveform	20
2.1	Dispersion curves for axis symmetric L (0,n) modes of rebar embedded in grout (a) attenuation; (b) energy velocity	22
2.2	Various arrangements of transmitter and receiver for experimental analysis	23
2.3	Waveform obtained above 2 MHz	25
2.4(a)	Linear regression of non-destructive ultrasonic parameters vs. fracture energy results of CFRP–concrete samples subjected to accelerated aging temperatures(average power v/s fracture energy)	26

2.4(b)	Peak amplitude v/s fracture energy	27
2.5	Peak-peak voltage ratio with surface seeking mode	28
2.6	Peak-peak voltage ratio with core seeking mode	29
2.7	(a) Specimen schematic (b) specimen wrapped with FRP	30
2.8	AE hits versus cycling loading for RC beam (corroded and uncorroded)	31
2.9	Comparison of chloride content and AE activities	32
2.10	AE activities and Half-cell potential in accelerated corrosion	33
2.11	AE activities and Half-cell potential in cyclic wet-dry test	34
2.12	Crack classification by AE indices	34
2.13	Total AE hits and half cell potential in sodium chloride portion (left) and water portion (right)	35
2.14	AE sources located at 2 nd high AE activity in test	36
2.15	Number of cumulative AE hits and AE events	37
2.16	Number of cumulative AE hits and half cell potential	37
2.17	RC specimen with dimensions	39
2.18	Time of corrosion initiation for specimen leads to ponding test with 3.5% sodium chloride solution	40
2.19	Diagram showing specimen with 2 entrenched bars (a) uncracked (b) pre-cracked	40
2.20	Corrosion current densities for uncracked concrete slab with corrosion inhibitors	41

2.21	Corrosion current densities for precracked concrete slab with 0.2mm crack	41
2.22	Corrosion current densities for precracked concrete slab with 0.4mm crack	42
2.23	Open circuit potential versus time of concrete specimens	42
3.1	Test program	47
3.2	Epoxy used	52
3.3	Paint used	53
3.4	Inhibitor used	53
3.5	Beam specimens	54
3.6	Beam showing arrangement for induced corrosion	55
3.7	Power supply (Aplab,64V,1A Current)	56
3.8	Systematic view of ultrasonic monitoring	57
3.9	Actual ultrasonic test set-up	57
3.10	DPR 300	58
3.11	Transducer used (Karl Deutsch, 0.1 MHz and 1 MHz)	58
3.12	Schematic representation of AE setup	59
3.13	Data acquisition setup	60
3.14(a)	Position of sensor on beam: Front face	60
3.14(b)	Position of sensor on beam: Back face	61
3.15	R3 α sensor for acquisition of data	61
3.16	Pre-amplifier	62
3.17	Experiment test setup used in present study	62
3.18	Apparatus of pencil lead break test	63

3.19	Pencil break test during study	63
4.1	Specimen B1	65
4.2	Specimen B2	66
4.3	Specimen B3	67
4.4	Specimen B4	68
4.5	Cell current of all beam specimens	69
4.6	Signatures for specimens B1 and B4 at various days (L(0,1) mode)	72
4.7	Peak to peak voltage ratio of specimen B1 (L(0,1) mode)	73
4.8	Peak to peak voltage ratio of specimen B4 (L(0,1) mode)	74
4.9	Signatures for specimens B2 and B3 at various days (L(0,1) mode)	75
4.10	Peak to peak voltage ratio of specimens B2 and B3 (L(0,1) mode)	76
4.11	Signatures for specimens B1 and B4 at various days (L(0,7) mode)	78
4.12	Peak to peak voltage ratio of specimen B1 (L(0,7) mode)	79
4.13	Peak to peak voltage ratio of specimen B4 (L(0,7) mode)	80
4.14	Signatures for specimens B2 and B3 at various days (L(0,7) mode)	81
4.15	Peak to peak voltage ratio of specimens B2 and B3 (L(0,7) mode)	82
4.16	Melcher model of corrosion loss	83
4.17	Cumulative AE hits of beam B1	85
4.18	Cumulative AE hits of beam B2	86
4.19	Cumulative AE hits of beam B3	86

4.20	Cumulative AE hits of beam B4	87
4.21	Amplitude variation of specimen B1	88
4.22	Amplitude variation of specimen B2	89
4.23	Amplitude variation of specimen B3	90
4.24	Amplitude variation of specimen B4	91
4.25	Variation of CSS of specimen B1	91
4.26	Variation of CSS of specimen B2	93
4.27	Variation of CSS of specimen B3	93
4.28	Variation of CSS of specimen B4	94

LIST OF TABLES

Table No.	Title	Page No.
1.1	Reinforcement state at various level of pH	5
1.2	Chloride content limits as recommended by some code of practice	6
2.1	Test conditions for RC specimens	38
3.1	Nomenclature of samples prepared	45
3.2	Physical properties of cement used	48
3.3	Compressive strength of cement used	48
3.4	Sieve analysis result of the fine aggregates used	49
3.5	Physical properties of fine aggregates used	49
3.6	Sieve analysis result of 20mm coarse aggregates used	50
3.7	Physical properties of 20mm coarse aggregates used	50
3.8	Sieve analysis result of 10mm coarse aggregates used	51
3.9	Physical properties of 10mm coarse aggregates used	51
3.10	Properties of steel reinforcement used	52
3.11	Sensor's specification	61

CHAPTER 1

INTRODUCTION

1.1 MOTIVATION AND BACKGROUND

Corrosion in reinforcement has been found as a major factor responsible for the deterioration of reinforced concrete structure. The durability and serviceability of the concrete structure is adversely affected by this corrosion of reinforcement. Therefore to avoid the untimely failure of reinforced concrete structure, control and monitoring of rebar corrosion assume to be important. Hence, it is important to check the structural behavior of corrosion affected part because it will help in making conclusion related to examination, repair, increasing the strength, replacement and demolition of this kind of structures.

For corrosion monitoring in RC structure, a number of corrosion monitoring techniques have been used by various research group. Ultrasonic guided waves and Half-Cell Potential techniques have been used successfully for corrosion monitoring. Half-Cell Potential is very simple, less costly and virtually non destructive technique for the assessment of corrosion risk of steel bar in concrete. But the main drawback of this technique is that it gives variable results under various conditions. Ultrasonic guided waves monitoring is the another technique which is being used now a days for corrosion monitoring. For assessment of rebar condition in RC structure, this is very useful method. Its main limitations are that it does not give information regarding corrosion of concrete and another limitation is that it needs accessibility to steel bar. This thesis bring out the demerits of ultrasonic guided waves and suggest that this demerits can be overcome using Acoustic emission or both these techniques can be used in combination for corrosion monitoring of RC structure. In the field of structural health monitoring, this acoustic emission technique has gained popularity since past few years. This technique involves the use of sensors for detecting any acoustic energy released during the formation or propagation of the crack.

1.2 GENERAL

Concrete is most widely used man-made material and with its very own special properties, it is versatile material. Concrete is weak in tension and possess less ductility therefore it is generally reinforced with steel or any other material having relatively higher ductility and tensile strength. Steel reinforced concrete (RC) is very famous construction material. As a construction material of choice, it has been used from decades and has verified to be very victorious in terms of both durability and structural performance. RC plays a very vital role in economic growth of nation because of nature and role of the concrete in rehabilitation, formation and restoration of infrastructure of a country. Lack of durability of RC structure is one of the major menaces to the sustainable development of concrete and concrete industry as well as it is massive economic implication to country's welfare.

Reinforcement corrosion is recognized as greatest problem which affect the durability of concrete structure as it degrades the bond between steel bar and concrete. Previously it was believed that cover could be a better protection against embedded steel corrosion and as a result RC structures were considered to be highly resistant against corrosion. But practically, RC structures do not perform so well and their service life is very smaller than what they are designed for. The steel embedded in concrete is always prone to be attacked by corrosion. It has been found that 40% failure of structure occurs due to corrosion of embedded rebars in concrete. That is why control of corrosion of steel reinforcement is an issue of paramount importance. Corrosion is that form of damage which is hidden and insidious until it strikes at the most terrible moment of a system operation.

When the steel bar in concrete is open to chlorides either granted from concrete components or penetrated from adjacent chloride-bearing environment then the problem becomes serious. This salt induced corrosion in steel bars for various users has certainly turns into substantial cost-effective burden. As we know that iron has a aptness to regress to its most steady oxide state, this trouble, regrettably still be with us, but to a very low extent because of the employ of different corrosion protection techniques in construction process.

The use of high-quality construction practices, good design, ample concrete cover depth, less permeability concrete, coated steel reinforcement and corrosion inhibitors are playing very important role in reducing the reinforcing steel corrosion in various structures. The other reasons of rebar corrosion are carbonation and infiltration of acidic gases in concrete. Beside these there are some more factors, few related to concrete quality like water cement ratio, presence of

surface cracks, cement-content, impurity in other constituents etc. and other associated with external environment like moisture, bacterial attack, stray current, oxygen, humidity and temperature etc., through which the rebar corrosion gets affected.

Presently, one of the major problems that concrete industry is facing is repair and maintenance of RC structures mainly due to corrosion damage. Whereas there are various other ways to avoid aforesaid damage, the optimum control system depends upon early diagnosis of problems. The reinforcing steel in fine grade concrete, still in presence of adequate moisture and oxygen does not corrode. It all occurs due to the generation of fine preventive oxide layer (passive film) on steel bar surface in extremely alkaline pore solution of the concrete. When enough chloride ion (from sea water or from de-icing salt) have penetrated to the reinforcement or due to carbonation, the pH of pore water approaches to a low value then this preventive layer gets damaged and reinforcing steel gets depassivated.

Although reinforcing steel corrosion may not influence the integrity and eventual load carrying capability of RC structural members immediately, it is insidious, more complicated and devastating type of destruction. Once it begin, it is totally unfeasible to discontinue it until ultimate stability, safety and desired service life are all severely condensed with time. Therefore, to build such type of structures which are environmentally sustainable, it is clear that durability should be the driving consideration rather than strength in modern construction.

1.3 MECHANISM OF CORROSION

Corrosion with rusting of steel bar in concrete occurs in two stages. Primary stage includes the transfer of aggressive elements (mainly CO_2 and Cl^-) of H_2O and of O_2 , including the corrosion initiation (depassivation of reinforcement). Second stage is the propagation stage in which these aggressive elements are in very high concentration at rebar's level. This corresponds to growth of rust, which bring about emergence of cracks and also sometimes breakage of concrete cover. This leads to spalling, cracks and damage etc. to the concrete.

Corrosion of the reinforcing bar embedded in concrete is an electrochemical process. Corrosion process is declared to be same in action, which occurs in a flash battery. The corroding rebar's surface behave as combined electrode that is a combination of anodes and cathodes connected electrically through the rebar's body itself, on which coupled (anodic and cathodic) reactions occurs. The water present in the pores of concrete works as an aqueous medium i.e., a complex electrolyte. Hence, a reinforcement corrosion cell is created, as presented in **Fig.1.1**.

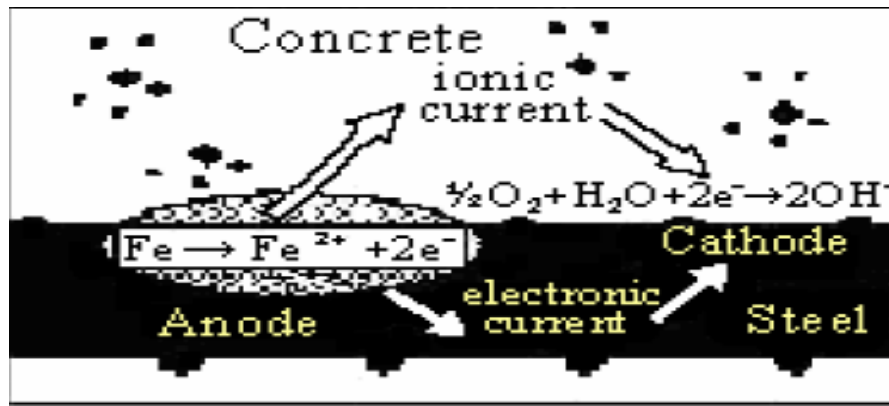
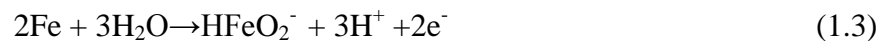
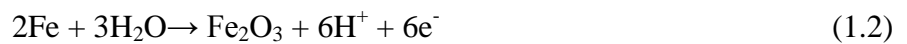
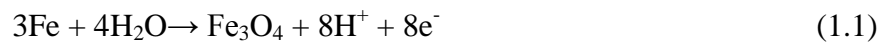


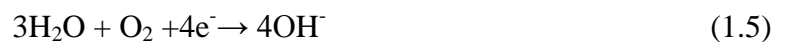
Fig.1.1: Corrosion of reinforcing bar in concrete as an electrochemical process [1]

1.3.1 ANODIC AND CATHODIC REACTIONS

Reactions at cathode and anode are generally referred as half cell reactions. The oxidation process occurs at anode and called as anodic reaction which results in dissolution or loss of metal whereas cathodic reaction is the process of reduction which leads to lessening of dissolved O_2 forming OH^- ions. For reinforcing bars implanted in concrete, following anodic reaction are promising.



The cathodic reactions which occur mainly are as follows;



OR



1.4 FACTORS AFFECTING THE CORROSION OF REINFORCING BAR IN CONCRETE

The factors which affect corrosion are separated into two main categories as below;

- (1) Internal
- (2) External

1.4.1 Internal factor affecting corrosion of reinforcing bar in concrete

It generally includes the environmental parameters, as follows;

- **Availability of moisture and oxygen at steel bar level**

Existence of moisture fulfils the electrolytic requirement of corrosion cell, and oxygen and moisture together leads to the generation of hydroxyl ions, thereby additional rust component is produced.

- **Temperature**

Increase in the temperature may bring about twofold effect:

- (a) Rate of electrode reaction increases generally.
- (b) Oxygen solubility reduces which leads to the reduction in the corrosion rate.

- **Carbonation and entry of acidic gaseous pollutant to the steel level**

The consequence of entry of acidic gases like SO_2 , NO_2 etc and carbonation is because of their tendency to decrease concrete's pH. The various states of steel bar corrosion are shown in **Table 1.1**.

Table 1.1: Reinforcement state at various levels of pH [2]

pH of Concrete	State of Reinforcement Corrosion
Below 9.5	Commencement of steel corrosion
At 8.0	Passive film on steel surface disappears
Below 7.0	Catastrophic corrosion occurs

- **Aggressive anions, mainly chloride ions, attaining to the steel bar level, whichever through the ingredients of concrete or from the external source**

It is generally recognized that corrosion process is influenced by free chloride ions. It is reported that with the increase in chloride content, the rate of corrosion increases and

resistivity decreases. **Table 1.2** shows the limits of recommended chloride content for various codes.

Table 1.2: Chloride Content's limit as recommended by some code of practice [2]

Country	Recommended limits of chloride content (% by mass of cement)
USA	0.15% for chloride exposure and 0.3% for chloride free exposure
UK	0.30%
India	0.15%

1.4.2 External factors affecting corrosion of reinforcing bar in concrete

- **Cement composition:** The cement present in concrete assures safety against the corrosion of reinforcement by keeping very higher pH of 12.5-13.
- **Impurities in aggregates:** Aggregates which contains chlorides originate severe corrosion troubles, chiefly those which are associated with sea water and those whose natural sites are in ground water where concentration of Cl⁻ ions is high.
- **Impurities in curing and mixing water:** Mixing and curing water may prove to be detrimental as far as reinforcement corrosion is concerned if it is either contaminated with enough amount of chloride or it is highly acidic due to presence of any undesirable element in it.
- **Admixtures:** Addition of an admixture, commonly calcium chloride which is used for accelerating cement's hydration is probably the main cause for existence of chloride in concrete in reinforced concrete structures.
- **(w/c) Ratio:** Basically the durability, strength and impermeability of concrete are controlled by the water/cement ratio. In some aggressive solution when RC structures are immersed, it is the permeability which affects the corrosion of reinforcement and permeability is the role of w/c ratio. With increase in the w/c ratio, the depth of incursion of chloride threshold level also enhances.

1.5 CORROSION PROTECTION MEASURES

Corrosion of steel bar in reinforced concrete can be prevented using different techniques given below.

- Corrosion Inhibitor

- Epoxy Coatings
- Paint
- Electrochemical Methods of Protection(Anodic and Cathodic)

Here, first three methods are discussed in detail.

1.5.1 Corrosion Inhibitors

Corrosion Inhibitors are the chemical compounds which on adding to a liquid or gas, slows down the corrosion rate of material, classically a metal or an alloy. The efficacy of an inhibitor relies upon the composition of fluid, flow regime and amount of water. The process for inhibition includes formation of passive layer, which stops entry of corrosive substances to the metal.

1.5.1.1 Classification of Corrosion Inhibitors

Inhibitors can be categorized mainly in 2 manners, as per their physical modes of application and according to their protection method.

1. Based Upon the Physical Mode of Application

The corrosion inhibitors can be classified into two groups depending on its physical mode of protection as:

- I. Admixed inhibitor
- II. Migrating inhibitor

I. Admixed inhibitors: Those compounds which are added to the fresh concrete at the time of mixing for new structures are known as **Admixed Inhibitors [3]**. These compounds are added instantly on adding water to cement. Admixed inhibitor affect initial set, afterward strength gain or other properties i.e. hydration processes of cement. To overcome this, retarders are added to concrete mix which balances the acceleration of the inhibitors and provided a slight extra retardation. The inorganic compounds which are based upon calcium nitrite[4], NaNO_2 , $\text{C}_6\text{H}_5\text{COONa}$ and Na_2CrO_4 are used as admixed inhibitors.

Another group of admixed inhibitors are the organic compounds based on the blend of alkanolamines, amines or amino acids, or on the basis of suspension of unsaturated fatty acid ester of an aliphatic carboxylic acid and saturated fatty acids.

II. Migrating inhibitors: These are the chemical which are applicable on the toughened surface of concrete and are capable to disperse across concrete to the repressed rebar where they act to control both the anodic and cathodic corrosion reactions by making a monolayer film at the steel-concrete interface[5]. According to physical mode of application these types of inhibitors are

also called as “**Surface Applied Corrosion Inhibitors**” or “**Penetrating Corrosion Inhibitors**”. These inhibitors are classically based either on mixtures of alkanolamines and amines or on inorganic compounds based upon Mono-fluoro-phosphate [MFP] [6] .

2. Based Upon the Mechanisms of Protection

The corrosion inhibitors based upon protection mechanisms can be classified into three groups as:

I. Anodic inhibitor

II. Cathodic inhibitor

III. Mixed inhibitor

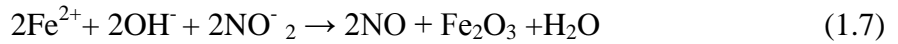
I. Anodic inhibitor: Anodic inhibitors are chemical substances which act as inhibitors because of their tendency to gain electrons. They put forth their operation by suppressing the reaction at the anode. The determination of necessary concentration is often done by the chloride level upto which the exposure of steel will be there. Anodic inhibitors work on the dissolution of the steel and they decrease the rate of corrosion by increasing the potential of the corrosion of the steel [7]. It functions by oxidizing corrosion product - ferrous ions to ferric ions that precipitated in the alkaline solution of the concrete and form a protecting layer on the reinforcement. The mainly employed anodic inhibitor is $\text{Ca}(\text{NO}_2)_2$, NaNO_2 , $\text{C}_6\text{H}_5\text{COONa}$ and Na_2CrO_4 have also been employed[5]. But when insufficient quantities of corrosion inhibitors are used, then intensity is localized and it generates acute pitting [8].

II. Cathodic inhibitor: Cathodic inhibitors work either by reducing the cathodic reaction or by particularly precipitating the sites of cathode. The materials used in this category are the strong acceptors of proton and in contrary to anodic inhibitors is typically not direct. Cathodic inhibitors work on the surface of steel and they slow down the rate of corrosion by decreasing corrosion potential. The majorly employed cathodic inhibitors are NaOH and Na_2CO_3 , which are believed to enhance the pH nearby steel, and decrease the transfer of oxygen by layering the surface of steel.

III. Mixed Inhibitors: Mixed inhibitors may concurrently influence anodic as well as cathodic processes. Due to the all encompassing effects of mixed inhibitor, wrapping corrosion occurred by chloride attack as well as that because of microcells on the surface of metal, a mixed is generally more enviable. It decreases the rate of corrosion with no noteworthy modification in the corrosion potential, typically by surface adsorption on the steel surface in association with the inhibitor and as a result generating a thin protective layer. The materials with hydrophobic group having polar groups like N, S, OH is efficient. The use of organic polymers like amine and aminoalcohol (AMA) can also be possible[9].

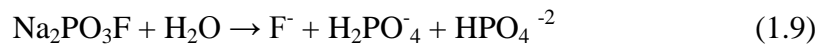
1.5.1.2 Mechanism of Some Commonly Used Commercially Available Inhibitors

(a) **Calcium Nitrite:** Nitrites of calcium or sodium are considered as an anodic inhibitors as they contend with the Cl^- ions for Fe^{2+} ions at the anode to make a layer of Fe_2O_3 as mentioned in the reactions below [10]:



The given reactions are very fast than the transfer of Fe^{2+} ions by means of formation of Cl^- ion complex. These reactions are very fast than the transfer of formation of Fe^{2+} ions via chloride ion complex formation. Therefore NO_2^- ions assist the formation of a steady passive film still in the existence of chloride ions (with γ FeOOH being the more stable oxide in existence of Cl^- ions). Conversely, complete safety depends largely on the concentration of vigorous ions such as the Cl^- ion, and critical pitting may cause when inadequate amount of inhibitor is employed in comparison to the chloride level in the concrete.

(b) **Mono Fluoro Phosphate (MFP):** The mechanism of inhibition of the Mono-fluorophosphate is quite unclear, that may either be anodic, cathodic or mixed. On hydrolysis of $\text{Na}_2\text{PO}_3\text{F}$ in aqueous and neutral media to form orthophosphate and fluoride via a reaction given by following equation:

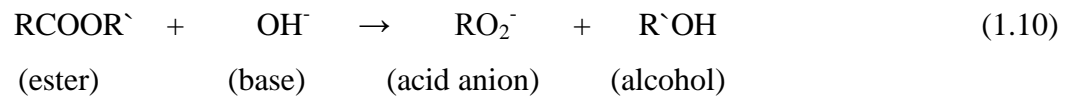


The inhibiting effect of $\text{Na}_2\text{PO}_3\text{F}$ may be recognized to the generation of phosphates, and therefore a passive layer of Fe_3O_4 , γ Fe_2O_3 and $\text{FePO}_4 \cdot \text{H}_2\text{O}$ formed on anode. On the other hand, as PO_3F^{2-} , PO_4^{3-} and OH^- are all probable corrosion inhibitors, this is not easy to say which type of ions are accountable for effects of inhibition of corrosion prompted by $\text{Na}_2\text{PO}_3\text{F}$. The outcomes of different researches affirm the combined effect of the phosphates.

(c) **Amino alcohol based (AMA) inhibitor:** In AMA containing organic inhibitor the chief constituent is aminoalcohol, whose nature is the volatile and aminoalcohol is carried largely by gas diffusion. Generally, the 2nd large constituent is an acid component. The acid component is described to react with hydration products[11]. The reaction with $\text{Ca}(\text{OH})_2$ results in the formation of gel which obstructs the pores of the concrete [7].

(d) **Amine ester based:** The inhibitors based on amines and esters exhibits twin actions in concrete as amine have dual actions in concrete as the compounds containing amine functional group works as an inhibitor while the compounds containing carboxylates ester acts as pore-

blocker, which blocks the entry of Cl^- ions[10]. For Surface applied type amino carboxylates containing inhibitors has the pore-blocking effect as a secondary protection mechanism against reinforcement corrosion. The hydrolysis of esters is done by mixing alkaline water to give corresponding carboxylic acid and alcohol. The reaction occurs in the manner as shown in **Eq. (1.10)**, where R and R' are various alkyl groups (hydrocarbons):



The COO^- anion is immediately transformed in concrete to the calcium salt of the fatty acid which is insoluble. The fatty acids and their calcium salts formed impart a hydrophobic coating inside the pores [12].

(e) **Mixed inhibitor:** An organic corrosion inhibitor comprising an emulsion of ester in water and amino alcohol is a **Mixed Inhibitor**, influencing corrosion across a mixture of active and passive mechanisms [13]. A decade over extending study explored the active part, a layer-forming amino alcohol which is usually considered to be a cathodic inhibitor. The passive part of the inhibitor mechanism lessens permeability by hydrolyzing an organic ester and depositing an insoluble calcium salt of fatty acid which blocks the concrete pores to decrease entry of Cl^- ions.

1.5.2 Epoxy Coating

The use of epoxy on the steel bar surface gives protection against corrosion. The epoxy coated rebar can be used in any concrete subjected to corrosive environments. This may include exposure to deicing of salts or marine environment. Epoxy coated rebar is also refers as “**Green Rebar**”. This epoxy coating is not consumed while performing its protection function. The coating has very low permeability to chloride ions. It is highly chemical resistant. An epoxy coating on the surface of steel bar acts as a very effective barrier to aggressive agents, particularly chloride ions, which will not easily diffuse through a continuous epoxy coating. Epoxy coated rebar is utilized in following kind of structures.

- Bridges
- Parking Structures
- Pavements
- Marine Structures

- Repair Works



Fig.1.2: Steel bar coated with epoxy [1]

1.5.3 Paint

Painting on the surface of steel bar is another method of protecting steel bar from corrosion. Its function is to build a barrier which prevents steel bar from the attack of corrosive agents. Paint inhibits contact between corrosive agents or chemical compounds from the steel surface. Paint generally consists of three components as below.

- Vehicle
- Pigments and Filler
- Additives

1.6 MONITORING OF CORROSION IN RC STRUCTURES

The following section provides a brief summary of the requirements of monitoring of corrosion and different methods through which it can be performed.

1.6.1 Need for Monitoring of Corrosion

Due to high stiffness and high tensile strength of reinforced concrete, the RC structures are expected to be durable. But this expectancy is not fulfilled in reality and failure of the structures happens upon exposing them to unfavorable environmental conditions over a time period. This can

lead to high repair cost, maintenance and less service life of RC structures. Therefore monitoring of growth of corrosion problems in new or existed RC structures is necessary, before it is rehabilitated or repair. Corrosion monitoring techniques are those methods which gives an entire picture of all the changes in condition of structures in time and also in all three dimension of structure. This technique provides an idea about external as well as internal damage caused, which enables the engineer to give proper safety measures to the structures.

In last few decades, a lot of damages detecting methods, like destructive and non-destructive techniques have been developed to analyze the variations in structures because of corrosion. Destructive techniques provide specific characteristics of the material by destroying the specimen and results in accurate measurement. On the other hand, the non destructive techniques monitor the quality of material without destroying the specimen. The different types of non destructive techniques which are used in monitoring the corrosion in reinforced concrete structures are given below;

- Half Cell Potential Method
- Surface Potential Measurements
- Ultrasonic Pulse Velocity Method
- Ultrasonic Bulk or Guided Wave Method
- Linear Polarization Resistance Method
- Open Circuit Potential Measurements
- Impact Echo method
- Acoustic Emission
- Electrochemical Impedance Spectroscopy
- Infrared Thermography

In present study, two wave based non destructive technique will be used for corrosion monitoring.

- **Ultrasonic Wave Approach**
- **Acoustic Emission**

1.7 ULTRASONIC WAVE APPROACH

Ultrasonic refers to the sound energy which is above the audible frequency of 20 kHz. Ultrasonic wave approach is a non destructive method which can be used to find the strength of

material and detect the internal damage in the structure like cracks, voids, honeycomb and decays etc. This method or technique is readily applied to the concrete structures in the form of ‘**Ultrasonic Pulse Velocity (UPV)**’ method. In this technique, electrical energy is converted into pulses of longitudinal, elastic stress waves with the help of a transducer which is in direct contact with the surface of concrete which is to be tested. A coupling gel is used to make good contact between surface and transducer. The sound waves generated with the help of transducer traverse through the concrete and after reflection, the waves are received by the transducer and converted back into electrical energy. With the help of an electronic mean, the time taken by the pulse or wave to travel through the structure and reflect back is measured and this time is used to calculate the parameter ‘‘pulse velocity’’. The quality of concrete is determined by the pulse velocity. This velocity is related to the soundness of concrete.

$$\text{Ultrasonic Pulse velocity (UPV)} = L/T \quad (1.11)$$

The upper frequency range of ultrasonic waves can be as high as 15-30 GHz. However, upper bound of frequency rarely overreaches 20 MHz for most of the structural health monitoring applications.

Ultrasonic monitoring is based on the ability of ultrasonic pulses to "see through" solid/opaque material and Bulk Wave identify internal or surface flaws without adversely affecting the material. It can be achieved only when the maximum applied stress does not exceeds the elastic limit so that the resultant strain is in proportion to the applied stress. It includes introducing a very low energy level, high frequency stress wave or ‘‘wave pocket’’ in to a material and observing the consequent propagation and reflection of this energy. The mean for introduction and detection of stress waves are generally based on piezoelectric effect. These pulses are responsive to the extent, position and character of defects in a structure, and wave characteristics change accordingly. By studying the attenuation, propagation and reflection of these waves, it becomes possible to determine the fundamental properties like damping characteristics and elastic modulus of the materials and employ them for the diagnosis of damages. Thus, ultrasonic method can be used as a mean for the monitoring of health/soundness of structures.

1.7.1 Ultrasonic Guided Waves

The elastic wave in all ranges of frequency - Ultrasonic, Sonic and Subsonic is categorised in 2 groups;

- Body waves or bulk waves
- Surface waves or guided waves

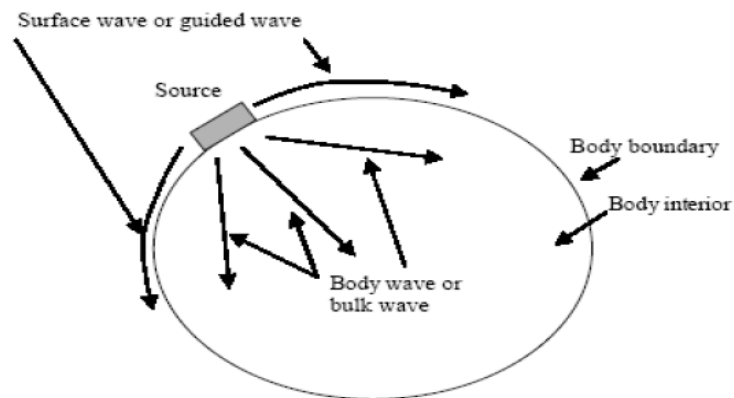


Fig. 1.3: Body and Surface waves generated with the help of Ultrasonic source[14]

Body wave or bulk wave travels through the bulk material and surface wave or guided waves travel along the surface. The sound velocity varies in material with their elastic properties and sound velocity can be found out by measuring flight time b/w 2 points.

This velocity can be linked to several kinds of different materials properties and condition and it is often used as a test to measure the uniformity of concrete, where a contour map displays the velocity. Voids and large cracks can be identified by increase in travel time. An ultrasonic wave becomes a guided wave when it is guided by the geometry of structure and constrained within the boundaries and this wave has the capability to propagate large distances with less energy loss. The structure which guides the wave is known as “waveguide”. The main requirement for an ultrasonic wave to be a guided wave is that the waveguide thickness must be comparable to the operating wavelength (**Fig1.4**). However, if material thickness is much higher than op

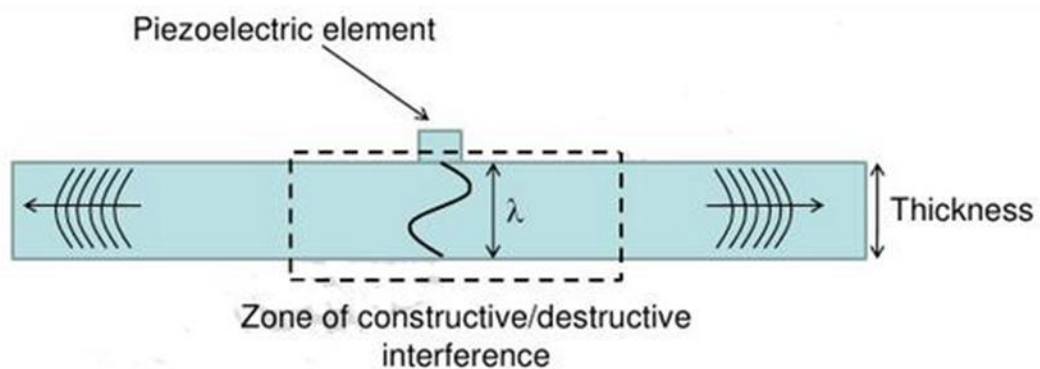


Fig.1.4: Guided waves propagation through a structure[14]

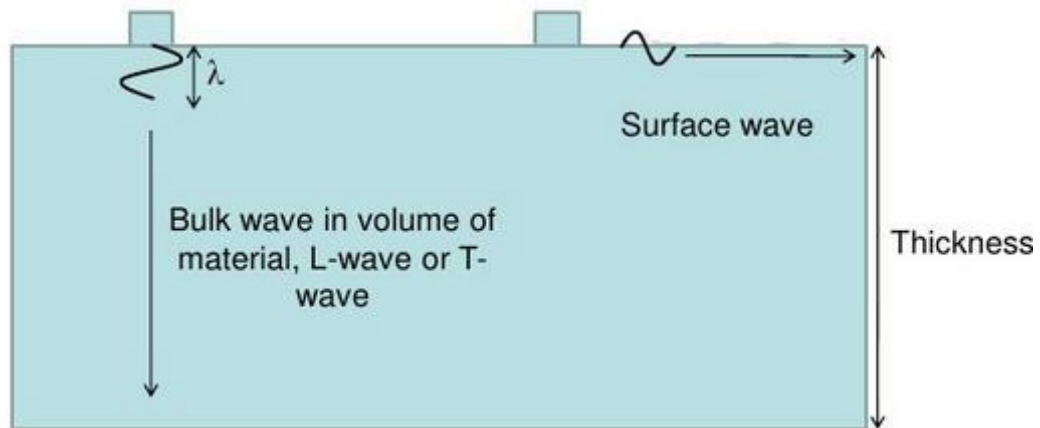


Fig.1.5: Propagation of waves when material's thickness \gg wavelength[15]

Major benefits of guided wave involve low cost, quickness and enhanced sensitivity to a number of defects. These guided waves can propagate at least 300 feet in a well conditioned steel bar.

Guided wave can travel in a structure as a whole and hence, have capability to examine the whole structure from a single point. Thus, an ultrasonic guided wave which is excited at exposed end of the steel rebar will be reflected from any defects in the rebar, allowing defects to be located accurately. There are a number of benefits of this UGW testing, as given below;

- Highly sensitive, which helps in the identification of small flaws
- Easily portable
- Non hazardous to the surrounding materials
- Capability of testing over large distance
- Testing is possible through the access of only one surface
- Some capability of estimating the shape, size, nature and orientation of the defects
- High penetrating power, that helps in flaws detection which are deep inside the structure

1.7.1.1 TYPES OF GUIDED WAVES

Depending on the geometry of waveguide or structure from which these guided waves travel, there are various types of guided waves.

- Plate wave or Lamb wave
- Rod wave
- Bar wave
- Cylindrical Guided wave
- Rayleigh wave
- Generalized Rayleigh-Lamb wave

They are presented in following **Fig.1.6**.

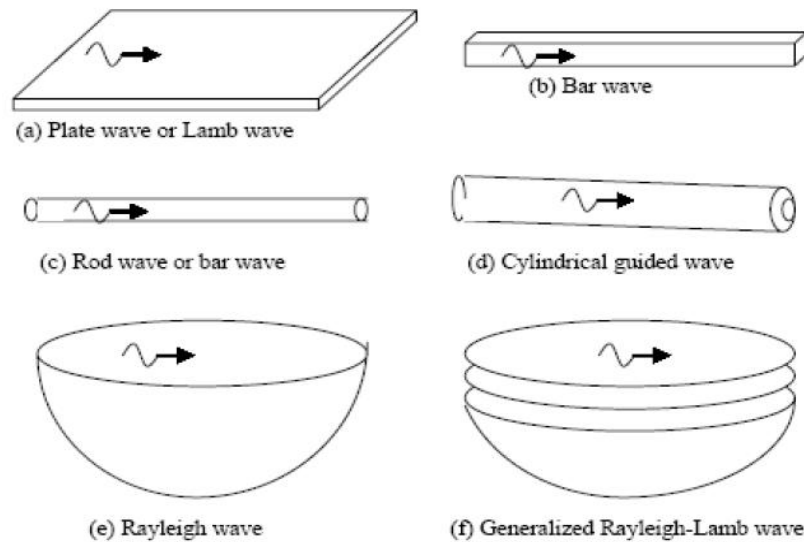


Fig1.6: Different kind of Guided waves[14]

If waveguide structure is homogeneous half space then the guided waves propagating along with the surface of half space is known as Rayleigh wave, which is named after its inventor. Lamb wave are those when wave propagate from a plate like structure with 2 parallel stress free boundaries. Elastic wave travelling through hollow pipe or cylindrical structure are known as cylindrical guided wave. Guided wave propagating through the solid bar or rod are called as Bar wave.

1.7.1.2. Propagation modes of guided wave

Ultrasonic wave travels in reinforcement bar in the form of guided wave. The present study uses the cylindrical guided waves as test specimens are cylindrical. In a cylindrical waveguide there are 3 types of mode or propagating waves.

- Longitudinal waves (L)
- Flexural mode (F)
- Torsional mode(T)

There is an axial and radial displacement in longitudinal mode, angular displacement in torsional mode and all the three radial, angular and axial displacement in flexural mode. $L(m,n)$, $T(m,n)$ and $F(m,n)$ are notations to represent these modes. In this notation 'm' is function of $\cos(m\theta)$ and it represents the circumferential displacement and 'n' denotes the chronological order of mode. The variable 'm' is 0 for the longitudinal mode as they have axial symmetry. The variable 'm' varies as $\cos(m\theta)$ around circumference of rebar for flexural mode. For e.g., the notation for first longitudinal mode is $L(0,1)$.

1.7.1.3 METHODS OF ULTRASONIC TESTING

Generally employed method of ultrasonic testing are;

- Pulse Transmission Method
- Pulse Echo Method

➤ PULSE TRANSMISSION METHOD

In this method, an ultrasonic transmitter is placed on one side of material and the detector or receiver is placed on reverse side. The beam from transmitter T, propagate through the material and reached to the opposite face where receiving transducer R is placed, as shown in Fig. 1.7.

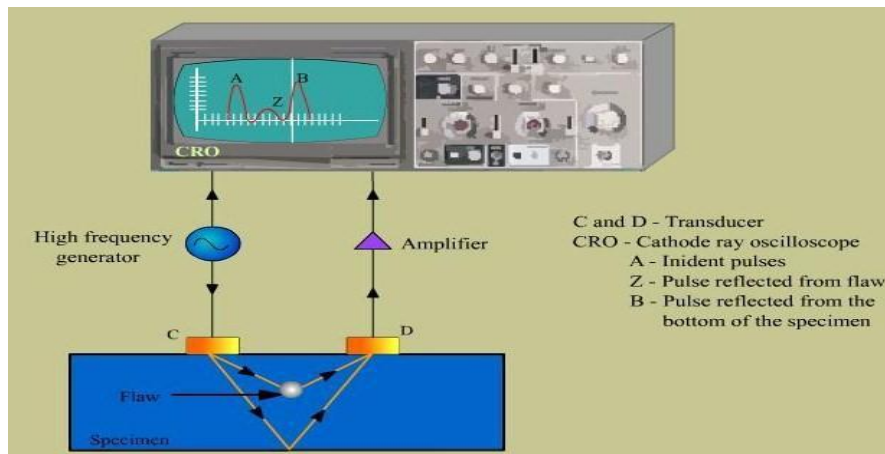


Fig.1.7: Pulse Transmission Method [16]

If a material is scanned by this method, it gives detail of location of flaws, defects and inclusions in XY plane. The relative severity of the flaw can be assessed by measuring the relative change in amplitude of inputs and received signals.

➤ PULSE ECHO METHOD

In this method, a piezoelectric transducer is used to transmit and receiving the ultrasonic energy, having its longitudinal axis perpendicular to and mounted on or near the surface of the specimen to be tested.

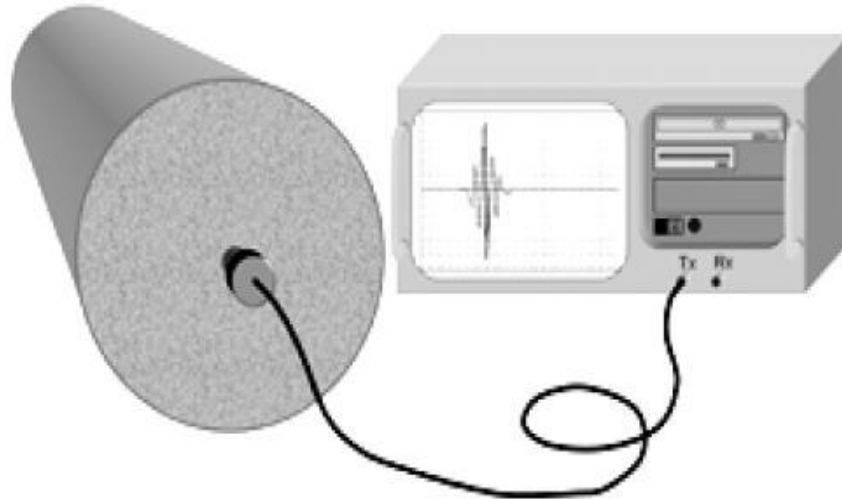


Fig.1.8: Test Set-up for the Pulse Echo Method [17]

1.8 ACOUSTIC EMISSION TECHNIQUE

For monitoring the structure at different levels of deterioration, the acoustic emission (AE) is one of the most promising methods. Acoustic emissions are those waves which generates in the form of energy due to any elastic or plastic deformation happening in material. ASTM E 1316 (2006) defines acoustic emission as “ that class of phenomenon whereby transient elastic wave are produced by quick discharge of energy from localized source within the material”. The source of AE wave generation can be microcrackinng, various sources dislocation and other variation due to rise in the strain. This is highly sensitive method and sensitivity makes possible to detect the damages long before it is visible. The vibration created by the waves when it reaches to the surface of material are recorded by AE sensors. The piezoelectric crystal converts the detected wave to electric signal and after amplification that electric signal is sent to the data acquisition system. This method also proves to be good in assessment of damage during the load test of different types of structure and materials including prestressed concrete(PC), steel reinforced concrete (RC) and fiber reinforced concrete(FRC).

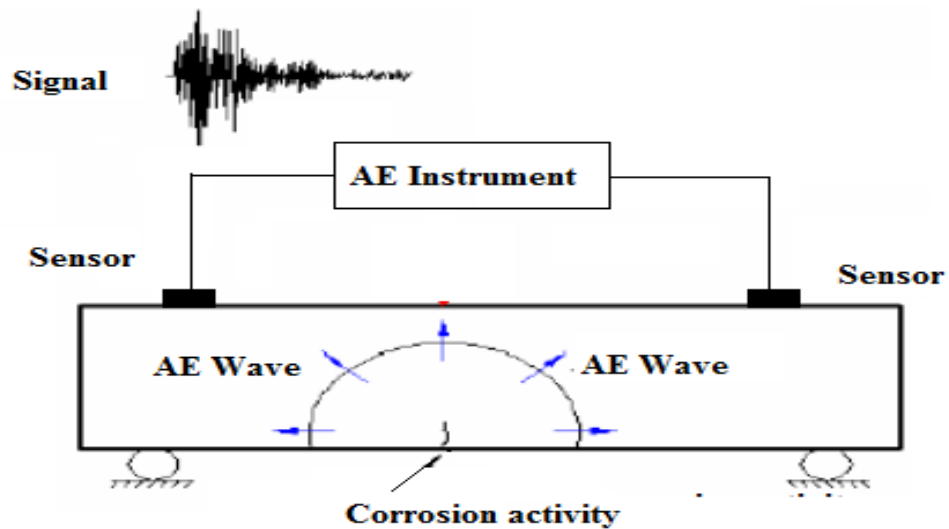


Fig.1.9: Schematic view of AE Monitoring Process[15]

The AE signal's strength depend upon a lot of factors, like orientation and distance from(wrt) sensor and also on nature of transferring material. The signals which are detected are generally termed as 'hit'. The definiton of a few general AE parameters is descibed below;

➤ **HITS**

It is the process of detecting and measuring an AE signal on an individual sensor channel (ASTM E1316).

➤ **EVENTS**

It is the increase of an AE activity which will cause the multiple hits on various sensors (ASTM E1316). A single event can be identified on the multiple sensors.

➤ **DURATION**

It is defined as the time between first threshold crossing and end of last threshold crossing of AE signal from AE threshold (ASTM E1316).

➤ **COUNTS**

The number of times the detection threshold crossed by AE signal is known as counts (ASTM E1316).

➤ **AMPLITUDE**

The highest voltage peak in AE signal waveform is know as amplitude or signal amplitude, normally expressed in decibels (dB)(ASTM E1316).

➤ **PEAK FREQUENCY**

It is that point in power spectrum where peak magnitude occurs. It is a 2 byte value reported in KHz.

➤ **AVERAGE FREQUENCY**

It is the ratio of no. of counts and duration of signal.

➤ **RA VALUE**

It is the ratio of rise time and highest amplitude in Volts from AE signal.

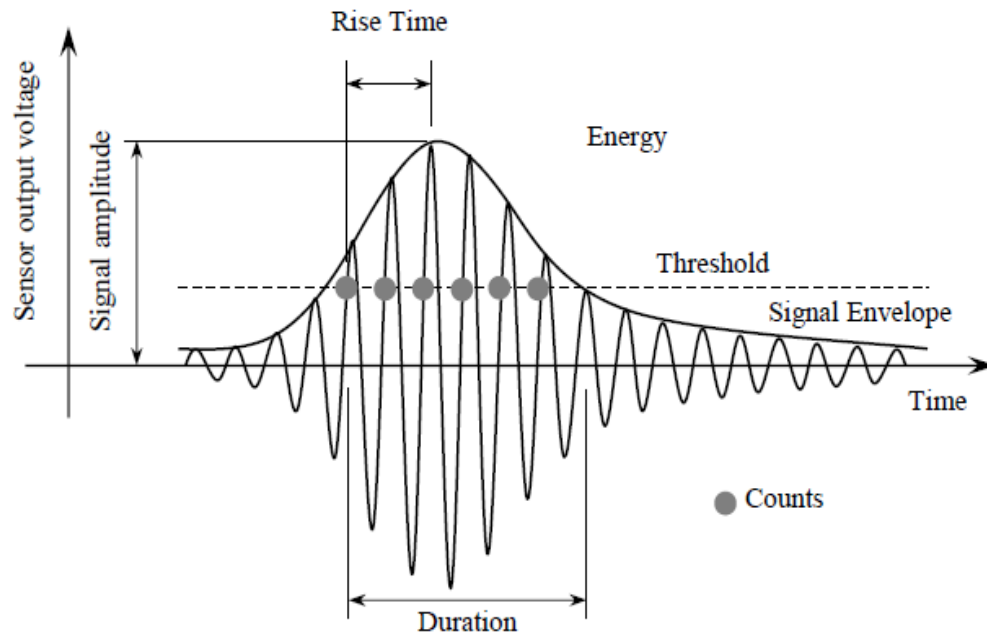


Fig.1.10: Schematic diagram showing some parameters of AE waveform[18]

➤ **RISE TIME**

Rise time is the time from an AE signal's first threshold crossing to its peak (ASTM E1316).

1.8.1 Acoustic Emission Source Location

AE can locate the source of emitted wave. The technique used in it is very similar to the technique used in seismology for locating the epicenter of earthquake [19]. If AE wave speed in tested material is known to us, then by the help of arrival time of AE signals at various sensor locations, we can perform the source location. Since, greater than one sensor is required there, so AE events are identifiable only through this method. The algorithms which perform the source location are established in well manner and embedded in data acquisitions software. Depending upon the number of sensors used the source location can be performed in linear, planar or three dimensional space. Previous research work has shown that the AE source location is possible in

reinforced concrete (RC) or prestressed concrete (PC) structures if adequate filters were used [20].

1.8.2 Advantages of Using Acoustic Emission Technique

Over the conventional NDT techniques, there are a number of benefits of using AE technique as listed below;

- High sensitivity
- Real time monitoring
- Defective area location
- Cost reduction especially maintenance cost
- Early and rapid detection of crack, defect and flaws etc.
- No need of access to whole area.

Hence AE technique is very helpful in testing of the materials and also in the study of corrosion, fracture and deformations. A material's behavior and response under stress is indicated by this technique immediately which in turns related to the damage, strength and failure.

1.9 CLOSING REMARKS

This chapter deals with the mechanism of corrosion in reinforced concrete structures, various factors which affect the corrosion process, protective measures against corrosion reinforcement, need of the studying of corrosion of those structures and different types of NDT used for the monitoring of corrosion in the structures. This fact cannot be denied that NDT techniques are very effective in examining and evaluating actual situations of structure. However, in present research, AE technique and UGW technique was selected for monitoring the corrosion because of various benefits of these techniques over other usual NDT methods. In next chapter, a detailed discussion of work done by a number of researchers on these two techniques will be done.

REVIEW OF LITERATURE

Various researchers have been focussing on the use of ultrasonic and acoustic emission technique to check corrosion of RC structures. A concise review of work carried out in these subject areas of research has been explained in this section. Apart from these two techniques the review related to the use of corrosion inhibitors is also done in present section.

2.1 USE OF ULTRASONIC GUIDED WAVES IN R.C STRUCTURES

Pavlakovic et. al. (2001) explored the operation of ultrasonic guided modes that illustrate smaller attenuation while propagation across the waveguide made by the rebar rooted in lesser impedance grout, so as to enlarge the detection span of tendons. The fabrication of 2 test sample were done, made up of a mild steel bar inside the centre of a plastic pipe which was packed with grout. The bar was intact for the first specimen, and from each end of the bar, notches were cut approximately 500 mm for the second specimen. Each pulse-through and pulse-echo tests were accomplished. This was established that a series of modes with attenuation minima at greater frequencies was shown by the dispersion curves of circular steel bar embedded in lower impedance medium. The minimum attenuation appeared at the identical frequencies at the point where energy velocity is maximum(**Fig.2.1**).

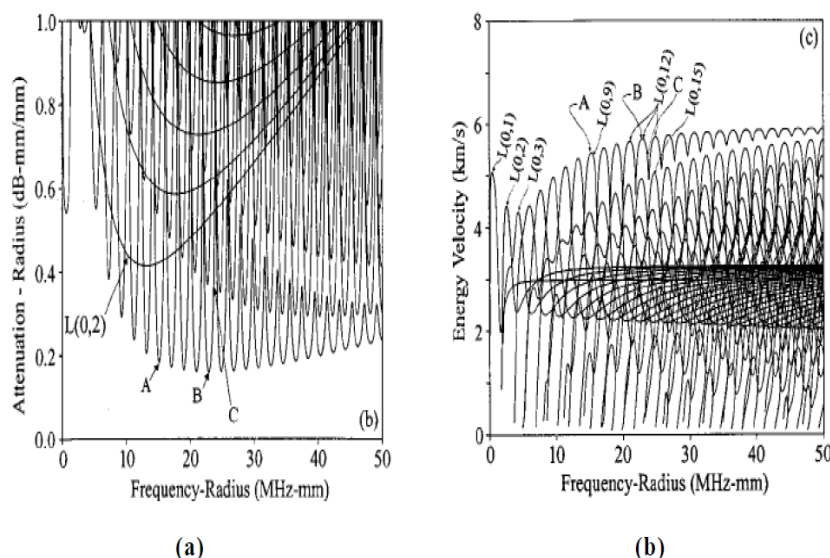


Fig.2.1: Dispersion curves for axis symmetric L (0,n) modes of rebar embedded in grout (a) attenuation; (b) energy velocity [21]

The attenuation minima and energy velocity maxima relative to location of leakage of energy into the embedded medium is limited. This can be observed as of the fact that with the rise in frequency, the value of minimum attenuation falls till a 23 MHz-mm frequency-radius. Past this position, the material attenuation present in the bar becomes a remarkable factor and attenuation gets bigger at the minima.

Na et al. (2002) considered the possibility of discerning and estimating de lamination on the steel-concrete interface employing ultrasonic guided waves. The investigations were attempted on three sets of specimens. The Specimen sets 1 and 2 are composed of four cylindrical structures both having dissimilar values of taking apart (0, 25, 50, 75 % of concrete steel interface). Specimen set 3 consisted of three concrete beam structures- specimen having dissimilar quantity of separation with no stirrups, specimen having distinct quantity of separation having stirrups and, specimen having identical quantity of separation at diverse locations with stirrups. Ultrasonic testing was administered in via transmission mode. The fabrication of two experimental set ups were framed for both moderately high and low arrangements (TRA1, TRA2, TRA3, TRA4) to generate, propagate and receive guided waves across steel bars and concrete (Fig. 2.2).

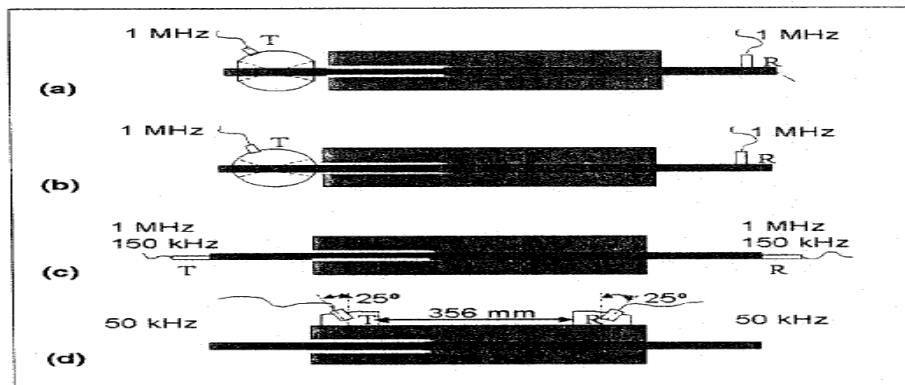


Fig.2.2: Various arrangements of transmitter and receiver for experimental analysis: (a and b) spherical solid coupler transducer holder; (c) transmitter and receiver having direct contact at the ends; (d) solid coupler transducer holder on concrete with 25° incident and reception angle [22]

For the launch of flexural cylindrical guided wave modes across the steel bar, two angular solid couplers of dissimilar dimensions were used, and for the launch of lamb waves in concrete beams, an angular solid coupler holder was used when steel bar was not attainable. The coolant

used was Petroleum jelly. To reveal the consistency of results, experiments were done 4 to 8 times with each arrangement. $V(f)$ curves were plotted found on the investigations.

It was established that TRA1 is very effective in forecasting and evaluating the extent of separation for specimen sets 1 and 2. The responsiveness was influenced by the choice of transducer frequency in TRA3. The detection responsiveness was influenced by the gap between concrete surface and separation region in case of TRA4. If the absolute transmitter angles were used then the results obtained with TRA1 and TRA2 were appropriate. The experimental observation revealed that the effectiveness of annular shaped holders employed for stimulating flexural cylindrical guided wave modes was reasonably greater than other holders. The signal generated from comparatively higher angle of incidence was most sensitive to discontinuities. This was confined that the guided wave method can be appealed to calculate or quantify the extent of separation or de lamination by the use of pulse through transmission mode.

Beared et al. (2003) suggested a technique employing guided ultrasonic waves to examine grouted steel tendons, anchors and rock bolts for corrosion and fracture. Two types of reinforcing tendons were formed- 5 or 7 mm single wire strand and seven wire strands of 15mm diameter. To determine the attenuation accomplished by the wave in short lengths of grouted tendons, pulse-echo method was performed from the free end of the structure to determine the attenuation sensed by the wave in short lengths of grouted tendons. The outcomes of the experiment elucidated that the range of the inspection for a complete break was restricted to about 1.2 and 0.8 m for 7mm and wires of diameter 5 mm respectively. For 15 mm stranded tendons, the examination range was restricted to about 1.5 m for the center wire and about 0.5 m for the six outer wires. It show that because of large level of attenuation and deprived reflection of modes, the use of guided waves for the examination of less diameter tendons would be restricted to give verification of defects in localized areas. Although, it was seen that attenuation decreases greatly with rise in tendon diameter(25-30 mm). This was also concluded that the range of inspection of such structures could be as much as 5 m. [23]

He et al. (2006) discussed the application of ultrasonic guided waves in a two-layered structure (comprised of solid steel and semi-infinite film of concrete) to find out the length of steel rod fixed in concrete and to calculate the quantity of delamination among a steel rock bolt and concrete. To calculate the large frequency theoretical wave structures for a rod rooted in concrete, a Semi-Analytical Finite Element Method (SAFEM) model was used. Six specimens

having different values of delamination (0, 25, 33, 50, 75 and 100% of the entire length of the rod), the pulse-echo technique was used to conduct ultrasonic testing.

The experimental findings reveal that, in order to find out the length of an embedded rod, one must employ guided wave modes at greater frequencies. It was found that, a transducer having a centre frequency of 1 MHz or greater is more appropriate for length determination. The lesser frequency guided wave modes displayed more appropriate findings whereas estimating delamination at the steel-concrete interface. This was accomplished that any transducer having a centre frequency greater than 2 MHz is unacceptable for the assessment of delamination.

Fig.2.3 exhibits that elevated frequency modes at excitation frequency of 2.6 MHz and 2.8 MHz are not sensitive to the existence of delamination, as there is a small variation in signal amplitude.

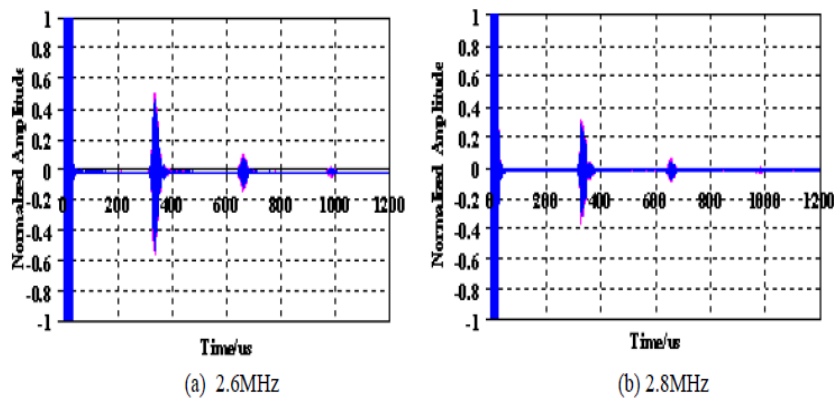


Fig.2.3: Waveforms obtained above 2MHz. [17]

This was inferred that ultrasonic guided wave pulse-echo method can be used to examine huge lengths of embedded rods.

Cawley (2007) investigated the employment of ultrasonic guided waves for long range assessment of big structures for instance airframes. In their study, the highlighted difficulty was the overlapping of reflections from different features in complex structures. The rise in feature density made it not possible to examine an individual reflection or, an extra reflection from a defect. This difficulty was determined by deducting the current response from a baseline measurement taken when the state of structure was well-known and this made it probable to observe the modifications in the response of the structure. Nevertheless, this technique needed a large extent of signal stability with the passage of time in the lack of destruction, or a scheme that could precise benevolent modifications such as temperature disparity. One such proposal,

‘temperature compensation’ was executed and significant outcomes were found. It was highlighted that for complex structures some other gentle variations like intake of moisture by adhesives are also an affair of perturbation and a big deal of research is vital to discern a consistent health monitoring. [24]

Mahmoud et al. (2010) explored the application of ultrasonic waves for non-destructive structural health monitoring of CFRP bonded concrete specimens administered to water immersion ageing at under control temperatures of 25-60°. To generate and receive surface waves at the external face of CFRP, narrow-band transducer with center frequency of 110 kHz were used. The amplification, digitization and processing of the signals received by the transducer and processed to dig out the parameters: average power (P_{avg}) and maximum amplitude (V_{max}). Due to water immersion ageing the alteration in these parameters occurred were recorded for 12 weeks. A decline in the measured ultrasonic parameters owing to ageing over time was specified by the results. Mode-11 fracture loading of CFRP concrete samples was lead to some ageing conditions, temperature, a parameter and a synchronous destructive study was carried out and fracture energy was obtained. At every ageing temperature, a correlation analysis was executed in between destructive parameters and the non-destructive parameters (P_{avg} , V_{max}), as shown in **Fig.2.4**.

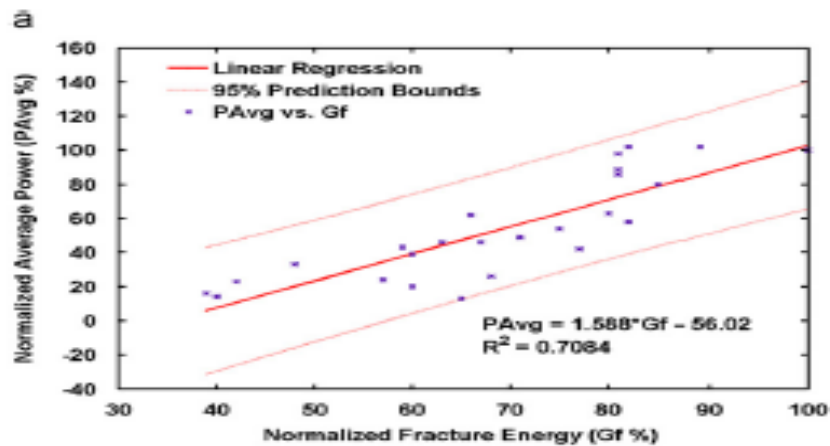


Fig 2.4: Linear regression of non-destructive ultrasonic parameters vs. fracture energy results of CFRP–concrete samples subjected to accelerated aging temperatures: (a) average power (P_{avg}) vs. Fracture energy (Gf). [25]

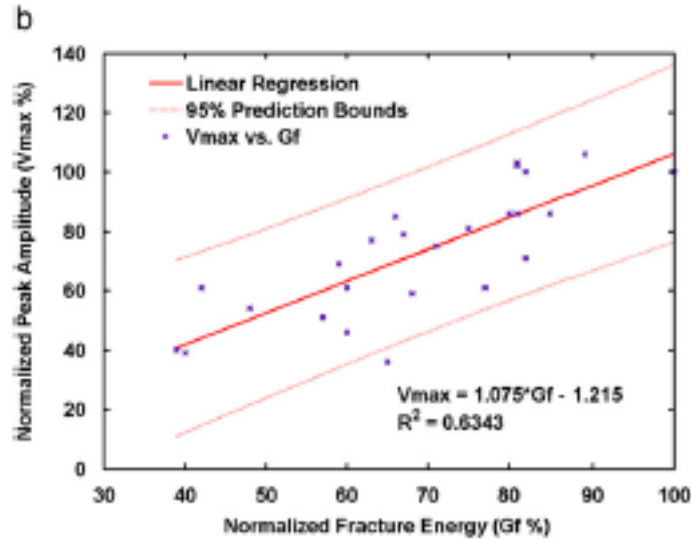


Fig 2.4(b): peak amplitude (V_{max}) vs. Fracture energy (Gf) [25]

At all temperatures, a sound relationship between the ultrasonic parameters and fracture energy was indicated by the results. This was inferred that for the structural health monitoring of CFRP confined concrete structures, non-destructive ultrasonic technique can be applied.

Raisutis et al. (2010) discussed the use of non-destructive ultrasonic guided waves for the examination of small diameter CFRP rods which are employed in gliders. For the investigation of the propagation of ultrasonic guided waves in defective CFRP rods with multiple delaminations, several models such as 3D numerical solutions, finite difference and finite element were used. This was demonstrated by the conducted experiments that ultrasonic guided waves can be applicable for the testing of faulty CFRP rods. To monitor the amplitude of leaky waves over the rod, the immersion technique whose basis is the excitation of longitudinal guided wave mode L(0,1) was proposed. Over a defected zone, a decline in amplitude or complete fading of leaky waves was indicated as de lamination type defects. This was indicated that the de lamination type defects was not hampering the propagation of L(0,1) guided. L(0,1) mode was just transformed into another modes which were not generating leaky waves. Consequently, a prospect of discerning a chain of flaws in CFRP rods was noticed. For online testing of CFRP rods, the emphasis was given on the future prospect for non-contact generation of longitudinal L(0,1) guided wave with the help of a more developed ultrasonic method. [26]

Sharma and Mukherjee (2010) explored the application of longitudinal guided ultrasonic waves to study notch and debond defects caused by corrosion in steel bars in concrete simulating pitting and de lamination phenomenon. For the before time detection of destructions in steel in

RC beams, the techniques of low and high frequency ultrasonic pulse echo and pulse transmission was employed. By the use of effective union of two ultrasonic monitoring techniques, the accurate position and magnitude of damage was specified. To recognize corrosion mechanism in a bar impacted in concrete, the application of Ultrasonic guided wave monitoring utilizing specific core and surface seeking modes was done. In general aspect, large pitting and non-uniform area loss was emphasized by acute signal attenuation marks chloride corrosion, which was well untangled by core seeking mode. It starts through de lamination exhibited by increase in signal with surface seeking mode. This was found that the whole mechanism of corrosion in RC structures can be fruitfully recognized through sensible selection of ultrasonic modes [27]

Sharma and Mukherjee (2011) studied the kind of mechanism of corrosion in chloride and oxide environments in RC beams. This was observed that the signal was highly attenuated when core-seeking mode was propagated in case of Chloride corrosion in, accordingly indicating pitting and non-uniform area loss. There was an rise in the signal strength and then a fall when surface seeking mode was propagated, hence signifying delamination, subsequently local loss of material. It was observed in case of oxide corrosion in beams that when core-seeking mode was transmitted, there was a deliberate decrease in signal strength, representing the lack of pitting. When the surface-seeking mode was communicated, there was an early decrease in the signal because of the pressure build up by the generation of products of corrosion, signifying a steady rate of corrosion and localized corrosion and finally, a steady climb in signal strength was recorded, representing bond deterioration. **Fig. 2.5 and 2.6** shows the ultrasonic voltage trends of the received signal using surface-seeking and core-seeking mode in both chloride and oxide corrosion specimens respectively.

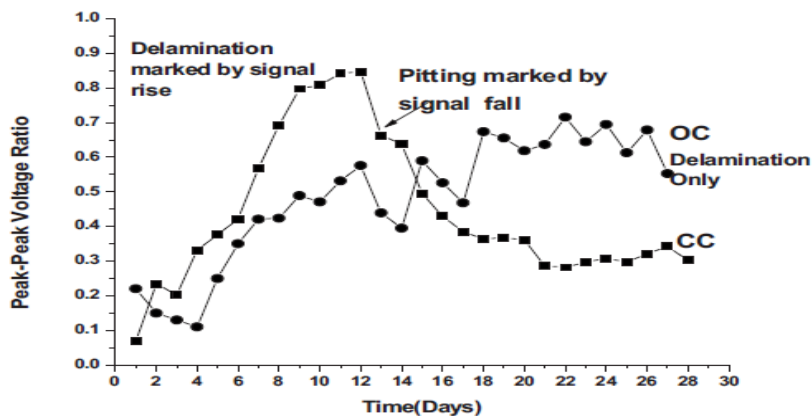


Fig.2.5: Peak-peak voltage ratio with surface-seeking mode [28]

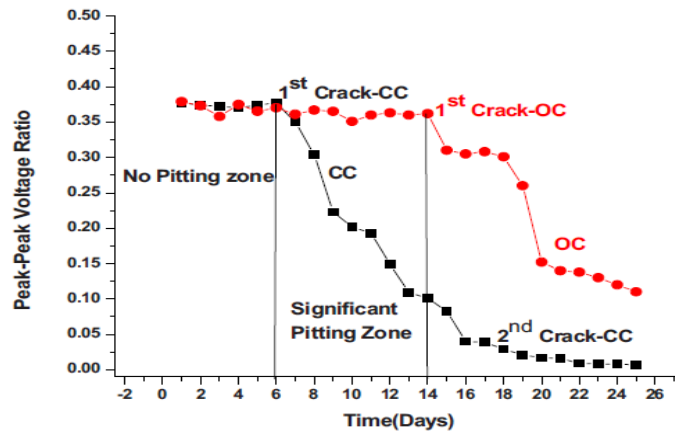


Fig.2.6: Peak-peak voltage ratio with core-seeking mode [28]

It was found by carrying out simultaneous destructive tests on RC beams that there is a well correlation between non-destructive Ultrasonic technique and destructive technique.

Sharma and Mukherjee (2013) exposed the application of ultrasonic guided waves in non-destructive evaluation of corroding reinforcing bars in the existence and nonexistence of chlorides. The monitoring of RC beams experiencing accelerated impressed current corrosion was done by the experimental investigation. In general, the acute signal attenuation marks chloride corrosion chosen by core seeking mode highlighted the huge pitting and non-uniform loss of area. The signal rise with surface seeking mode showed that it start with de lamination. As illustrated by strength of signal increase in surface seeking mode, the pace of corrosion was slow, localized, and marked by slow bond deterioration in oxide corrosion. In core seeking mode in OC, Pitting was irrelevant. In both oxide and chloride environments, at different stages of corrosion bars were monitored ultrasonically to investigate the capability of ultrasonic to envisage the deterioration level of the bars. By relating the ultrasonic voltage ratio with critical parameters of tensile strength, mass loss and bond strength in two ordinary environments of corrosion. This was accomplished that, even though the employ of guided waves is effectual in recognizing the existence of corrosion in rebar is broadly changeable environments, the technique requires ingress to the ends of rebar. [29]

Sharma et al.(2015) utilized UGW technique in monitoring the process of corrossions initiation and its development in steel bar which were entrenched in concrete, after samples were bonded with fibre reinforced polymer (FRP) sheets. Cylindrical specimens of concrete ofsize 300mm height and 150mm dia of grade M20 with a rebar of dia. 25mm at the core of the X- section, were subject to accelerated corrossion in chloride environment using impressed current technique.

Both GFRP and CFRP sheet were utilized in study. The fiber sheet was wrapped around specimens to be tested with the fiber along the circumferential direction of cylinders after definite days of introduction to corrosive surroundings.

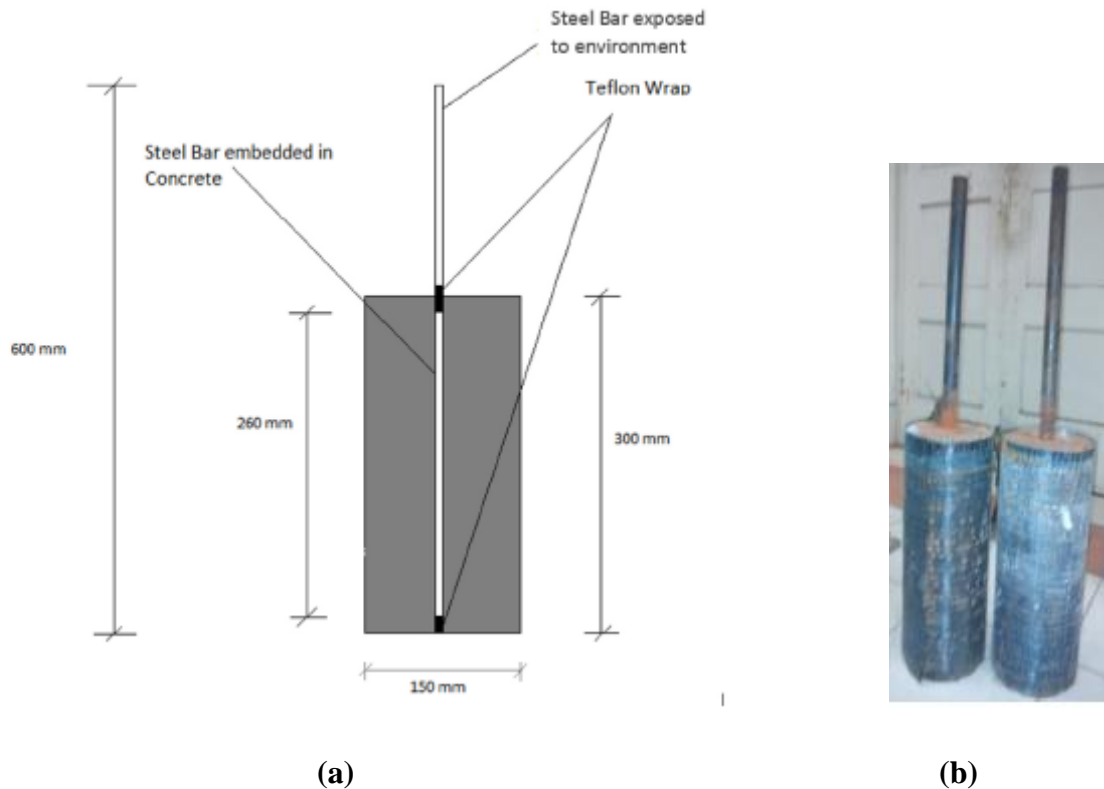


Fig.2.7: (a) Specimen schematic (b) Specimen wrapped with FRP[30]

Surface and core seeking modes were utilized to ultrasonically determine the opposition provided by FRP wrap to the corrosion. The ultrasonically measurement were linked with destructive parameters of pull-out strength and mass-loss. Using surface-seeking and core-seeking modes, it was recognized that PE technique is appropriate to determine corrosion in FRP wrapped specimens. It was marked by decrease in surface-seeking signal as against the rise of the signal due to delaminations of the rebar from the surroundings concrete in control specimens. Core-seeking mode signal which measure the deteriorations of the rebar because of pitting and area losses at later stage of corrosion indicate a very slow and marginal fall after wrapping as against a huge and drastic fall in signals with control specimen. It indicates that shield by FRP wraps very much decreases the corrosion rate. There is a link b/w the observed phenomenons and the PE signal. Using these two modes of the signal, it was probable to distinguish the pitting from surface corrosion. It was observed that Glass FRP give better shield than Carbon FRP. The protected samples exhibited lower mass and higher pull out strength than the control samples.

2.2 USE OF ACOUSTIC EMISSION FOR CORROSION MONITORING

Yoon et al. (2000) inspected the outrage in reinforced concrete corrosion by the use of the acoustic emission. He carried out a chain of normal strength concrete beams tests by the use of four point flexural loading. The dimensions of the beam were 100 mm x 150 mm x 1150 mm long. Various kinds of beams were trailed to activate various sources of damage. As a result of cyclic loading for various unreinforced and reinforced specimen, the incident of AE events showed in Fig. 2.8 The AE activities lessen as the load was held continually or unloaded, on the whole, in every cycle. The lesser AE events were seen in the corroded specimen, while a huge no. of AE events were developed in the uncorroded specimens; the greater the extent of corrosion, the lesser the AE activity in the reinforced beam.

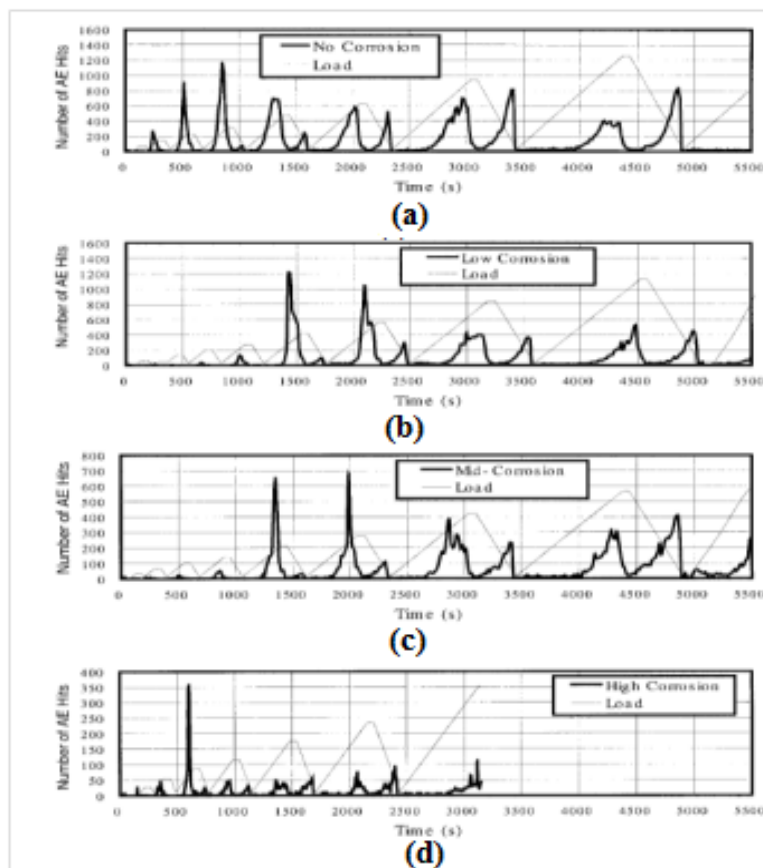


Fig.2.8: AE hits versus cyclic loading for RC beams (corroded and uncorroded)[31]

Ohtsu and Tomoda (2003) investigated the monitoring of corrosion in reinforced concrete by acoustic emission. Two types of mixture were engaged in the accelerated corrosion test. The ratios of water to cement (W/C) were 45% and 55%. For the accelerated corrosion test, the dimensions made for the reinforced concrete slabs made were 10 cm x 25 cm x 40 cm and for the crack-expansion test, the dimensions made for a concrete plate were 10 cm x 25 cm x 25 cm.

Expansive agent of dolomite paste was fed into a hole of 30 mm diameter in order to simulate radial pressure generated because of corrosion product. For every W/C ratio, the preparation of three specimens was done and after the accelerated corrosion, the chloride content was calculated. Core samples were taken at the elapsed of 4 days, 10 days, and 12 days for W/C = 45%, whereas for W/C = 55%, core samples were taken at the elapsed of 4 days, 8 days and 10 days.

In a sample with W/C = 45%, after 12 days chloride ions per m³ reaches greater than 1.2 kg at the point of concrete cover. In compare, for W/C = 55%, it reaches more than 1.2 kg after only 8 days. This is for the reason that with rise in W/C ratio in concrete, permeability increases. As per the Standard Specification (JSCE, 2001) the prescribed lower and upper bounds for prompting corrosion are 0.3 kg/m³ and 1.2 kg/m³ respectively.

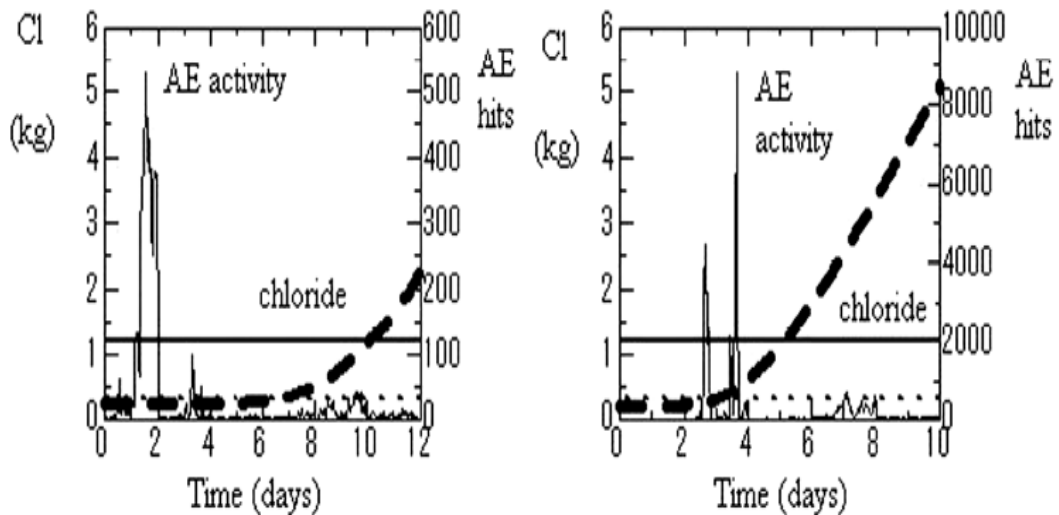


Fig.2.9: Comparison of chloride content and AE activities [32]

Therefore, on the basis of Fick’s law, the amount of chloride content, $C(t)$ was found out.

$$C(t) = C_0 (1 - \text{erf} (x/2[Dt]^{1/2})) \dots \dots \dots (2.1)$$

Where, C_0 is the surface concentration, D is diffusion coefficient, t is time and erf is Gauss’s error function. The comparative outcome of AE activity and chloride content has been shown in **Fig.2.9**. Here, from potentiometric titration, the contents of chloride in concrete were determined first. The first high AE activity is noticed in both the cases of W/C = 45% and 55%. One more high AE activity is observed, at the stage when the chloride content crosses the upper bound (1.2 kg).

Ohtsu et al., (2007) discussed the process of corrosion in reinforced concrete recognized by Acoustic Emission. The dimensions of RC slabs tested were 300mm x 300mm x 100mm. For longitudinal arrangement, reinforcing steel bars having diameter 13 mm are embedded with 15 mm cover thickness. Both an accelerated corrosion test as well as cyclic wet-dry test was carried out. The measurement of half cell potentials at the surface of the specimen was done by portable corrosion-meter. Immediately after terminating the current, the measurement was done two times a day in the accelerated corrosion test. At various stages, the concentrations of chloride were measured. Firstly, the beginning concentration was recorded by the use of a standard cylinder sample after moisture-curing of 28 days. **Fig.2.10.** show the connection among the AE activity and the half-cell potentials recorded.

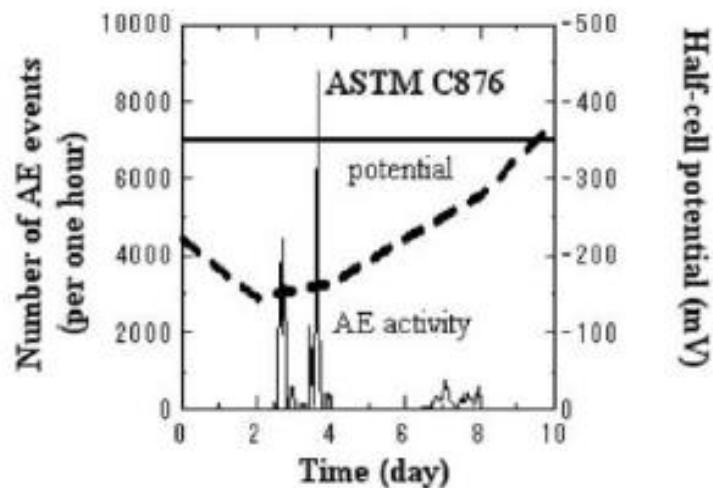


Fig 2.10: AE activities and Half-cell potential in accelerated corrosion [33]

A plot of the number of AE events as a total of two channels counted for 1 hour was taken. At approximately 3 days elapsed and 7 days elapsed, two periods of high AE activities are evidently remarked. This is confirmed that half cell potentials begin to fall after the primary activity, but are even larger than -350 mV nearby the second activity. As the half cell potential less than -350 mV is recommended as higher than 90% prospect of corrosion. Outcomes implies that the corrosion in the rebar is identified by AE activity additionally sure than the half cell potential. During the cyclic test, the number of AE events and the half cell potentials for AE events in cyclic test are shown (**Fig.2.11**). For 1 hour, the number of AE events is plotted again. Beside the cycles of wet and dry, AE events are occasionally examined. At 40 days elapsed, the first high AE activity in noticed, whereas the second activity is not clear. The values begin to fall at about 100 days elapse in agreement with half cell potential.

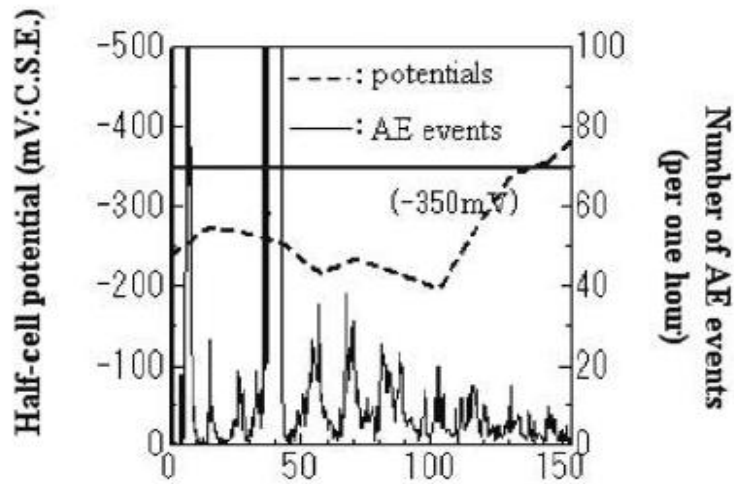


Fig.2.11: AE Activities and Half-cell potential in cyclic wet-dry test [33]

To facilitate the second activity, the RA values and the average frequency were examined analytically. Relative to first period as designated by a symbol of arrow, the value of RA becomes high and the value of average frequency is less.

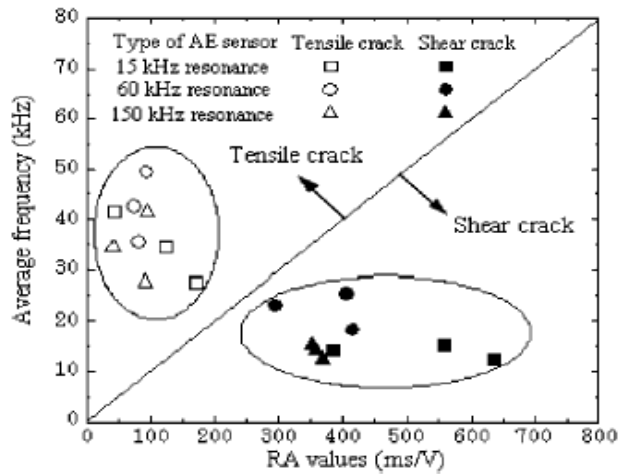


Fig.2.12: Cracks classification by AE indices [33]

According to **Fig.2.12**, the classification of AE sources was done as shear cracks. The rise in the RA value is found toward the 100 days elapsed. Therefore, at around 100 days elapsed the second period is rationally diagnosed, at which the RA values are less and the average frequencies are large. At this period, tensile cracks are to be nucleated as seen in **Fig.2.12**.

Ohtsu et. al. (2008) studied the AE Technique for steel bar corrosion in reinforced concrete. A RC specimen of size 1000mm X 570mm X 100mm was tested. 2 deformed steel bars of nominal diameter 13 mm, were entrenched into the specimen with 20mm thick cover. A cyclic wet-dry

test was performed. On surface of sample using portable corrosion meter, half cell potential was evaluated. The concentrations of chloride were measured at different time periods. Total no. of AE hit and half-cell potential during test are presented in **Fig. 2.13**. Figure shows that a solid curve which is plotted using total no. of AE hits observed while testing. The first AE activity is clearly visible at an elapse of around 14 days, whereas 2nd activity occurred at an elapse of around 60 days in sodium chloride portion.

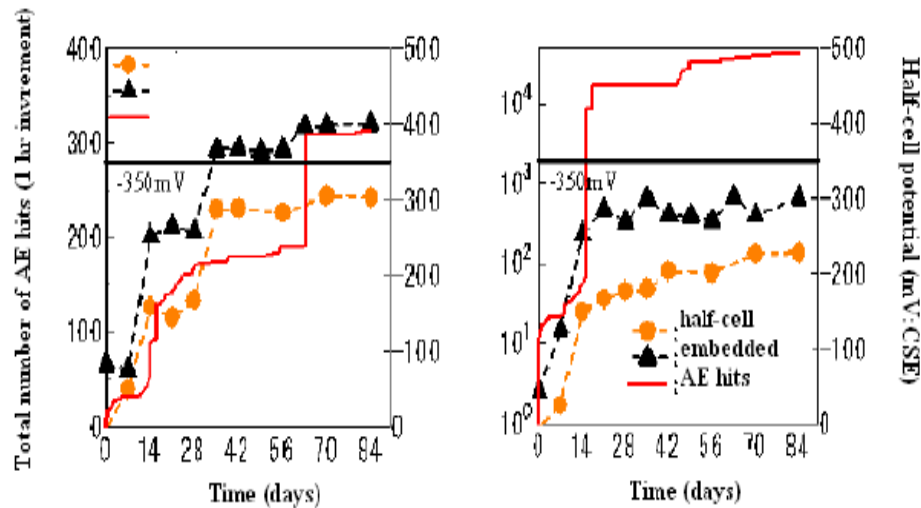


Fig. 2.13: Total AE hits and half cell potential in sodium chloride portion (left) and water portion (right) [34]

The AE activity curve in sodium chloride region is in important agreement with typical corrosions loss of phenomenological-model. Cracking can occurs in concrete because of expansion of corrosion products which ultimately results in generation of AE activity. It gives suggestion that AE activity can be detected in concrete sample. On comparing AE activity with half cell potential, it was found that potential shifts to more negative values with rise in no. of AE hits.

Consequently, at the 2nd period of high AE activity, the points of AE source are presented in **Fig.2.14**. This is noticed that AE sources are reasonably located that AE sources are fairly placed just about rebar locations. This implies that in rebar, the activity of corrosion generated due to extension of corrosion products because of concrete cracking is detected readily and positioned by AE method.

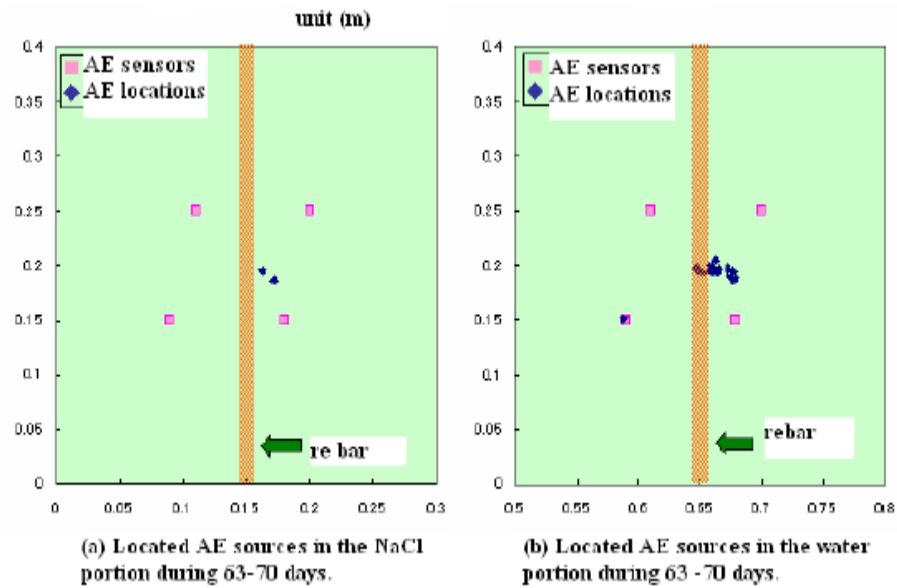


Fig.2.14: AE sources located at 2nd high AE activity in test [34]

Kawasaki et al. (2013) explore the corrosion mechanisms in reinforced concrete by AE technique. In their studies, they examined acoustic emission activities beneath a cyclic dry and wet test and the findings drawn are studied by an electron probe microscope (EPMA). As a result of rebar corrosion in reinforced concrete, AE sources are localized by SiGMA analysis (Simplified Green's functions for Moment tensor Analysis) to facilitate the Kinematical information of AE sources and nucleation of micro-cracks inside concrete. In addition to this, with the use of AE parameter analysis and Ib-value analysis features of AE signals are studied.

The dimensions of three beams made were 100mm X 75 mm X 400 mm. A contorted rebar having diameter 13 mm is lodged with 20 mm cover-thickness. The simulation of the corrosion process as a result of salt attack was done by a cyclic dry and wet test. AE was monitored constantly by the use of an AE measuring system. Six sensors of 150 KHz were linked with the beam's surface. Every week, the measurement was done within the frequency range of 10 KHz to 2 MHz, to perform a half cell potential measurement.

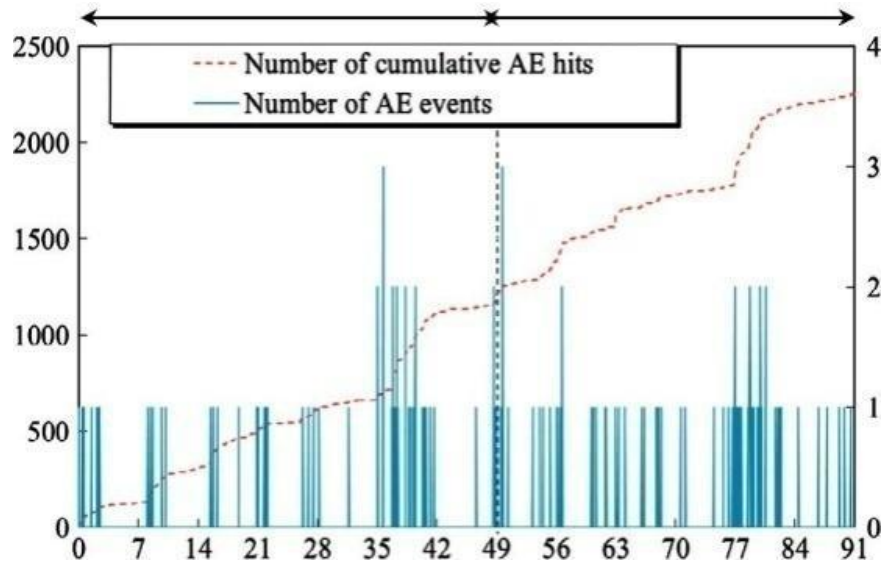


Fig.2.15: Number of cumulative AE hits and AE events [35]

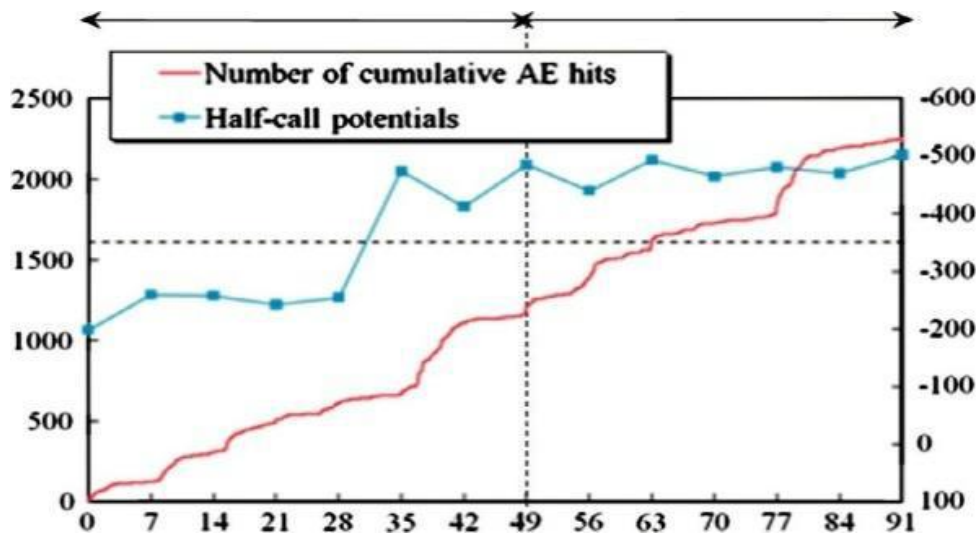


Fig.2.16: Number of cumulative AE hits and half-cell potential [35]

Fig.2.15 shows the Cumulative AE hits and AE events among all the 6 channels for every one hour. Six signals which constitute one AE event were observed and investigated. During the first 42 days, AE hits and AE events begin to increase reasonably and the calm period of AE activity is noted. From 35 days to 42 days, the calm period is brings into being after rise of AE hits and AE events. Additionally, the second rise of AE events was examined at 49 days. Subsequently the calm phase, AE hits and AE event increase constantly. Both the curve of cumulative AE hits and corrosion losses are in agreement with each other. Consequently, this leads to the surety that

during the first 42 days, the onset of corrosion existed and from 49 days to 91 days, the corrosion-induced cracks because of expansion of corrosion products could exist.

2.3 USE OF CORROSION INHIBITOR FOR PROTECTION OF STEEL IN CONCRETE

Ormellese et. al. (2006) used four kind of commercial inhibitors in the concrete for protection against corrosion. Three were Organic Compound Inhibitor Admixture (OCIA) mainly amine-esters (C), aminoalcohol (D) and alkanolamines (E) and one was nitrite based(N). Three series of concrete specimens were casted as shown in **Table2.1**.

Table2.1: Test conditions for RC specimens [6]

Series	Concrete mix	Chloride(%)	Inhibitors	Dosages		
1	Mix 1	0	No	-		
			Nitrite based	7.5 L/m ³		
				20 L/m ³		
					OCIA-C	5 kg/m ³
					OCIA-D	10 kg/m ³
					OCIA-E	1.6 kg/m ³
				1.5	No	-
					Nitrite based	7.5 L/m ³
						20 L/m ³
					OCIA-C	5 kg/m ³
					OCIA-D	10 kg/m ³
					OCIA-E	1.6 kg/m ³
				2.5	No	-
					Nitrite based	7.5 L/m ³
						20 L/m ³
			OCIA-C	5 kg/m ³		
			OCIA-D	10 kg/m ³		
			OCIA-E	1.6 kg/m ³		
2	Mix 2	1	OCIA-C	7.5 kg/m ³		
			OCIA-D	16 kg/m ³		
			OCIA-E	4 kg/m ³		
				1.5	OCIA-C	7.5 kg/m ³

			OCIA-D	16 kg/m ³
			OCIA-E	4 kg/m ³
3	Mix 3	0	No	-
			Nitrite based	7.5 L/m ³
			OCIA-C	5 kg/m ³
			OCIA-D	10 kg/m ³
			OCIA-E	1.6 kg/m ³

In every specimen of concrete, a carbon steel rebar having diameter 10mm and length 270mm was placed. A thermoretractil sheath was covering the terminals of every rebar such that only a length of 170mm was kept on to concrete. Inhibitors were added according to producer recommendations. The exposure of these specimens to ponding cycles i.e. accelerating chlorides diffusion by wetting with 3.5% sodium chloride solution for 1 week and drying in the laboratory for 2 weeks was done.

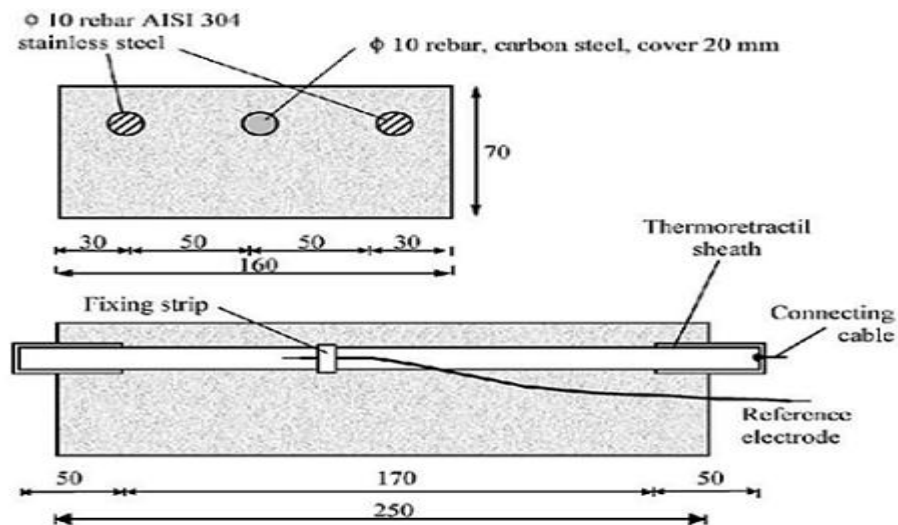


Fig.2.17: RC specimen with dimensions [6]

The inhibitors that are tested seem to be capable to enhance initiation time of corrosion in concrete lead to accelerated chloride diffusion as presented in **Fig.2.18**. Nevertheless the results are scattered. The finest effect is shown by Inhibitor OCIA-D, whereas nitrite containing inhibitor and OCIA-C acts in a same manner. The organic inhibitors available commercially decrease the entry of chlorides by packing the pores of concrete and choking the porosity of concrete by the disposition of compounds which are complex.

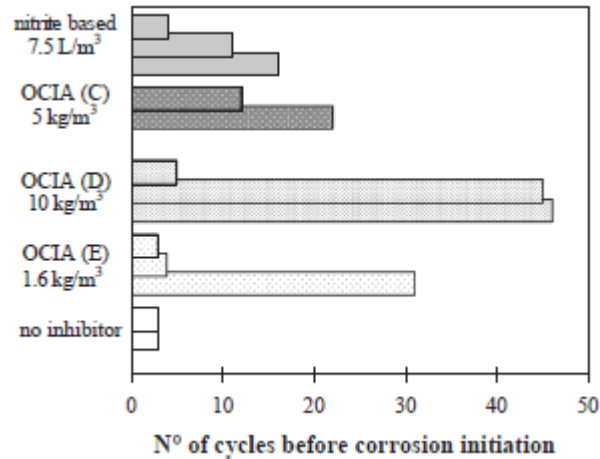


Fig.2.18: Time of corrosion initiation for specimens lead to ponding test with 3.5% Sodium Chloride solution [6]

Kondratova et. al. (2003) prepared RC slabs with a cover of 20mm having dimensions 55mm X 230mm X 300mm. All the slabs of concrete contain two straight bars of 15.9mm diameter. In order to perform electrochemical measurements, a rod of stainless steel was casted in concrete slab to act as counter electrode. A classic concrete slab is shown in **Fig.2.19**.

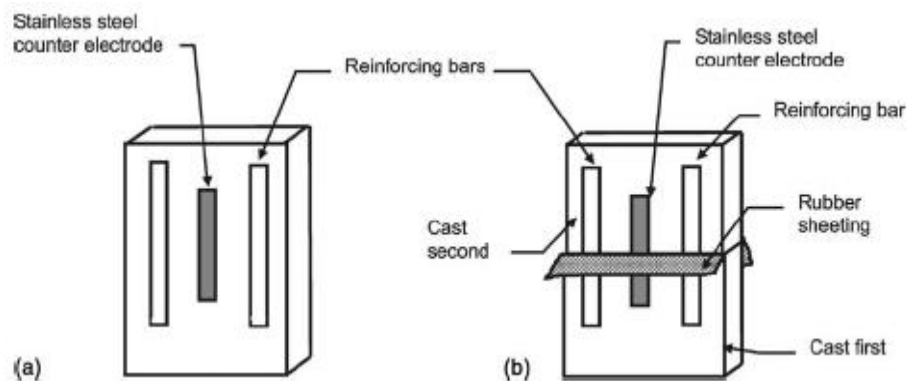


Fig.2.19: Diagram showing specimen with 2 entrenched bars (a) uncracked (b) precracked [36]

The w/c ratio was 0.4 and the concrete slabs were either precracked or uncracked. A simulating crack of width 0.2 or 0.4 mm was made transverse to the axis of rebar at the time of casting. Two kinds of corrosion inhibitors available commercially, mainly OCI-mixed type and CNI-calcium nitrite based inhibitor were mixed to concrete mixture for protection of corrosion. Slabs were fixed around 1 m beneath high tide at the Treat Island, Maine, USA, natural marine

exposure site. The specimens were visibly examined and the rates of corrosion were recorded yearly by the use of linear polarization method. A few concrete slab were wrecked open subsequent to exposure of 12 months and damage due to corrosion was assessed. The analysis of chloride content which is soluble in water was accomplished at this time. On the exposure of three years, it was recorded, that either of corrosion inhibitors were efficient in dropping the rate of corrosion for uncracked slabs, but moderately not effective in arresting localized corrosion of reinforcing steel in the crack regions for the concrete slabs which are precracked.

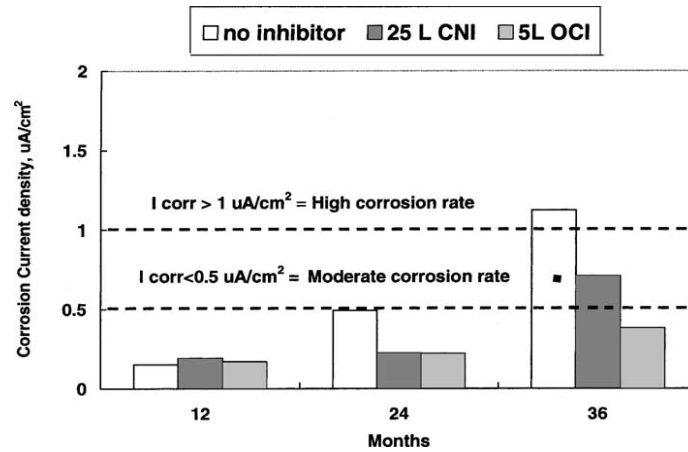


Fig.2.20: Corrosion current densities for uncracked concrete slabs with corrosion inhibitors [36]

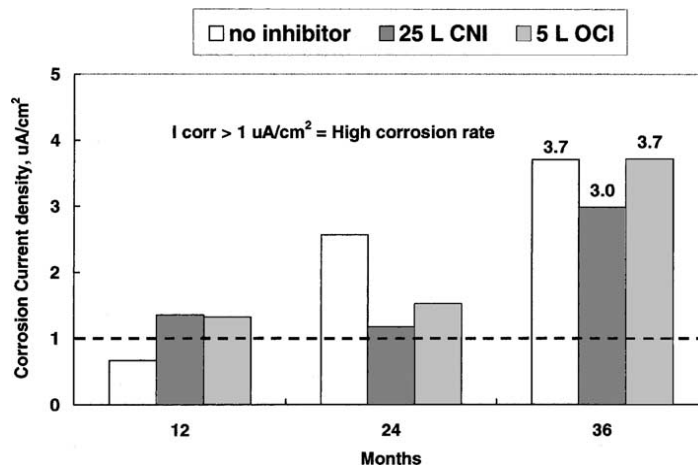


Fig.2.21: Corrosion current densities for precracked concrete slabs with 0.2 mm crack [36]

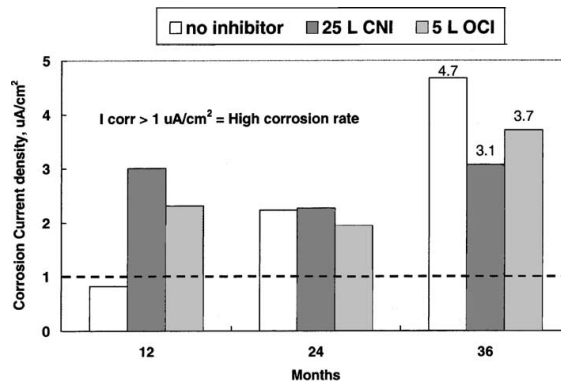


Fig.2.22: Corrosion current densities for precracked concrete slabs with 0.4 mm crack [36]

Dhouibi et. al.(2003) reported that the efficiency of inhibitors decreases with the time, after two year of immersion in chloride solution. The specimen were made in form of prism of RC having dimensions 40mm X 40mm X 160mm. Reinforcement was a rod 6.5mm in diameter and 120mm long, made of carbon steel. The inhibitors were added to the concrete mixing water. Their weight content were 0% (reference specimen), 6 % against cement weight. The open circuit potential (OCP) of reinforcing bars were measured once a year. Fig.2.23 shows the steel OCP results obtained. It appears that for concrete free form inhibitors, steel OCP is more negative ($E_c = -550 + \text{or} - 20\text{mV}_{\text{SCE}}$), when specimens were immersed in chloride solution, than when they were in distilled water ($E_c = -120 \text{ mV}_{\text{SCE}}$). After one year of immersion, chloride ions content at steel surface was very high resulting in steel depassivation and corrosion initiation. Moreover, the value of OCP potential becomes more positive only for specimens containing nitrite, and after one year immersion. With the other tests, the OCP values are similar to those of control specimens, which were immersed in same solution.

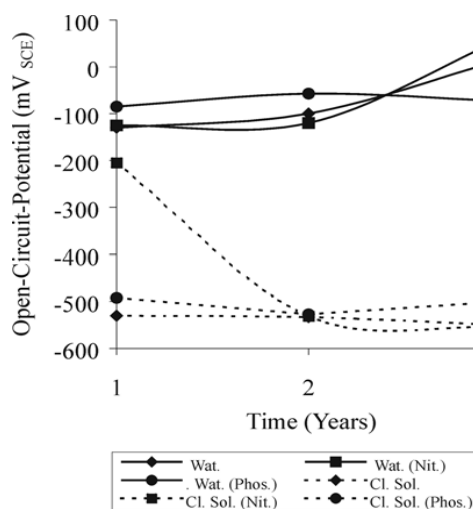


Fig.2.23: Open circuit potential versus time of concrete specimens [37]

Chaussadent et al. (2005) presented some main features on the application of monofluorophosphate (MFP) as a corrosion inhibitor for reinforcements of concrete. The corrosion inhibitor used to the surface of concrete, was proposed to disperse into the concrete in order to get into the reinforcement and end or delay corrosion. The experimental work involved analyzing the chemical interactions taking place between Monofluorophosphate and Ca^{2+} ions, when the portlandite $\text{Ca}(\text{OH})_2$ exist excluding other calcium comprising compounds such as CaCO_3 . The complexity of diffusion of MFP into non-carbonated concrete and therefore inhibiting the process of corrosion was established by recording corrosion potential on steel in mortars throughout the 48h subsequent MFP application on the surface of mortar. Chemical analysis on carbonated cement pastes exhibited that MFP ions could get to a depth of 40 mm under laboratory conditions. This level of diffusion was verified by electrochemical measurements executed on steel in carbonated mortars and exhibited that when MFP ions get to the surface of steel, they become efficient in raising protection of steel. [38]

Loto et al. (2012) performed a test on Type 316 austenitic stainless steel with the varying intermediate as well as concentrated concentrations of sulfuric acid and phosphoric acid. Identical tests were as well executed by adding 2% (20g/l) NaCl, to every specific acid concentration to form their respective acid chlorides. Potentiostatic polarization technique was employed for the study of corrosion on the specimen of Austenitic stainless steel –SS316 in cylindrical shape having diameter 10mm and length 10mm with mounted in araldite resin and linked with a flexible wire connection, ground and refined to fine diamond (1 μm), cleaned and rinsed/degreased in an ultrasonic bath with the use of acetone. For further experimental studies of corrosion, the samples were instantly placed in a desiccator. The active as well as passive characteristics are exhibited by the electrochemical corrosion. In the test of 9.1M H_2SO_4 observe that the rate of corrosion is 2.09×10^{-5} mm/yr and the corrosion polarization resistance (R_p) is - $3.8 \times 10^{-7}\Omega$. The corrosion current density of 5×10^{-6} A/cm² was less and the corrosion current is 3.56×10^{-7} A which was also quite less. The confirmation of the less corrosion of the test specimen in sulphuric acid was done by these results. But on adding 20g/l sodium chloride to the acid environment, the outcomes found here were relatively unusual from H_2SO_4 . There was rise in rate of corrosion 4.84×10^{-2} (mm/yr) and the E_{corr} (OCP) of -0.380V. The polarization resistance value was -2.3×10^{-5} and with a corrosion density of 1.2×10^{-4} A/cm². The corrosion current measured was 8.25×10^{-5} A. Correspondingly, the results of corrosion reactions specified more corrosion exhibited than in the environment in the absence of sodium chloride. The

behaviour of corrosion polarization for the experiments done in phosphoric acid, H_3PO_4 , also exhibited active corrosion reactions behaviour at all the employed concentrations (7.4M; 42.5% and 14.8M; 85%). With the obtained results, it is found that the mixing of sodium chloride gave low resistance to corrosion of the test electrode. [39]

Sancak and Coban (2015) found the usability of Forsterite Mine Tailings (FOT) in protection against corrosion of steel bar in concrete. For this purpose, C30 grade concrete specimens were produced with and without FOT. The amount of FOT used was 5%, 10%, 20% and 40% by volume in 150mm side cubic specimens. After 28 days of curing, compression testing of specimen with FOT was done. The specimen with 5%, 10%, and 20% FOT showed greater strength than that of C30 grade concrete. The different mixes without and with 5%, 10% and 20% FOT were poured in the mould of size 50mm diameter and 100mm height with centrally embedded a steel bar of 10mm diameter. The specimens prepared, were placed in the 5%NaCl solution to increase the corrosion in steel bars, after 14 days curing. For 120 days(17 weeks), the Corrosion current, Polarization resistance, corrosion rate and corrosion potentials values of the specimens were measured on a weekly basis my means of the Linear Polarization method. The results showed that the corrosion rate of specimens with 5% and 10% Forsterite Mine Tailings decreased as compared to the reference specimens without Forsterite Tailings.[40]

2.4 CLOSING REMARKS

In this chapter, the literature survey on application of ultrasonic guided wave and acoustic emission approach for studying the mechanism of corrosion in RC structures has been presented. The corrosion monitoring of the structures by the use of both techniques were found to be potent. During this investigation, the accelerated induced corrosion on the RC beam specimen has been monitored by using both these techniques. Along with these two techniques a literature survey regarding use of corrosion inhibitors is also done here. The corrosion inhibitors are found to be very effective in protection against corrosion.

EXPERIMENTAL PROGRAM AND METHODOLOGY

3.1 GENERAL

The aim of this study is to investigate the protection offered to corrosion by various suitable methods of epoxy coating and paint coating on rebars and the effect of admixed inhibitors, by NDT of Ultrasonic Guided waves and Acoustic Emission Techniques. RC beam samples were cast in four categories i.e., Control, Epoxy Coated rebar, Paint Coated Rebar and Corrosion Inhibitor admixed RC beam. The corrosion was accelerated in all the beams using impressed current technique and the effectiveness of protection offered by these various methods was studied by Ultrasonic Guided Waves (UGW) and Acoustic Emission Technique (AET).

3.2 TEST PROGRAM

The test program includes:

- 1) To determine the basic properties of ingredient materials of concrete (cement, fine and coarse aggregate) and steel, according to relevant IS specification. To assure the quality of reinforcing bars they were also monitored by using ultrasonic guided waves.
- 2) Casting of four RC beams, each having dimension of 150mm X 150mm X 700mm with a MS rebar of 25mm diameter and length 1000mm embedded in centre of cross-section in such a way that 700mm length was inside the concrete and 150mm projected out from both sides.
- 3) Four different beam samples were:

Table 3.1: Nomenclature of Samples Prepared

Beam	Detail
B1	Control
B2	Epoxy Coated Rebar
B3	Paint Coated Rebar
B4	Inhibitor Admixed Beam

- 4) All the four beam specimens were subjected to accelerated corrosion using impressed current technique at a constant voltage of 30V.
- 5) The beams were subjected to brine solution in middle 300mm length of beam
- 6) Ultrasonic Guided Wave monitoring of all the specimens was done after every 24 hours till the signals vanished.
- 7) Real Time monitoring using Acoustic Emission Technique was done throughout the duration of accelerated corrosion exposure.
- 8) To find the effectiveness of corrosion protection system using NDT tools of UGW and AE.

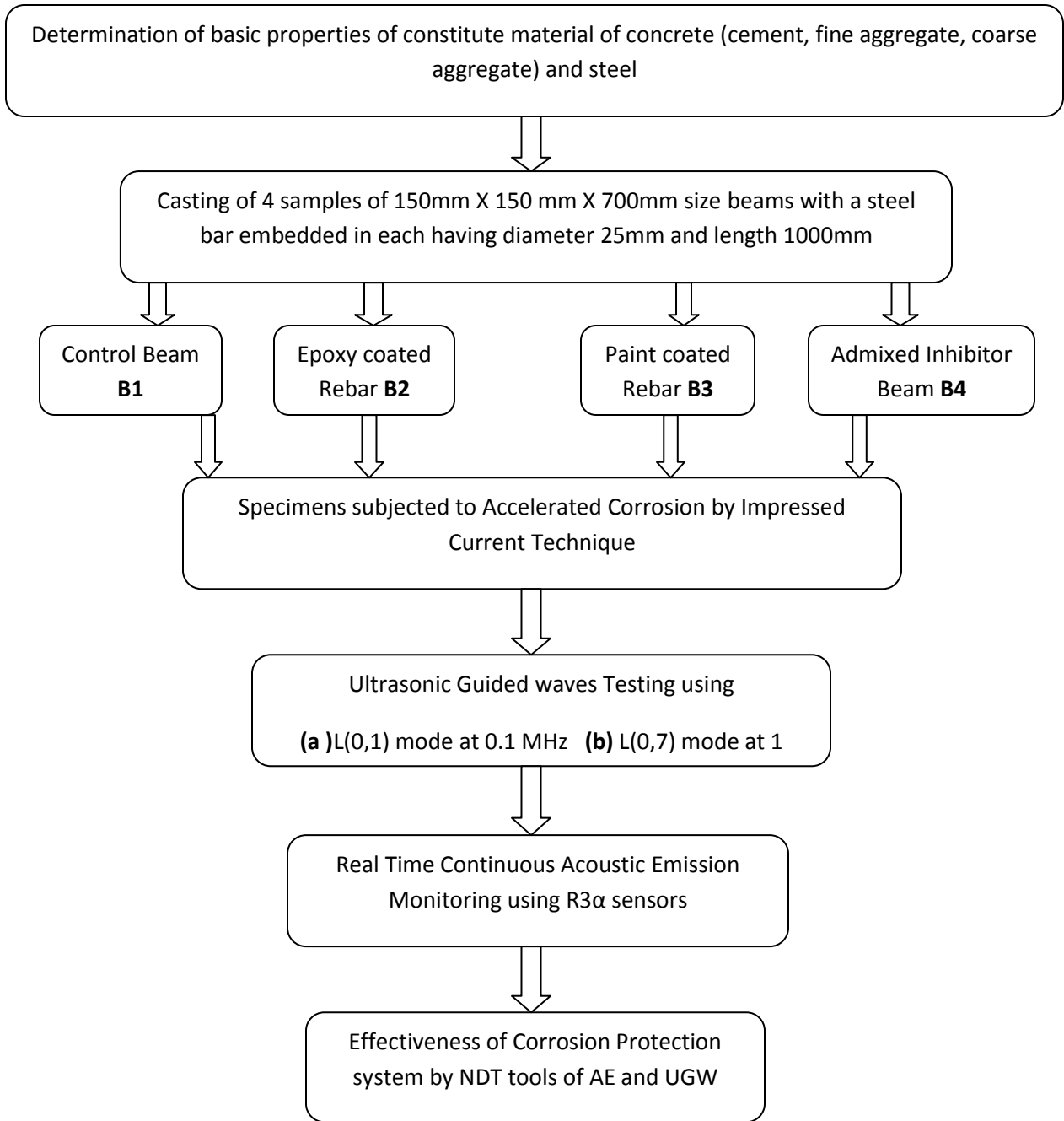


Fig.3.1: Test Program

3.3 MATERIALS USED

The reinforced concrete beams were casted in a mould having size 150mm X 150mm X 700mm with a provision of embedment of steel in it. The properties and specifications of constituent materials are as follows:

- **Cement:** The investigation of Ordinary Portland Cement (OPC 43 grade) manufactured by Ultratech Cement was done. The cement was free from hard lumps and it had uniform color i.e., grey with light green shade. Result of the various test performed on cement is presented in **Table 3.2** and **Table 3.3**. All tests were done as per the procedure given in **IS: 8112-1989**.

Table 3.2: Physical properties of cement used

Sr.No	Characteristics	Experimental Value	Standard Values
1	Normal consistency	33%	–
2	Initial setting time	48 min	Not less than 30 min
3	Final setting time	240 min	Not more than 600 min
4	Fineness	4.8 %	–
5	Specific gravity	3.09	–

Table 3.3: Compressive strength of cement used

Sr. No.	Days	Experimental Results in (MPa)
1	3	24.8
2	7	37.5
3	28	46.8

- **Fine Aggregate:** The fine aggregate were procured locally for the experimental work and conformed to grade zone II. As per **IS: 383-1870** sieve analysis was carried out in laboratory. Firstly the aggregate were sieved from 4.75mm sieve to separate out the aggregates having size bigger than 4.75mm in the size and then they were washed for removing dust. The results of sieve analysis and physical properties are shown in **Table**

3.4 and Table 3.5 respectively.

Table 3.4: Sieve analysis result of the fine aggregates used

Sr.No.	IS-Sieve (mm)	Wt. Retained (gm)	%age Retained	%age Passing	Cumulative % retained
1	4.75	40	4	96	4
2	2.36	397	39.7	56.3	43.7
3	1.18	277	27.7	28.6	71.4
4	600 μ	124	12.4	16.2	83.8
5	300 μ	95	9.5	6.7	93.3
6	150 μ	40	4	2.7	97.3
7	Pan	22	2.2		
	Total	1000.00		SUM	393.5
				<i>FM =</i>	3.93

Table 3.5: Physical properties of fine aggregates used

Sr.No	Characteristics	Values
1	Specific gravity	2.67
2	Fineness modulus	3.93
3	Water absorption	0.4%
4	Zone of Grade (based on the percentage passing 600 micron)	Zone II

- **Coarse aggregates:** In this experimental study crushed stone aggregate having size 20 mm and 10mm were used. To remove dust from the aggregate they were washed and dried up to the surface dry condition. The testing was done according to the **IS: 383-1970**. The outcomes of various tests are presented below.

Table 3.6: Sieve analysis results of 20mm coarse aggregates used

Sr. No.	Sieve size	Weight retained(gm)	Percentage retained	Percent Passing	Cumulative percentage retained
1	80	0.00	0.00	100.00	0.00
2	40	0.00	0.00	100.00	0.00
3	20	205.00	4.1	95.9	4.1
4	10	4541.00	90.82	5.08	94.92
5	4.75	239.00	4.78	0.3	99.7
6	Pan	15	0.3	0.00	
	Total	5000.00		SUM	198.72
				<i>FM =</i>	<i>6.98</i>

Table 3.7: Physical properties of 20mm coarse aggregate used

Sr. No.	Characteristics	Value
1	Type	crushed
2	Specific gravity	2.69
3	Water absorption	0.55 %
4	Fineness Modulus	6.98

Table 3.8: Sieve Analysis Result of 10mm Coarse Aggregate used

Sr. No.	Sieve Size	Weight Retained(gm)	Percentage Retained	Percent Passing	Cumulative Percentage Retained
1	12.5	292	5.84	94.16	5.84
2	10	1328	26.56	67.6	32.4
3	4.75	2763	55.26	12.34	87.66
4	2.36	475	9.5	2.68	97.16
5	Pan	134	2.68		
	Total	5000.00		SUM	123.06
				<i>FM =</i>	<i>6.23</i>

Table 3.9: Physical properties of 10mm coarse aggregate used

Sr. No.	Characteristic	Values
1	Type	Crushed
2	Specific Gravity	2.66
3	Water Absorption	0.64 %
4	Fineness Modulus	6.23

- **Water:** For casting of beams clean and fresh tap water was used in this investigation. The water was free from impurities like organic matter, acidic materials, sugar, silt etc. as per Indian Standard.
- **Steel Reinforcement:** Mild steel bars were used in this study as reinforcement. The diameter of the bars were 25mm and length of the bars were 1000mm. 700mm length was embedded in concrete and 150mm on each side was kept exposed to environment so that electrical connections can be made later on. The properties of rebars which were used in casting of reinforced concrete (RC) beams are shown in **Table 3.10**. This data was provided by the manufacturer of steel.

Table 3.10 Properties of Steel Reinforcement used

Size and Type of the Bar	Ultimate Tensile Stress (MPa)	Yield Stress (MPa)	Young's Modulus (GPa)	Percentage Elongation
25 mm, mild-steel	410	240	200	23

- **Epoxy:** The epoxy used in the experiment was manufactured by the Asian Paints Ltd. It was a colorless liquid having very high viscosity. It was applied on the bar with the help of a brush. It takes very less time to get dry and then makes a hard film on the surface of steel. The active ingredient of this epoxy is epichlorohydrin and bisphenol A which gives bisphenol A diglycidyl ethers based epoxy.



Fig.3.2: Epoxy used

- **Paint:** The paint used in the testing was manufactured by Asian Paints Ltd. The paint was of grey color. The specific gravity of paint was 1.08. It was applied with the help of a brush on the steel rod to be used. The paint was mixed with the hardener in the ratio of 4:1(paint/hardener). The pigment in the paint was zinc phosphate, binder in the paint was ethyl propenoate. Two layers of paint was applied on the surface of steel before casting in the concrete specimen.



Fig.3.3: Paint used

- **Inhibitor:** The inhibitor used in the study was **Masterlife CI 220** manufactured by **BASF**. It actively inhibits both anodic and cathodic reactions. The recommended usage of this inhibitor is $5\text{L}/\text{m}^3$ of concrete, irrespective of the severity of the exposure environment. It is added in the concrete while mixing. The active ingredient of this inhibitor is a water-based combination of amines and esters.



Fig.3.4: Inhibitor used

3.4 Preparation of Beams

3.4.1. Preparation and Preconditioning of the Reinforcing Steel Bars

Reinforcement bars are cut in to required length of 1000mm. Then all bars are cleaned with wire brush for the removal of scale if any, present on the bars. Then one bar is coated with paint and one with epoxy layer respectively. Prior to their embedment in concrete, these bars were monitored with Ultrasonic Guided Waves to check for their soundness and health. The bars should be without any kind of inherent or manufacturing defects before casting so that UGW can be propagated later.

3.4.2. Casting of RC beams

The concrete mix is prepared using fine aggregate (river sand having medium size), crushed stone coarse aggregates with a nominal size of 20 mm(60%) and 10 mm(40%) and 43 grade OPC. Indian Standard guidelines are followed to design the mix. Mix design is calculated as 1: 1.41: 2.53. The water/cement ratio is kept as 0.45 and the compressive strength of concrete is 29 MPa after 28 days. In the present study, RC beam specimens were casted in a mould of 150mm X 150mm X 700mm with 700mm of reinforcing bar embedded into concrete and 300mm length exposed to the environment. Firstly oiling of beam mould was done so that easy removal of specimen could be achieved after 24 hours. The initial weight of reinforcing steel bars was measured. After placing bars at their position, pouring of concrete in the mould was done and the vibration was given to the mould for removal of air gap from concrete. After demolding the beam specimens were cured for 28 days in an open tank.

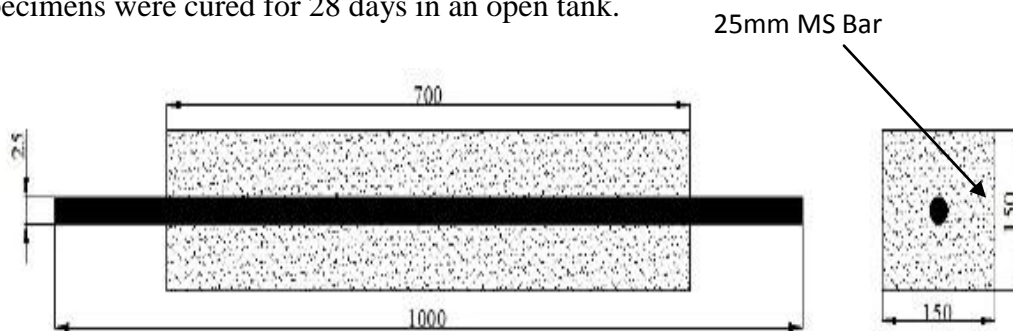


Fig.3.5 Beam specimens

3.4.3. Inducing Corrosion in Concrete

Corrosion is very slow process and hence has to be accelerated to carry out our study. Salts spray, chloride diffusion and impressed current methods are the common methods for introducing accelerated corrosion in RC specimens. Past studies have shown that salt spray method did not prove to be effective in showing visible sign of corrosion even after 100 days. This method was unsuitable due to time constraints also.

The corrosion can also be induced by alternate immersion of specimens in sodium chloride (NaCl) solution and drying of the specimens. But impressed anodic current method is the fastest method to induce the corrosion. Middle 300mm length of beam was subjected to brine solution (3.5% NaCl) dripping and the current is impressed by making the rebar as anode and stainless steel wire mesh wrapped in middle 300mm as cathode.



Fig.3.6: Beam showing arrangement for induced corrosion

In this study, brine solution (3.5% NaCl) is supplied to the beam specimen by continuous dripping to make the beam saturate with solution as shown in **Fig.3.6** For even distribution of NaCl solution, mats are placed on the top of the specimens. The steel bar is used as anode. 300mm wide stainless steel mesh is rolled around the beam and united collectively with the aid of metal ties to make electrically continuous and it is used as the cathode (**Fig. 3.6**). For making electrical connection, the reinforcing steel is extended 150mm on

both sides past the concrete. To accelerate the corrosion, a constant voltage of 30V is applied using a power supply system (Aplab Make, 64V,1 A Current) (Fig 3.7).



Fig. 3.7: Power supply (Aplab, 64V, 1A Current)

3.4.4 Testing

The ultrasonic signals were used for detecting extent and mechanism of corrosion in RC beam by measuring the signals while steel bar is subjected to accelerated induced corrosion. For 30 days acoustic emission monitoring was also done.

3.5. ULTRASONIC GUIDED WAVES INVESTIGATIONS

3.5.1. Specimen and Set-Up Details

Pulse Transmission (PT) testing method is used for guided waves investigation. In this method two piezoelectric transducers are used to transmit and receive the signals respectively. The transducer are placed in direct testing arrangement which generates longitudinal waves **Fig.3.8** shows the setup for guided waves investigation. The digital to analog converter (DAC) digitizes the input and received pulse and is displayed on the display. The signals which are received, appears in the form of Voltage-Time (V-t) graphs. DPR-300 pulse receiver system (**Fig.3.10**) and Karl Deutsch contact transducers (**Fig.3.11**) were used in this ultrasonic study. The actual setup is shown in **Fig.3.9** below.

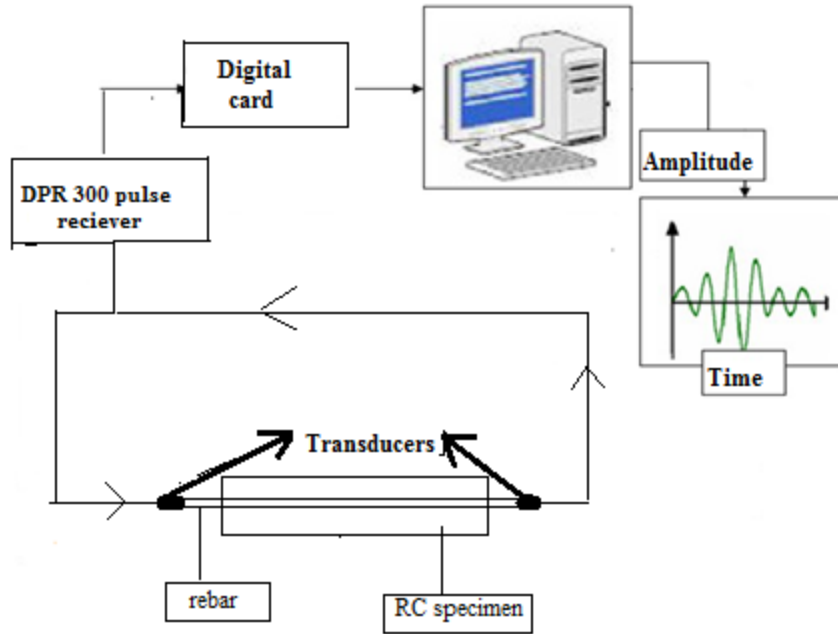


Fig.3.8: Systematic view of ultrasonic monitoring[15]

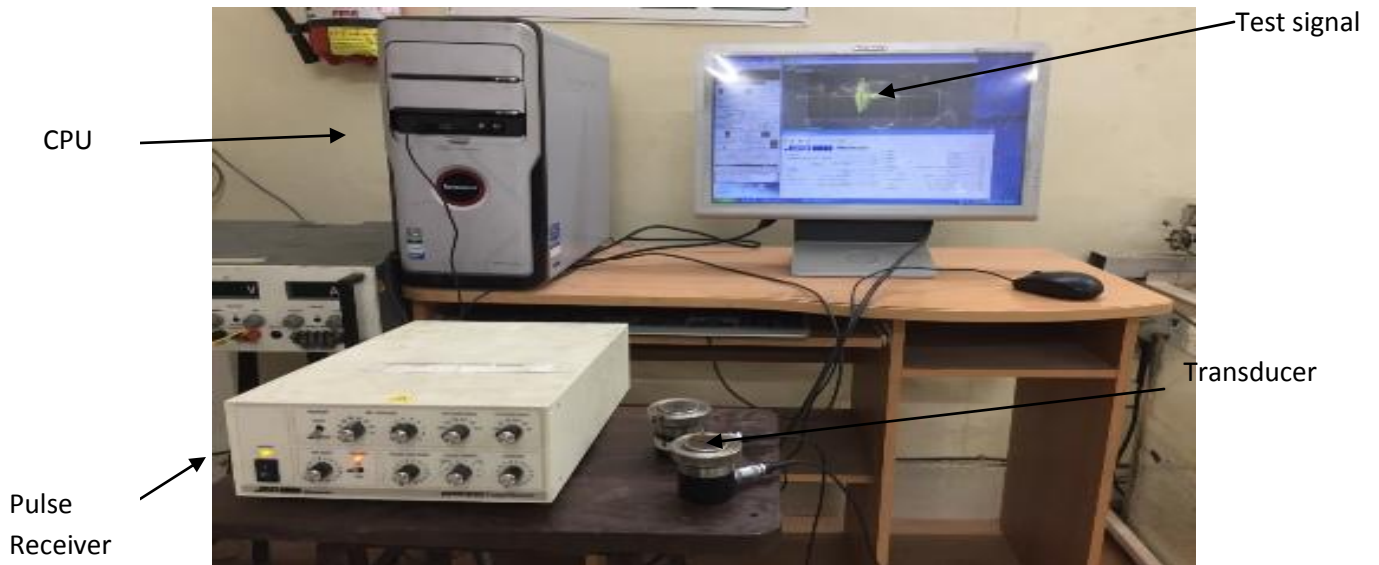


Fig.3.9: Actual Ultrasonic test setup



Fig.3.10: DPR 300



Fig.3.11: Transducers used (Karl Deutsch, 0.1 MHz and 1MHz)

3.5.2 Selection of excitation mode and frequencies

DISPERSE software was used for the selection of suitable test mode and frequencies after analyzing dispersion curves. Mode which can be easily distinguished and have less attenuation are chosen. Generally, modes having less attenuation help in maximizing the inspection range and minimize the effect of dispersion and also minimize the interference due to other modes in received signal.

L(0,1) at 0.1 MHz and L(0,7) at 1MHz was the longitudinal modes which were selected for Ultrasonic investigation [28,29].

L(0,1) mode at 0.1MHz has been recognized as lower frequency, less attenuative, fundamental mode which interrogates the surface modifications in the embedded rebar hence referred as Surface Seeking Mode. This mode picks up the initial delamination of the bar undergoing

corrosion. On the other hand, L(0,7) at 1 MHz is a high frequency, less attenuative mode which is a core sensitive mode and picks up the pitting effect of the corrosion.

Hence, these two particular modes [L(0,1) and L(0,7)] at 0.1MHz and 1 MHz was selected for UGW excitation in 25mm reinforcing bar in concrete using the arrangement shown in **Fig.3.8**.

3.6. ACOUSTIC EMISSION MONITORING

The acoustic emission phenomenon can be described as the propagation of the elastic waves because of discharge of localized internal energy, such as minute fracture in the elastic materials. The sources of acoustic emission (AE) activities are processes like crack formation, plastic deformation and other kind of materials degradation in structures. This monitoring method typically consists of sensor, preamplifier and AE acquisition system and analysis system.

The aim of investigation was to find the effect of corrosion in surrounding concrete using AE technique in RC specimens. UGW interrogates only rebar in concrete whereas AET picks up cracking, spalling and deterioration in surrounding concrete. **Fig.3.12** shows the schematic representation of AE setup.

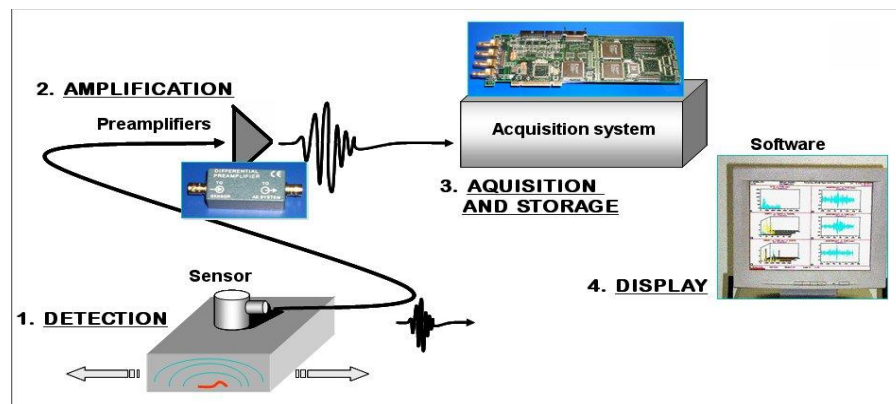


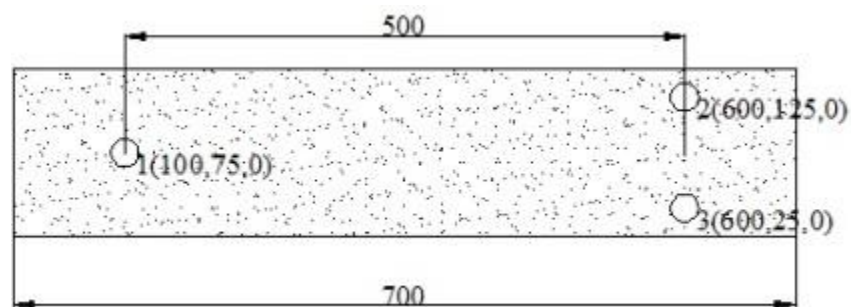
Fig. 3.12 Schematic Representation of AE Setup[15]

In our study, Micro II digital AE system, provided by Physical Acoustics Corporation (PAC) **MISTRAS GROUP** (**Fig.3.13**) was used for AE data acquisition in experimentation.

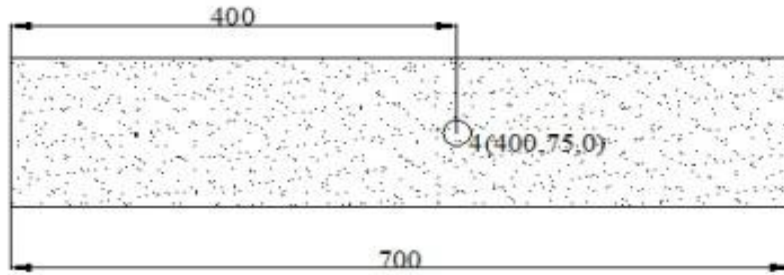


Fig.3.13: Data acquisition set up

For recording the acoustic signals the sensors were positioned on the surface of the structure with the arrangement of sensor placement is shown in **Fig.3.14** The sensor used in the present study for monitoring of corrosion were R3 α (**Fig.3.15**) with specifications (**Table 3.11**). We utilized 4 R3 α Sensors (resonant at 150 KHz) and Preamplifiers with the gain set at 40 db and range of frequency from 20-1200 KHz. 3 sensor were fixed on front face of RC specimens and 1 sensor was mounted on back face of specimens.



(a) Front Face



(b) Back Face

Fig.3.14: Position of Sensors on Beam

Table 3.11: Sensor's specifications

Sensors Specification	R3 α
Range of Operating Frequency	35-100 KHz.
Resonant Frequency	150 KHz
Physical Dimensions	19mm Dia.× 22.4mm Height
Weight	31 Grams
Casing	Stainless Steel



Fig.3.15: R3 α Sensors for acquisition of data

Fig.3.16 shows the preamplifiers used in study.



Fig.3.16: Pre-amplifier

These AE sensors are fixed to the surface with the help of tapes. A film of couplant (grease), is used between the 2 surfaces for effective transmission of AE signals. For AE testing in civil structures the common frequency range remains in between 100 - 300 KHz.

In software control of data acquisition system, a band pass filter of 20-400 KHz was set. For experimental purpose, 45 dB was fixed as threshold value. The experimental setup is presented in **Fig.3.17**.

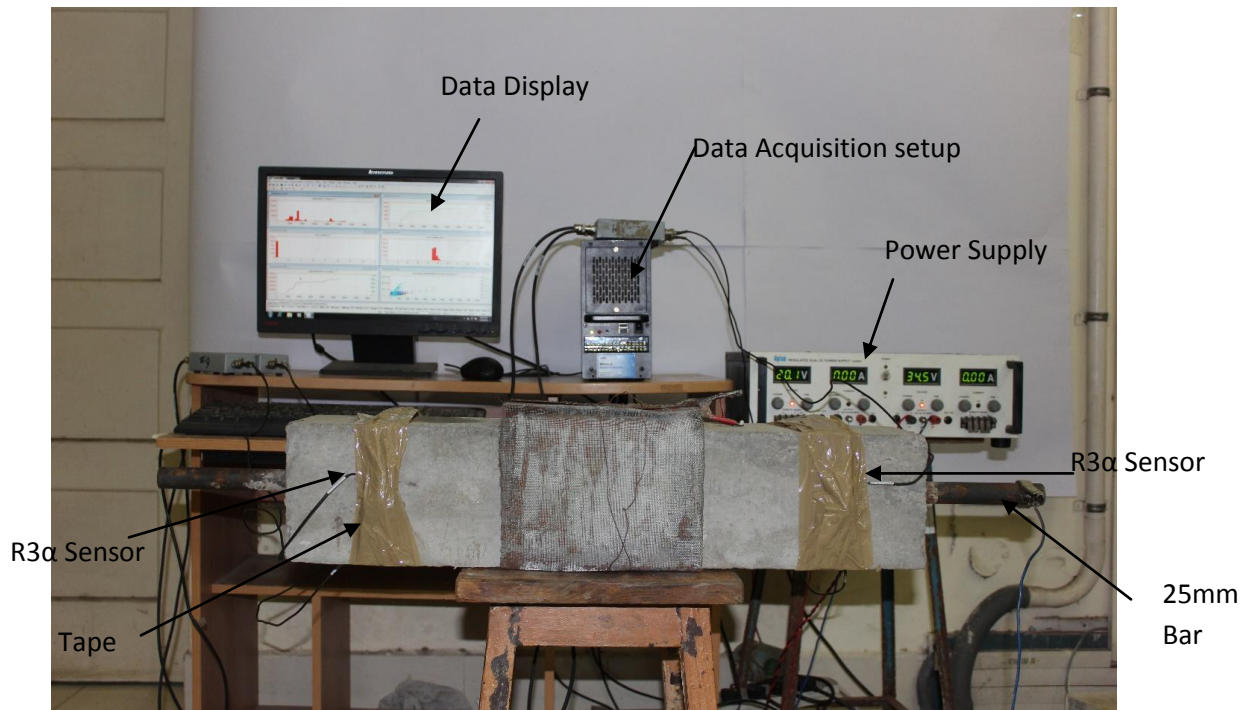


Fig. 3.17: Experiment test set-up used in present study.

These AE sensors can detect any acoustic activity occurring in the specimens. Preamplifiers amplify the signals before they enter into data acquisition system. The data acquisition system processes the data and in the end, displays the data on monitor screen. AE signals were produced by breakage of 0.5mm lead of pencil at chosen points on the plate and on each point pencil lead break tests were performed three times (**Fig.3.18**).



Fig.3.18: Apparatus of Pencil lead break test [1]



Fig.3.19: Pencil break test during study

It was done to assure that sensors were mounted correctly on specimens and they can identify the reflections though their amplitude would be lesser than the signal which is related to the crack. This process includes the sensor's utilization to identify the released strain energy from cracks which are in developing stage. Hence, for health monitoring in field of civil engineering, this technique is widely used.

3.7. CLOSING REMARKS

In present chapter, corrosion monitoring in reinforced concrete (RC) beam test specimens using both UGW technique and AE technique are discussed in detailed. Corrosion monitoring accords clear picture of different modifications in behaviour of structure due to corrosion. Thus, it is established that proper monitoring of structure to find extent of corrosion can help us in determining appropriate measures needed to be taken in primary stages of degradation due to corrosion before it reaches to an alarming level.

4.1 GENERAL

The focus of this work was to investigate the effectiveness of various corrosion protection methods of epoxy coating and paint coating on rebars and the effect of admixed inhibitors in RC beams using advanced NDT and Acoustic Emission Techniques. The variations in Cell-currents were also monitored. Visual Inspection of the corroding beams was done periodically. The results were analyzed and are discussed below:

4.2 VISUAL INSPECTION

The specimens **B1**, **B2**, **B3**, **B4** were subjected to accelerated corrosion and monitored periodically to note the progression of damage on the surface of concrete due to corrosion after 30 days.

(a) Control Specimen B1

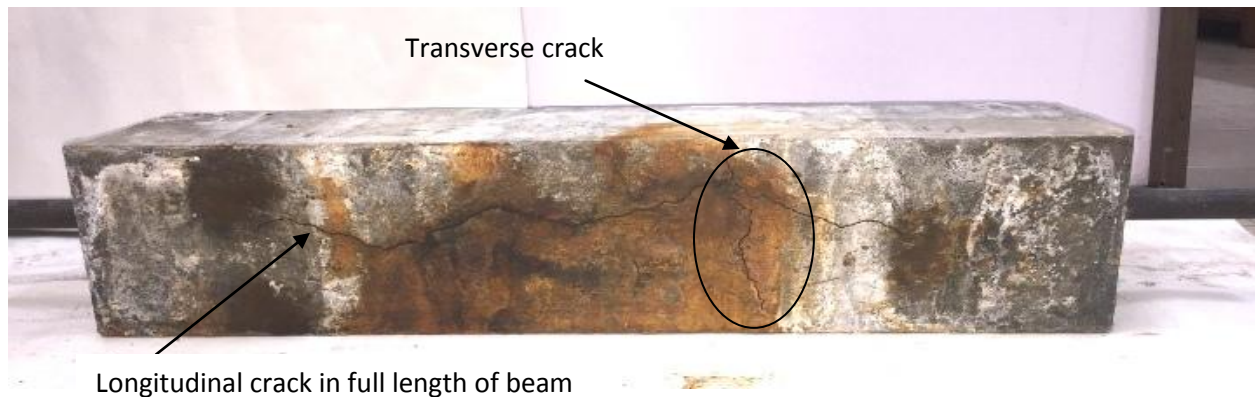


Fig.4.1: Specimen B1

Fig.4.1 shows the control sample corroded for a period of 30 days at a constant voltage of 30 V. The wrapped wire mesh was opened after every 24 hours to study the surface deformation.

It was observed:

- A micro-crack was observed after 4 days of accelerated corrosion in the longitudinal direction.
- A brown colored liquid oozed out of this micro-crack.

- Further the crack was observed to expand in the longitudinal and the transverse direction of the rebar.
- As the corrosion progressed inside the beam, the amount of brown coloured liquid increased thereby widening the cracks on the beam.
- After 30 days of corrosion, a longitudinal crack parallel to the rebar in the full length of beam and a transverse crack is observed.

(b) Epoxy Coated Rebar Specimen B2



Fig.4.2: Specimen B2

Fig.4.2 shows the image of specimen in which the epoxy coating was applied before the casting on steel bar. This specimen was also subjected to an accelerated corrosion of 30 days. It was observed:

- No deterioration was observed visually on the surface of beam.
- Only observation was a white coloured deposition on the surface of beam which was actually the NaCl used to accelerate the corrosion.
- Hence, it proves that epoxy coating on the surface of the rebar was effective.

(c) Paint Coated Rebar Specimen B3



Fig. 4.3: Specimen B3

Fig.4.3 shows the image of specimen containing steel bar protected with paint. The specimen was subjected to an accelerated corrosion for 30 days at 30 V.

- No crack or any other sign of deterioration was observed on the surface of the beam for the entire 30 days.
- Corrosion was observed up to some extent on both sides at the interfaces where the bar enters the concrete
- This again indicates that a simple coat of paint could really block the passage of corrosion into the rebar.

(d) Inhibitor Admixed Specimen B4



Fig. 4.4: Specimen B4

Fig.4.4 shows the image of specimen protected with admixed corrosion inhibitor. The specimen was also subjected to an accelerated corrosion at constant voltage 30 V. During the periodic inspection of the beam, it was observed:

- A small crack was observed after a period of 11 days of accelerated corrosion which in control beam was observed at around 4 days.
- Reddish brown color liquid also oozes out from the micro crack.
- Longitudinal crack and rust product were limited and localized to 200mm length.
- Therefore, it can be concluded that the corrosion inhibitor was effective in delaying corrosion to a greater extent.

Therefore, visual inspection gives an idea about the deterioration of the reinforced concrete beams in very late stage, where it is not of any use. The basic idea is to get, information of initiation of corrosion so that any remedial measure can be adopted before it deteriorate the structure and cause catastrophic damage. Hence it was collaborated with the Cell Current measurement, Acoustic Emission results and Ultrasonic Guided Waves results.

4.3 CELL CURRENT

The RC beam samples were subjected to accelerated corrosion at a constant voltage of 30 V. Corrosion progressions in all the beams was monitored by the cell current values recorded after every 12 hours are presented in Fig.4.5.

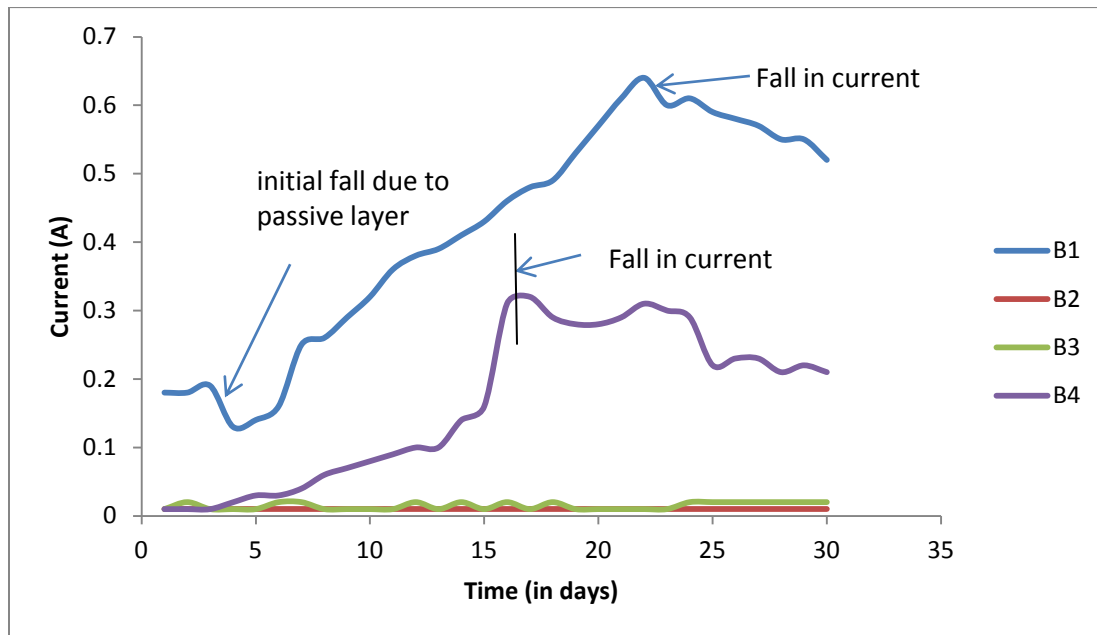


Fig. 4.5: Cell Current of All Beam Specimens

(a) Beam B1

- The values of cell-current are less initially and this could be due to protection provided by the passive layer in concrete.
- Cell-current increased afterwards, indefinitely, indicating the loss of resistance of the RC beam to corrosion. This further indicated that corrosion in rebar progressed continuously for the entire process of corrosion.
- However, after 23 days, the cell-current falls, indicating that most of the corrosion has occurred.
- The Peak Value of Cell Current attained in this case is 0.65 A

(b) Beam B2 and B3

- Beam B2 and B3 shows a very high resistance to the corrosion.

- Beams B2 and B3 did not show any change in the value of the cell-current.
- The values of cell-current for both the specimens ranged between 0.01 to 0.02.
- This indicates that the treatment of rebar with epoxy and paint, prevent the corrosion from initiating itself.
- Hence, epoxy and paint coating on rebar can be an effective measure for impeding the corrosion to a greater extent in actual structures
- Beam B2 and B3 in accelerated corrosion did not show any significant deterioration which is a striking result since it corresponds to many months, years of corrosion impediment in actual structures.

(c) Beam B4

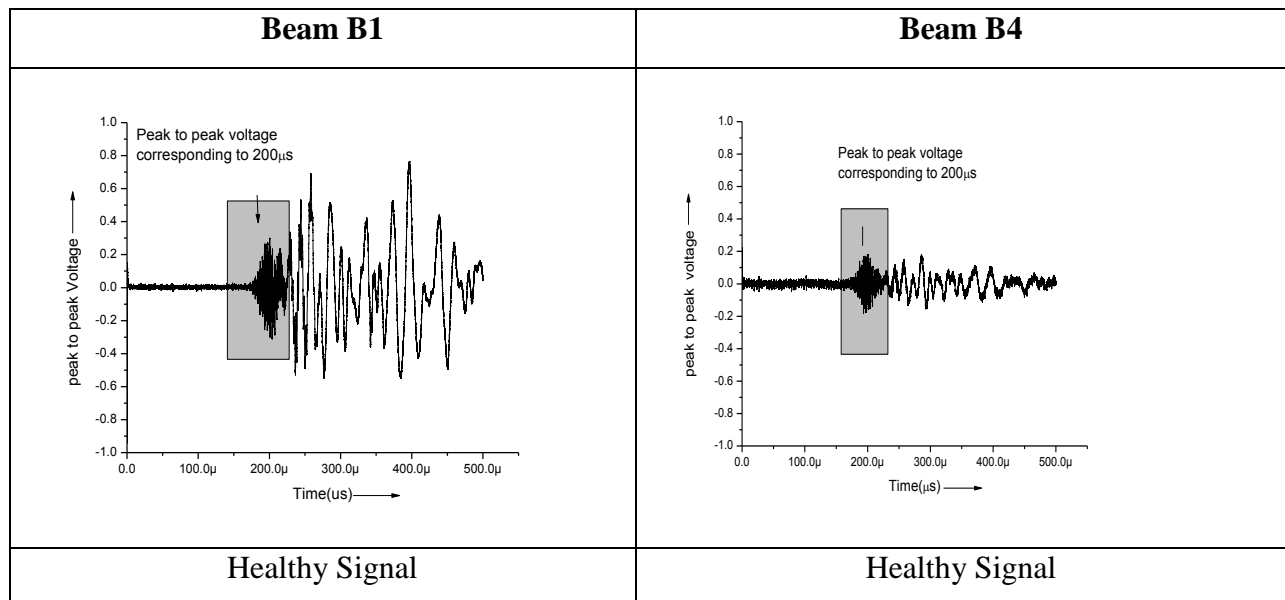
- There is a delay in the rise of the cell-current indicating that the inhibitor was able to prevent the initiation of corrosion for 11 days.
- Up to 11 days, the corrosion inhibitor maintains the alkalinity of concrete due to which the passive layer is protected.
- The cell current values remains very low throughout the duration in comparison to control Beam B1
- Highest recorded cell current value in control Beam B1 is 0.6 A whereas it is almost half 0.3 A in Beam B4.
- Therefore, corrosion inhibitor makes the corrosion very slow and delayed.
- It can be inferred that the rate of corrosion is very much reduced by adding inhibitors, hence, it can be very effective in practical structures where corrosion is not accelerated but slow.

4.4 ULTRASONIC GUIDED WAVE MONITORING

In this experimental study Pulse transmission method is utilized to monitor the different corrosion stages in all RC specimens. Core seeking and surface seeking mode are used to detect various phenomenon of corrosion i.e. delamination and pitting. Surface seeking mode is much suitable for detecting the delamination of rebar covered with the concrete and pitting corrosion can be detected using core seeking modes effectively[28,29] Therefore both the modes are helpful in detecting corrosion pattern in rebar. Results obtained through both these modes are presented in following section.

4.4.1 Surface Seeking Mode L (0, 1) at 0.1 MHz

The mode L(0,1) at 0.1 MHz is a low-frequency mode due to which it remains on the surface of the material and hence known as Surface-seeking mode. As the name suggests, it is only able to detect the discontinuities that appear on the surface of the material. From corrosion point of view, this mode can be successful in detecting, both the delamination and pitting phenomenon of corrosion. In this section, the variation obtained in received signal using L (0, 1) mode at 0.1 MHz is discussed. The signature of control specimen B1 and Inhibitor admixed specimen B4, for different days are shown in **Fig.4.6** using surface seeking mode.



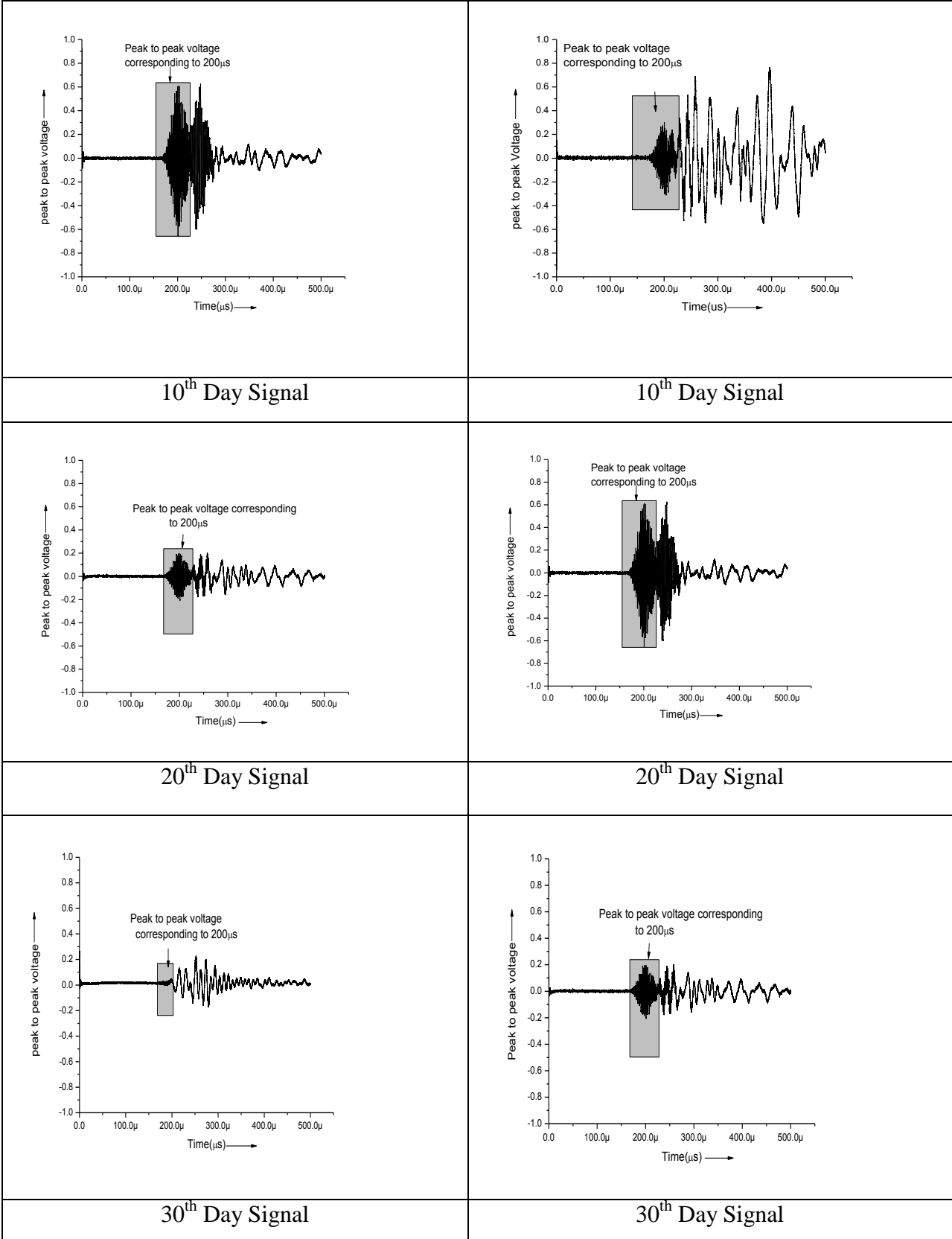


Fig. 4.6: Signature for Specimens B1 and B4 at various Days (L(0,1) mode)

(a) Beam B1

- It can be clearly seen in **Fig.4.7**, that L(0,1) mode at 0.1 MHz is capable to pick up the initial corrosion.
- Up to 9 days the curve of peak to peak voltage ratio rises. This is entirely because of the fact that the layer of rust prevents the signals from leaking into concrete, indicating the delamination phenomenon of corrosion.
- Between 9 to 20 days the corrosion occurs slowly and the signal starts to fall. And the peak to peak voltage ratio curve rises very slowly. This indicates that in this phase the corrosion is shifting from delamination stage to pitting stage.
- After 20 days the fall in signal amplitude totally, indicates the pitting phenomenon, resulting in scattering and loss of the signal amplitude. Peak to peak voltage ratio curve shows a sudden fall.
- The signal vanishes after 30 days.

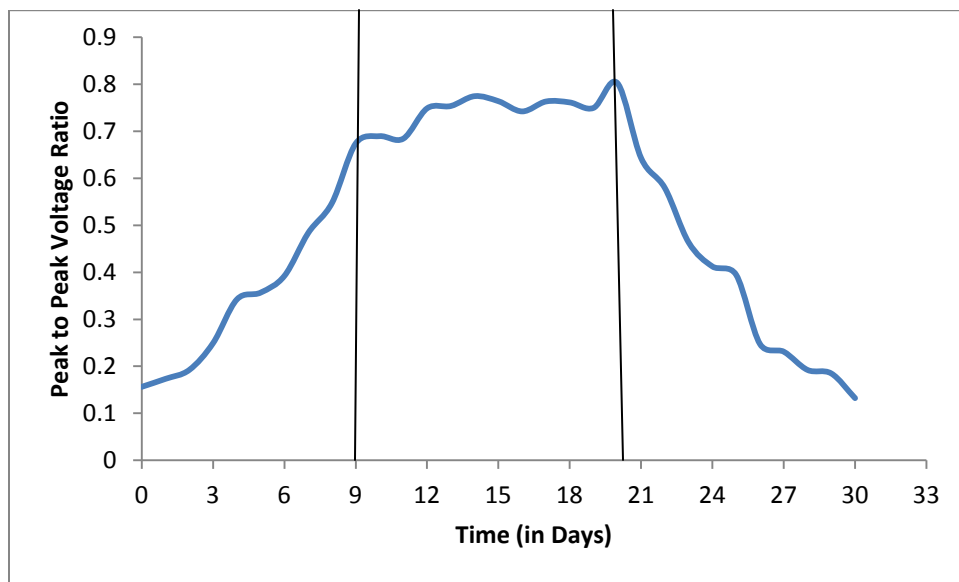


Fig.4.7: Peak to Peak Voltage Ratio of Specimen B1 (L(0,1) mode)

(b) Beam B4

- Peak to Peak voltage ratio curve (**Fig.4.8**) rises very slowly up to first 16 days. This indicates that the delamination stage remains for 16 days.
- From 17 to 25 the curve rises very slowly. This shows the shifting stage of corrosion from delamination to pitting.

- After 25 days onwards the curves starts falling down which indicate the pitting corrosion stage.
- All the processes of delaminations and pitting corrosion are delayed.
- Hence L(0,1) mode picks up the impediment of the corrosion in B4 Beam.

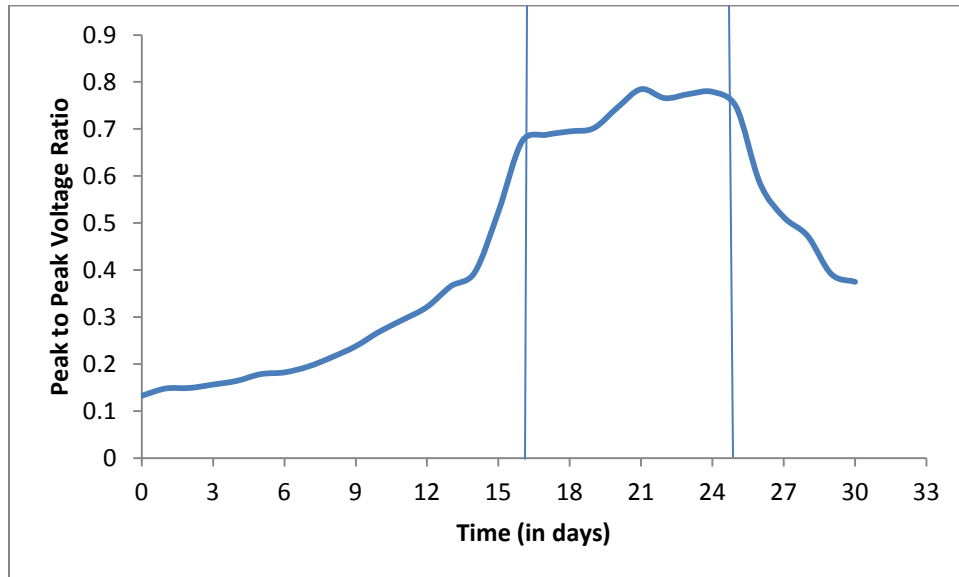
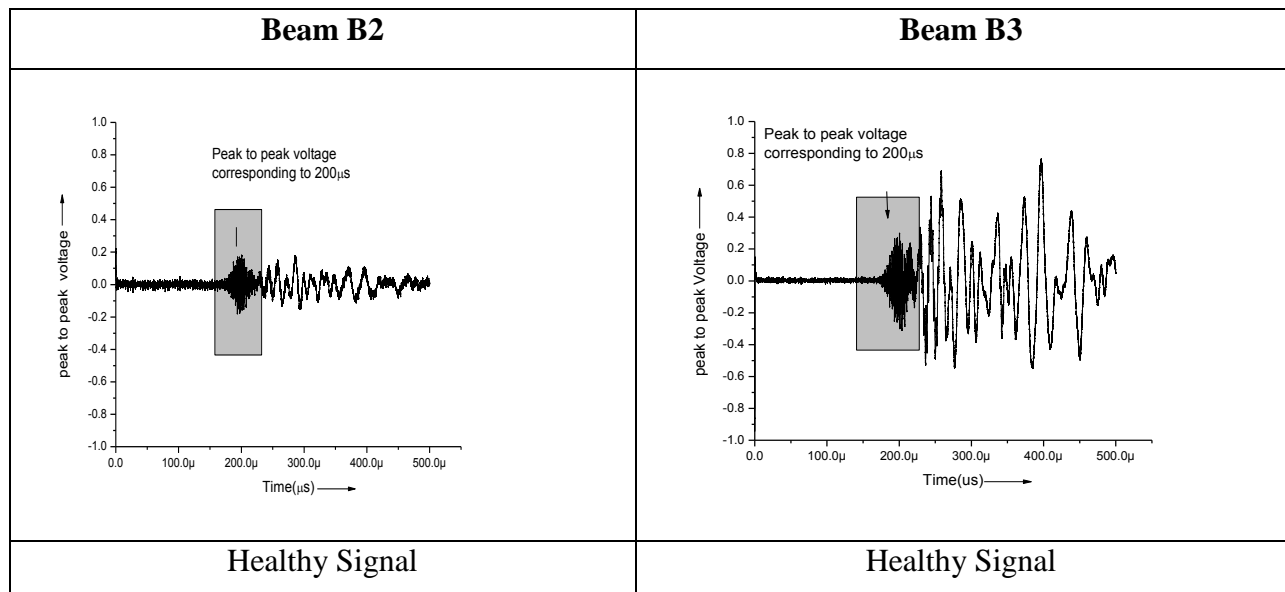


Fig. 4.8: Peak to Peak Voltage Ratio of specimen B4 (L(0,1) mode)

The **Fig. 4.9** shows the signatures of B2 and B3 beams at different days for surface seeking mode.



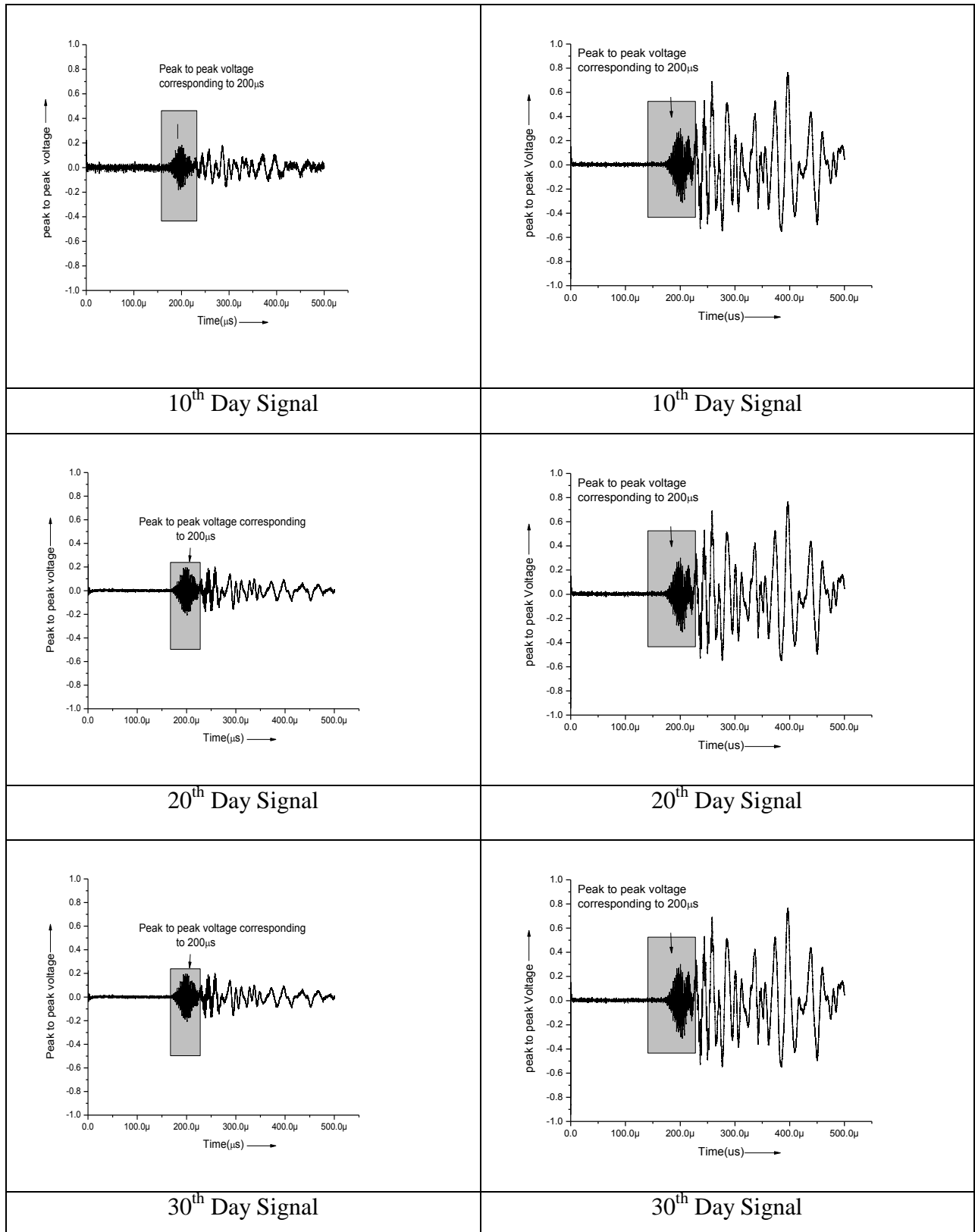


Fig. 4.9: Signatures for specimens B2 and B3 at different days (L(0,1) mode)

(c) Beam B2 and B3

- There is no increase or decrease of signals observed from **Fig.4.10**, pointing towards that no corrosion is initiated or progressed in B2 and B3.
- The peak to peak voltage ratio curves are not showing any increasing or decreasing trend. This implies that throughout the test duration no corrosion occurs in both the beams.
- Both the specimens have very less values of peak to peak voltage ratio.

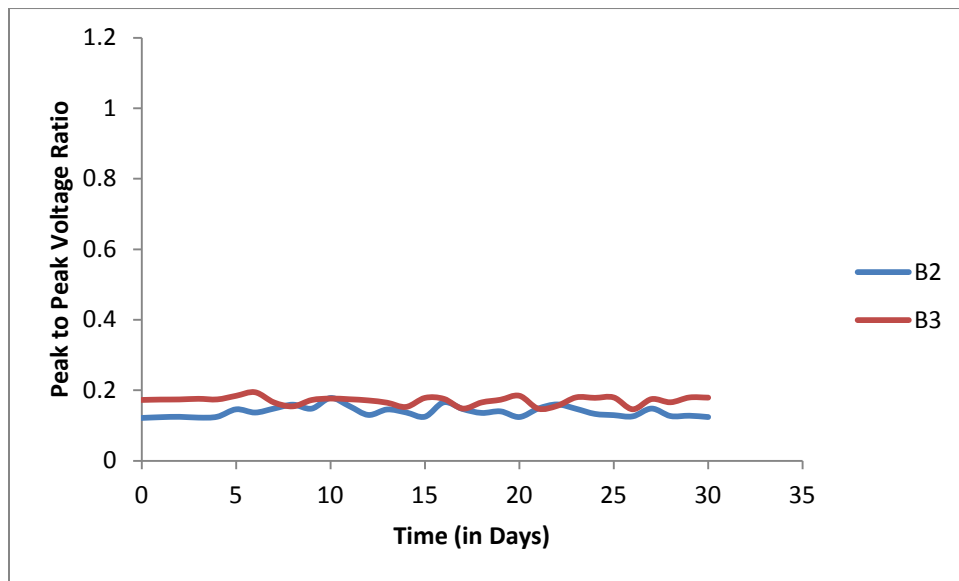


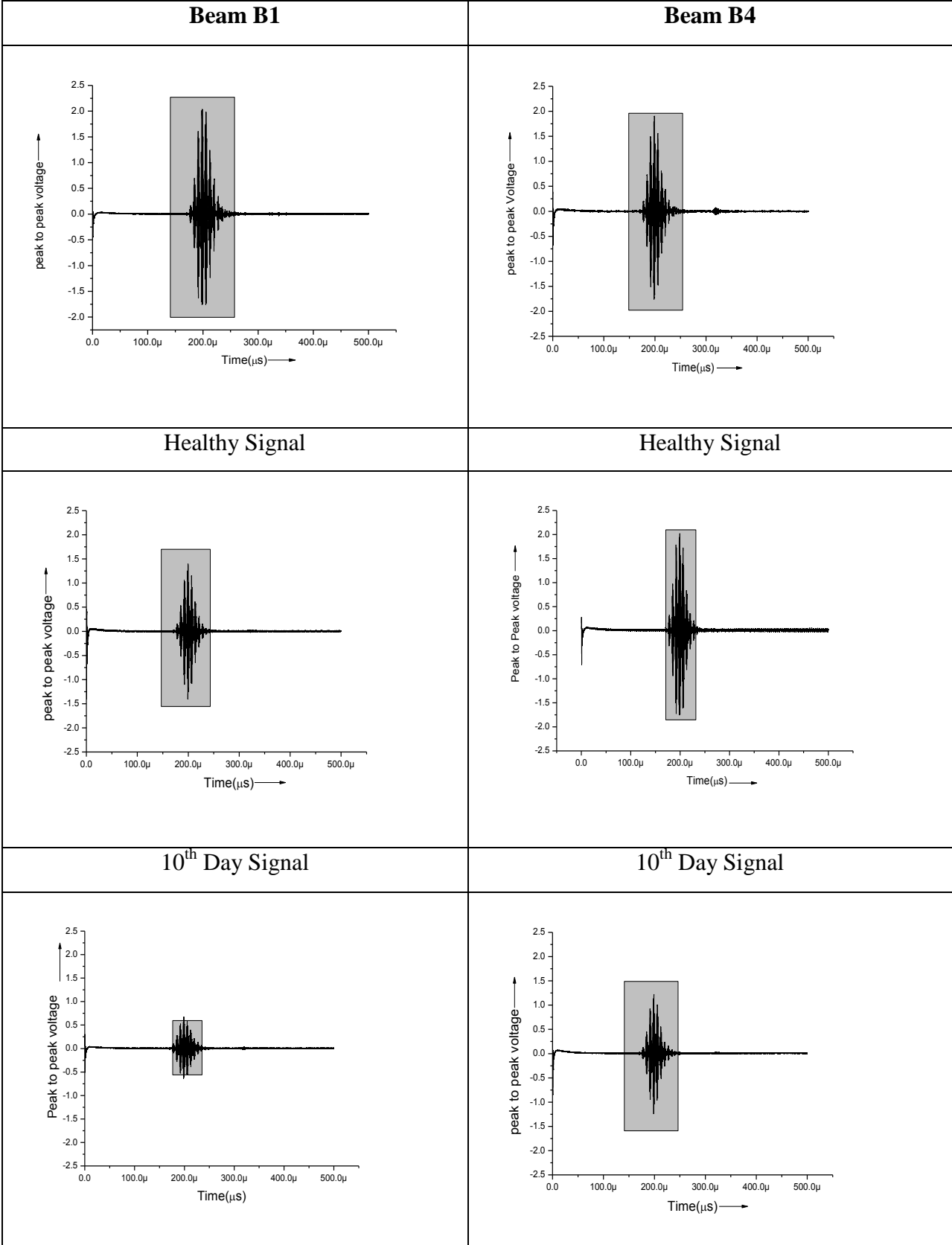
Fig. 4.10: Peak to Peak Voltage Ratio of Specimens B2 and B3 (L(0,1) mode)

4.4.2 Core Seeking Mode L(0,7) at 1 MHz

The mode L(0,7) at 1 MHz, is a high frequency mode, due to which it has tendency to enter into the core of the material and hence , it is known as the core –seeking mode. Because of its nature, it can only detect the deterioration that occurs in the core of the material. Hence, it is very effective in picking up the loss of cross-section and the pitting phenomenon of corrosion.

In this section, the variation in received signal using L(0,7) mode at 1 MHz is discussed. The signature at various days is shown in this section to study the trend of corrosion variation in detail.

The signature for specimens B1 and B4 are shown in **Fig.4.11** for core seeking mode.



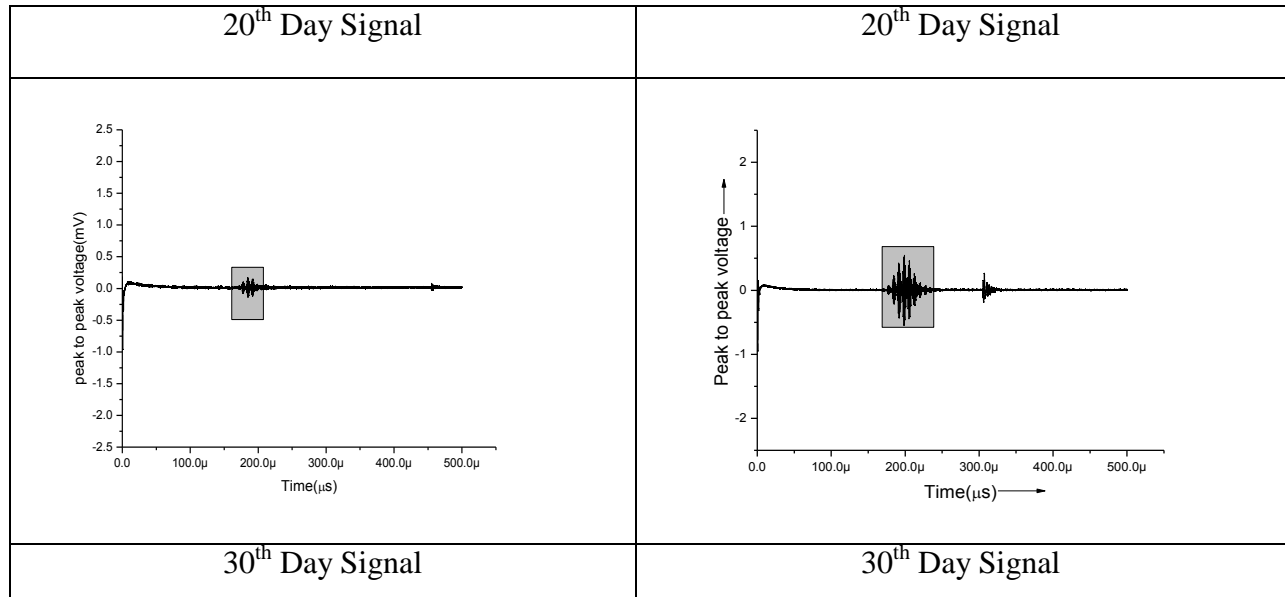


Fig. 4.11: Signatures for Specimens B1 and B4 at various days (L(0,7) mode)

(a) Beam B1

- No change in the curve (**Fig.4.12**) occurs up to 4 days which shows that initially up to 4 days no corrosion occurs. This is essentially because of the delamination taking place that core-seeking mode cannot pick up.
- After 4 days the signal starts to drop which indicate the commencement of pitting corrosion and core seeking mode picked this up from the very moment it started.
- The signal continues to drop for the entire duration of test program once initiated.
- However, the surface seeking mode was able to pick up pitting only after delamination was completed i.e., in the later stages of corrosion exposure.

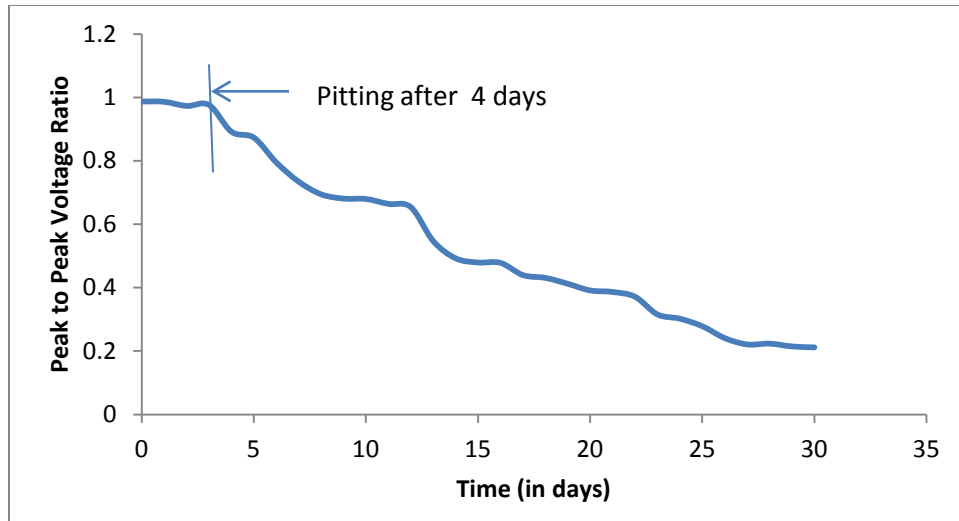


Fig.4.12: Peak to Peak Voltage Ratio of Specimen B1 (L (0,7) mode)

(b) Beam B4

- No change is observed till 15 days (**Fig.4.13**) during which delamination occurs. This mode is sensitive to changes in core only that is why it cannot pick up the changes occurring on the surface due to delamination.
- After 15 days the transition phase comes which continues up to 25 days. Between 15-25 days the corrosion occurs very slowly hence, signals falls slowly.
- After 25 days the pitting corrosion starts and signal falls for the entire duration of the experiment.
- All the processes of delamination and pitting are delayed using inhibitor as protective measures. Therefore, L(0,7) mode easily picks up the impediment of corrosion in B4 Beam.

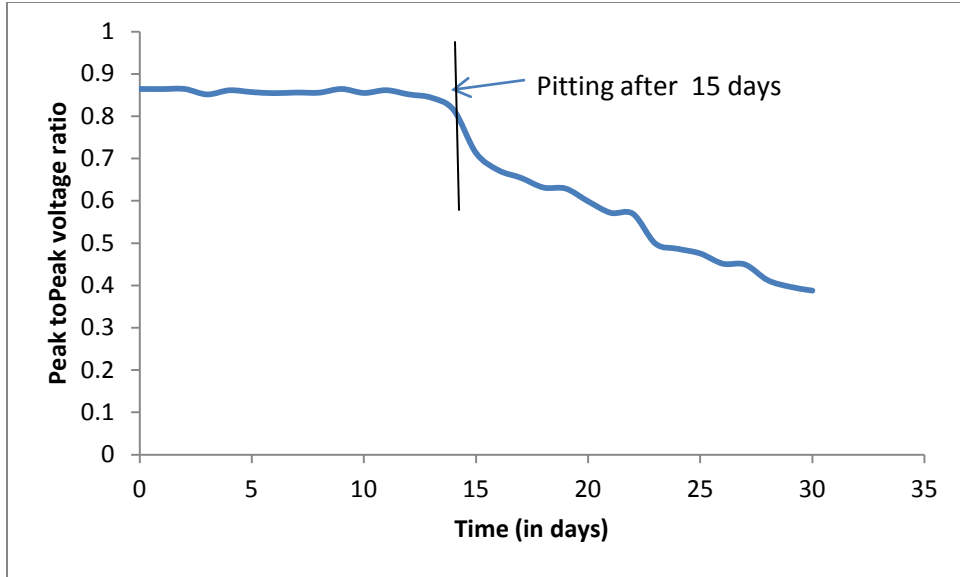
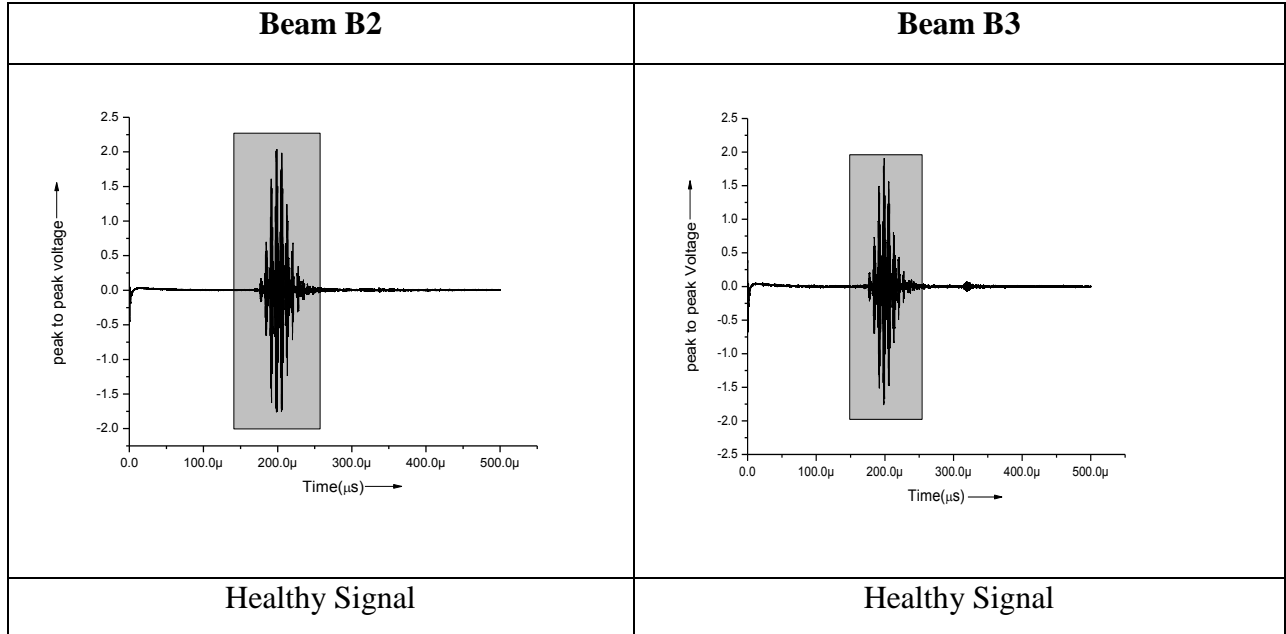


Fig.4.13: Peak to Peak Voltage Ratio of Specimen B4 (L(0,7) mode)

The Fig. 4.14 shows the signatures of B2 and B3 beams at different days in Core Seeking Mode.



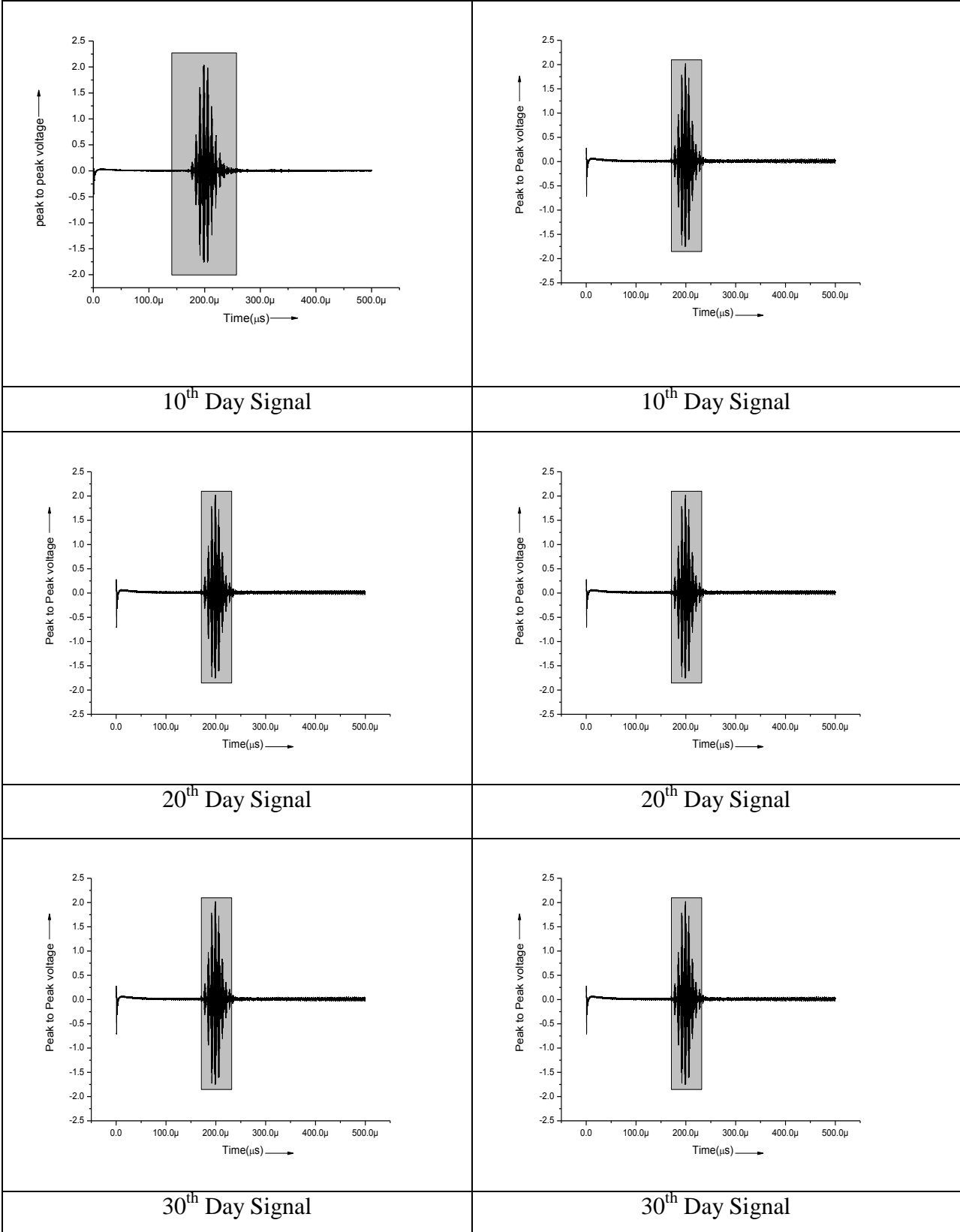


Fig. 4.14: Signatures for specimens B2 and B3 at different days (L(0,7) mode)

(c) Beam B2 and B3

- The curves in **Fig.4.15** follow a straight pattern in case of B2 and B3 beams.
- No change in the signal was observed in both specimens throughout the duration of experiment.
- This indicates that both epoxy and paint are very good protection measure against corrosion.
- Hence core-seeking mode easily picks up the impediment of corrosion in both these beams from very beginning.

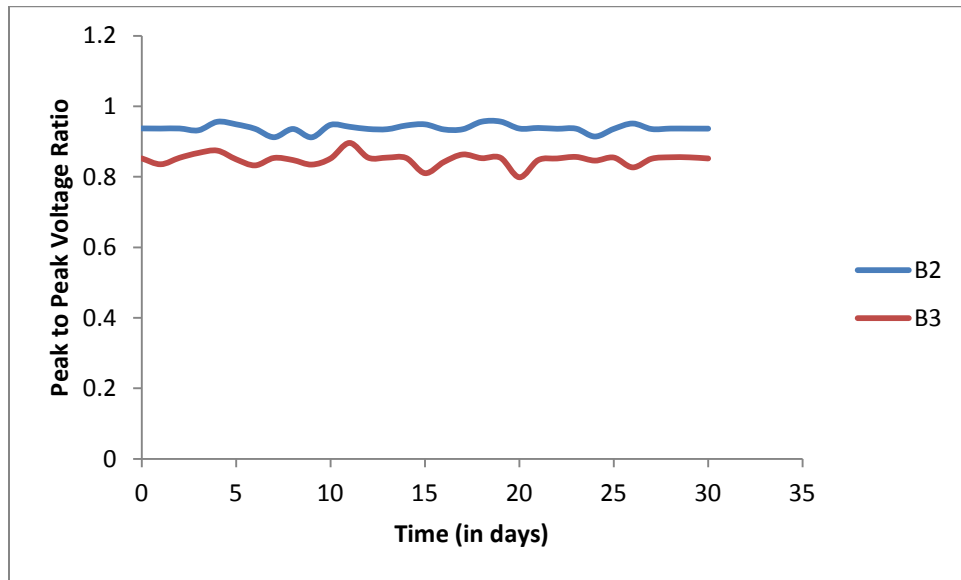


Fig. 4.15: Peak to Peak Voltage Ratio of Specimen B2 and B3 (L(0,7) mode)

4.5 ACOUSTIC EMISSION TESTING RESULTS

Another elastic wave based technique “AET” was also used to monitor corrosion onset and its further progression in control RC beams and beams protected with epoxy, paint and corrosion inhibitor B1, B2, B3, B4. Four acoustic emission sensors were used to record the damage induced due to corrosion in RC beams. Acoustic emission data was recorded for the entire duration of experiment i.e. 30 days.

Acoustic emission data is further studied in contrast with Melchers model of corrosion loss [41] The model divides the entire corrosion process into 4 phases. During the first phase, the passive layer is considered to be broken and the ignition of corrosion takes place. This is succeeded by

the development of a layer of rust around the rebar as a result of corrosion. During the second phase, the layer of rust prevents the excess air, water and oxygen from being in contact with the steel bar. Therefore, in this phase not much corrosion activity takes place and hence this phase is called as ‘Calm phase’. The third phase is accompanied by a very active corrosion process. This is probably due to the reason that layer of rust developed around the rebar depletes and the supply of oxygen, water and air increases greatly around the rebar, thereby accelerating the corrosion process. Finally in the fourth phase, not much corrosion activity is observed, as most of the corrosion has taken place.

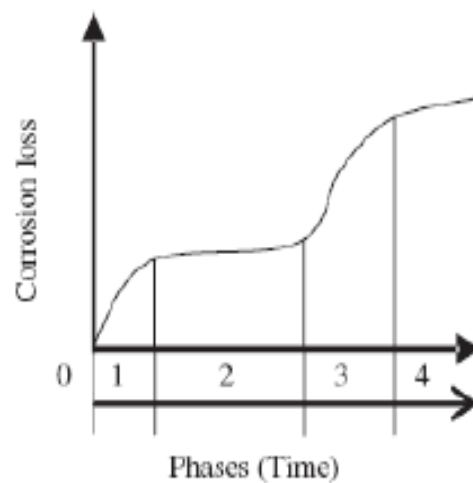


Fig.4.16: Melcher Model of Corrosion Loss[41]

AE analysis can be done in two ways: (1) AE parametric analysis and (2) AE intensity analysis. In this study we have done both of them to investigate the efficacy of AE to pick up the corrosion onset, and progression in RC beams and also to quantify the extent of damage in RC beams. Two AE parameters i.e. AE hits and Amplitude of AE hits are studied to investigate the corrosion process. For intensity analysis, Cumulative Signal Strength is studied to quantify the damage.

4.5.1 CUMULATIVE AE HITS:

(a) Beam B1

Fig.4.17 shows the plot of cumulative AE hits versus time for control specimen B1 subjected to an accelerated corrosion at a constant voltage rate of 30 V. It can be clearly seen that the AE hits

were recorded immediately after the corrosion was started. This very well explains the capability of AET to pick up the corrosion process in RC structure in very early stages.

- It can be seen that AE hits increased for a period of first 9 days. This can be regarded as the beginning of corrosion and is analogous to the 'Phase 1' of the phenomenological model of corrosion loss.
- Afterwards, the number of recorded AE hits reduced and therefore, the slope of the curve became much gradual up to 18 days. This further explains that because of the development of rust around the bar, blocks the entry of water and oxygen, thereby blocking the corrosion process to proceed. Therefore, this phase is termed as '**Minor Cracking**' Phase or Calm Phase.
- After this, the slope of cumulative AE hits increased greatly from 18 to 22 days. This could be attributed to the fact that the layer of rust must have depleted and therefore, in the presence of surplus oxygen and water, the process of corrosion accelerates much faster. During this phase, most of the corrosion loss occurs and therefore, the resulting spalling of concrete is more, during this period. This is known as '**Major Cracking**' Phase or Phase 3.
- After Micro Cracking Phase, very less number of AE hits were recorded i.e. the slope of cumulative AE hits is constant after 22 days to entire duration of experiment. This is termed as '**Low Activity**' Phase or Phase 4. This is essentially due to the fact that most of the corrosion process has occurred in the Phase 3 or Micro Cracking Phase.
- From the changes in the slope of the AE hits v/s time curve, the various effects of micro and macro cracking are picked up. Hence AET has the potential to pick up the effect of corrosion in rebar on the surrounding concrete very effectively

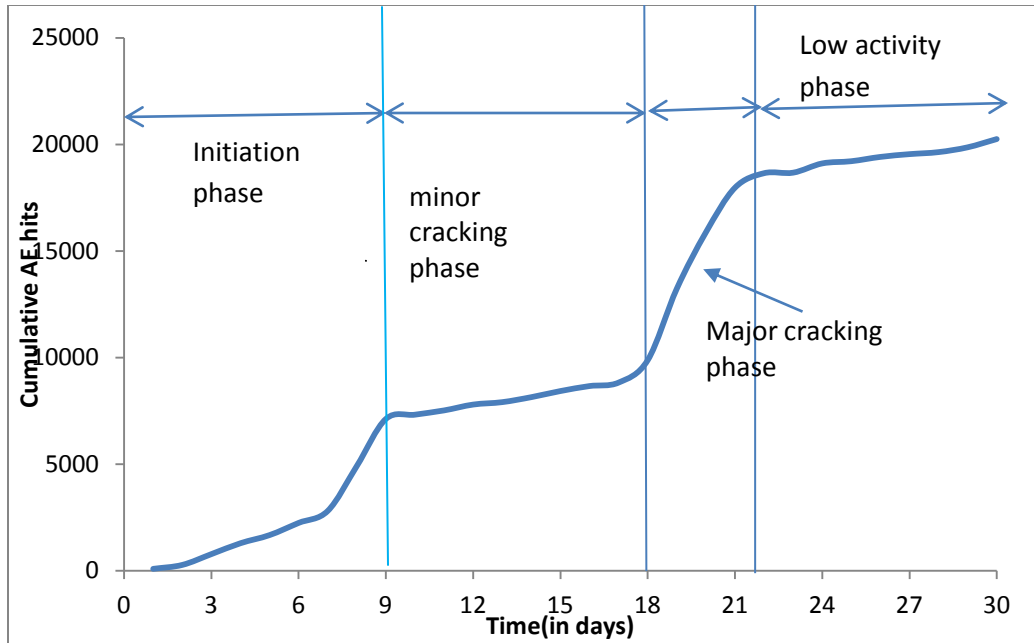


Fig.4.17: Cumulative AE hits of Beam B1

(b) Beam B2 and B3

- The cumulative AE hits plot (**Fig.4.18** and **Fig.4.19**) for the specimens B2 (epoxy coated) and B3 (paint coated) did not experience much change in gradient pointing towards no acoustic activity due to crack development in the epoxy and paint protected rebar.
- The number of hits that were recorded was even far lesser, around 3000 in comparison to 20000 in B1. This further indicates that there was almost no activity inside the beam during the entire duration of the experiment.
- This implies that epoxy and paint on the rebar in concrete were quite successful in preventing the RC beams from corroding.
- Hence, it points towards the effectiveness of coating of epoxy or layer of paint on rebar which can altogether stop the corrosion from intensity in actual RC structures.

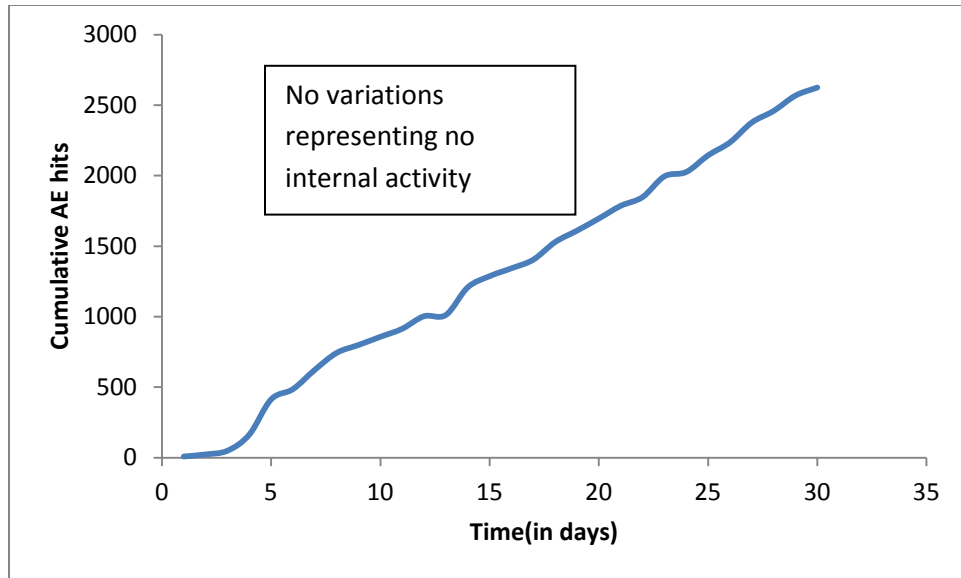


Fig.4.18: Cumulative AE hits of Beam B2

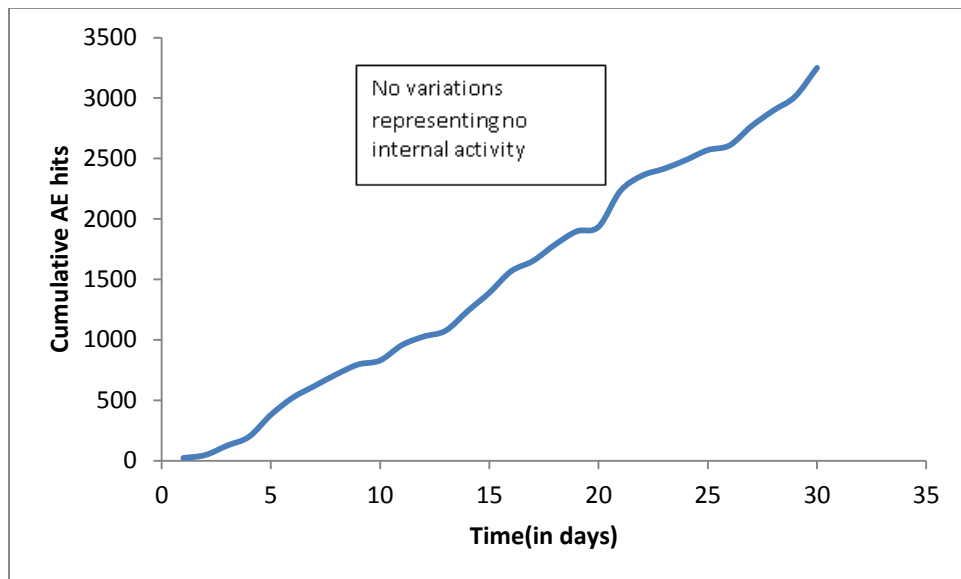


Fig.4.19: Cumulative AE hits of Beam B3

(c) Beam B4 (Inhibitor Admixed Beam)

- Very less number of hits was recorded during the initial stage of corrosion up to 15 days. And the gradient of the AE hits curve changes very slowly. This phase is also known as **‘Initiation Phase’**. A very low activity occurs during this phase due to corrosion.

- Between 15-22 days, the change in curve is also gradual. And this phase represents the ‘**Minor Cracking**’ phase. During this phase minor cracking in the beam is noted down due to corrosion.
- After 22 days to entire duration of experiment, the curve rises sharply. It indicates the ‘**Major Cracking**’ phase. During this phase most of the corrosion loss occurs.
- No ‘**Low Activity**’ phase occurred in the Beam during experimentation.
- This implies that corrosion inhibitor was successful in delaying the initiation and progression of corrosion and AET has the potential to pick up the impediment of corrosion.

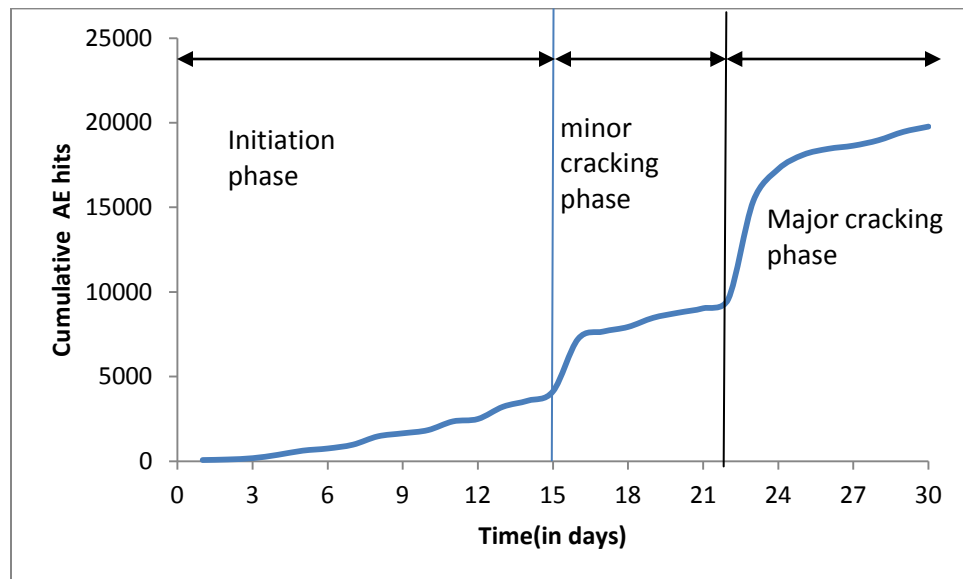


Fig.4.20: Cumulative AE hits of specimen B4

4.5.2 AMPLITUDE OF AE HITS

The amplitude of AE hit represents the magnitude of AE hit or the nature of the crack (whether the crack is major or minor).

(a) Beam B1

- The **Fig.4.21** clearly indicates that the amplitude of AE hits varied with corrosion exposure.
- During the initial stage (up to 9 days), very low values of amplitude were recorded ranging from 45-60 dB. This is during the same period when the rust is developed around

the bar and is regarded as the initiation phase in the Melchers model. Due to the development of rust around the rebar, there is a development of tensile stresses in the concrete, which are further recorded by the AE sensors as micro-cracks.

- After this period, the amplitude of AE hits that were recorded increased in their absolute values ranging from 45-75 dB up to 18 days. This was essentially due to increasing number of micro-cracks resulting in higher stress wave of higher amplitudes. It is to be noted that during this period, cumulative AE hits plot did not show much variation where amplitude of AE hits totally indicate that damage is getting severe with increasing corrosion exposure.
- Further, the value of amplitude of AE hits increased drastically ranging from 45 to 100 dB from 18 to 22 days. This further indicated that the micro-cracks have turned into macro-cracks leading to a combination of tensile and shear stress in the RC beam specimen.
- During the last stage of corrosion exposure, it is observed that lesser number of hits was recorded but the values of amplitude were mostly high ranging from 45 to 100 dB after 22 days to entire duration of experiment. This further indicates that from stage 3 onwards, most of the cracking is in the form of macro cracks i.e. the major damage due to corrosion occurs during this period.

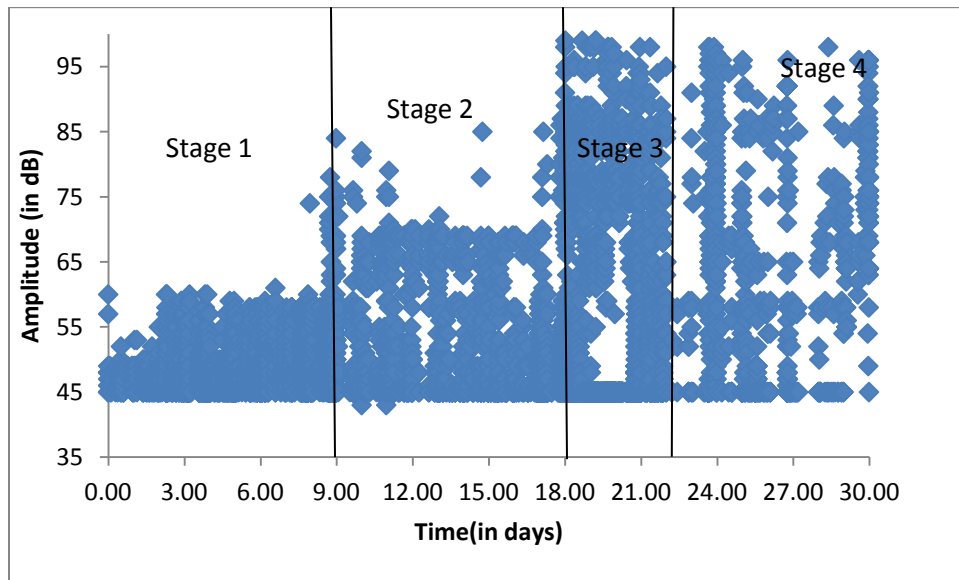


Fig.4.21: Amplitude variation of Specimen B1

(b) Beam B2 and B3

- **Fig. 4.22** and **4.23** shows the amplitude v/s time plot of specimens having rebar coated with epoxy (B2) and paint (B3) respectively.
- Most of the hits that were recorded ranged between 45 dB to 50 dB and therefore, it indicates that no cracking or any other damage is occurring in these 2 beams due to accelerated corrosion.
- This plot in combination with AE hits signify that no damage was observed in these two beam specimens and thus, it can be inferred that no corrosion activity was initiated even after 30 days of accelerated corrosion.
- This implies that both epoxy and paints are quite effective in impeding the corrosion inhibition.

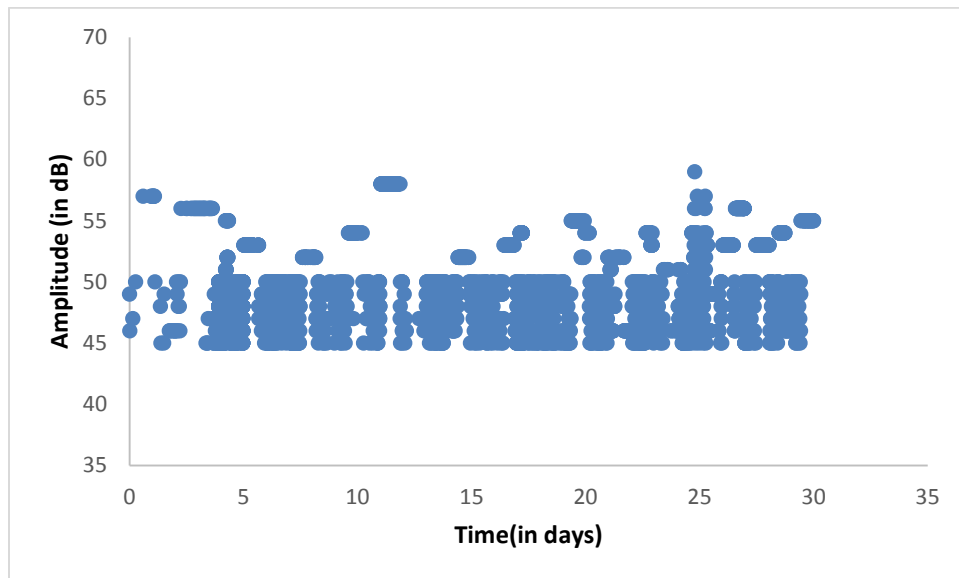


Fig.4.22: Amplitude variation of Specimen B2

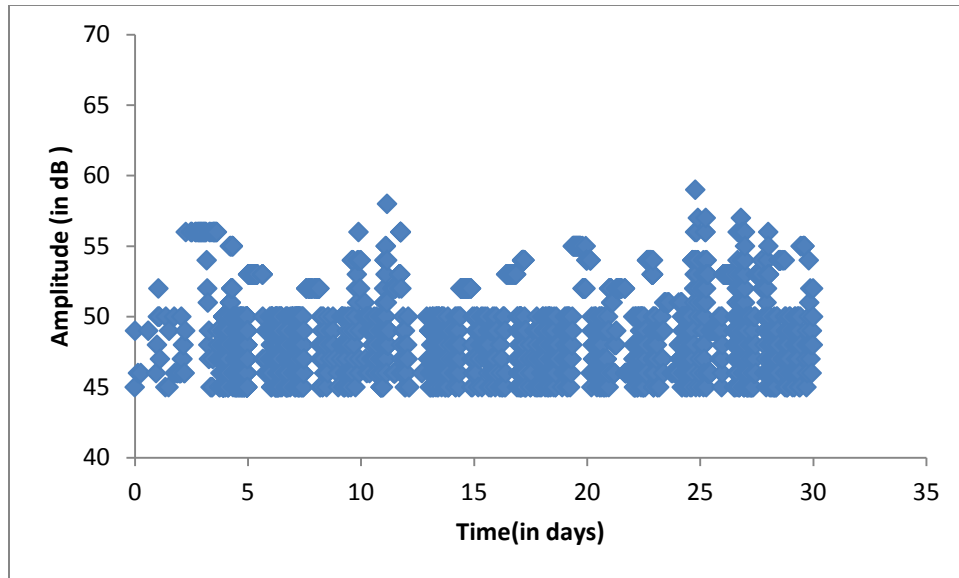


Fig.4.23: Amplitude variation of Specimen B3

(c) Beam B4

- **Fig.4.24** shows that very low amplitude ranging from 45 to 55 dB was observed for the first 15 days of accelerated corrosion. This further indicates that very less or no corrosion activity during the initial stages of corrosion exposure.
- But eventually, the amplitude values started rising and reached up to 70 dB up to 22th day of corrosion exposure. This further implies that the corrosion agents such as water and oxygen destroyed the combined protective layer offer by the corrosion inhibitor and the pseudo passive layer and the corrosion has begun and it corresponds to second stage.
- However, after second stage, the values of amplitude increased ranging between 45 to 100 dB indicating severe damage as most of the macro cracking took place during this stage.
- This implies that corrosion inhibitor was successful in delaying the initiation and progression of corrosion and AET has the potential to pick up the impediment of corrosion.

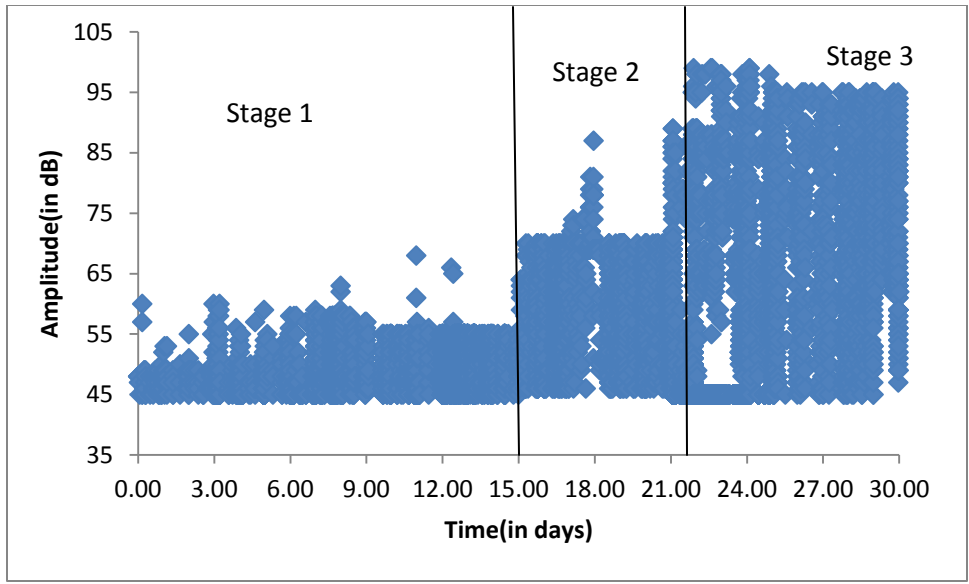


Fig.4.24: Amplitude variation of Specimen B4

4.5.3 CUMULATIVE SIGNAL STRENGTH

Another parameter mostly used to quantify the damage is cumulative signal strength. It generally represents the energy released by a crack inside the material. This parameter relates both amplitude and duration of AE hits. The formation of knee in the curve basically represents excessive release in energy or the severe damage for a CSS curve.

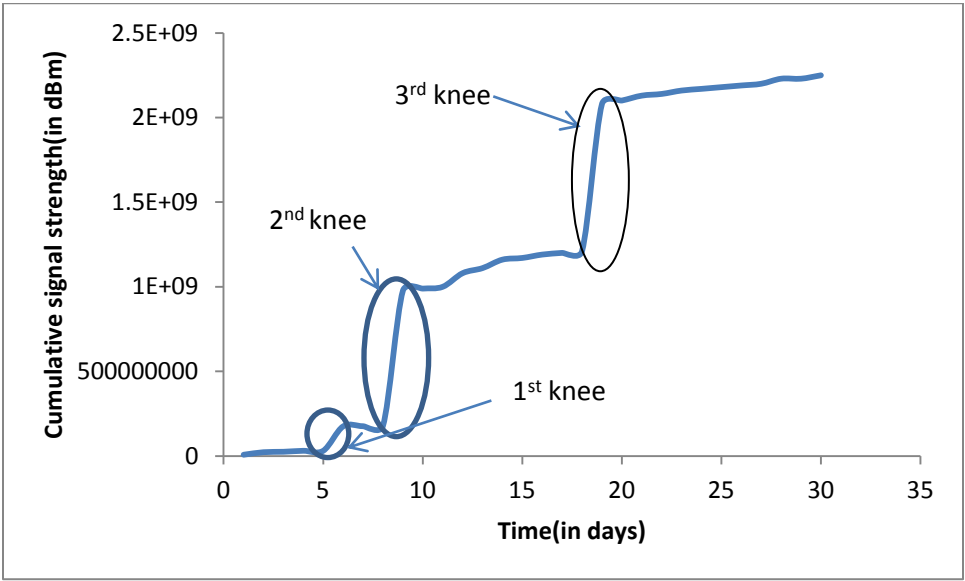


Fig.4.25: Variation of CSS of Specimen B1

(a) Beam B1

- It can be clearly observed from **Fig.4.25** that three knees are observed at 5th, 9th and 18th day of corrosion exposure. However, the height of knee varied as in the knee observed at 5th day was smallest, knee observed at 9th day was of the medium height and the knee observed at the 18th day has maximum height.
- The three different knees could be related to the severity of damage. The knee observed at the 5th day of corrosion exposure corresponds to the micro damage and it can also be confirmed by the fact that this period is in the initial stages of corrosion.
- And from the plot amplitude of AE hits wherein the values of recorded amplitude were very less ranging between 45 to 55 dB, it can be confirmed that this spike is due to the development of the micro cracks inside the RC beam specimen.
- The knee observed at the 9th day of corrosion exposure, further indicates the intensity of micro-cracking and therefore, the corrosion induced damage has increased greatly. This is in confirmation with the plot of AE amplitude where after this 9th day, the values of amplitude increased up to 75dB indicating the transition of micro-cracks to macro-cracks.
- Finally, the third knee observed at the 18th day indicates the major damage due to corrosion. This is also in confirmation with the corrosion model, phase 3, wherein it is observed that most of the damage has occurred during this period only. Also the values of AE amplitudes are highest during this period itself therefore reinforcing the fact that the spike in CSS curve is because of the macro-damage occurred inside the RC beam specimen.

(b) Beam B2 and B3

- From **Fig.4.26** and **Fig.4.27**, there is no spike in the CSS curve was observed for the specimens in which rebar is coated with epoxy and the paint.
- The value of CSS in case of B2 and B3 is very low in comparison to the B1.
- As there is no corrosion in these two beams which means no cracks is formed, therefore no energy is released. Hence, CSS values are less.

- It can be inferred that no damage was induced in concrete due to corrosion exposure. This is also in coherence with the results obtained from the AE hits and AE amplitude.
- It implies that both epoxy and paint are very effective remedial measure against corrosion, and AET has the potential to pick up the impediment to corrosion.

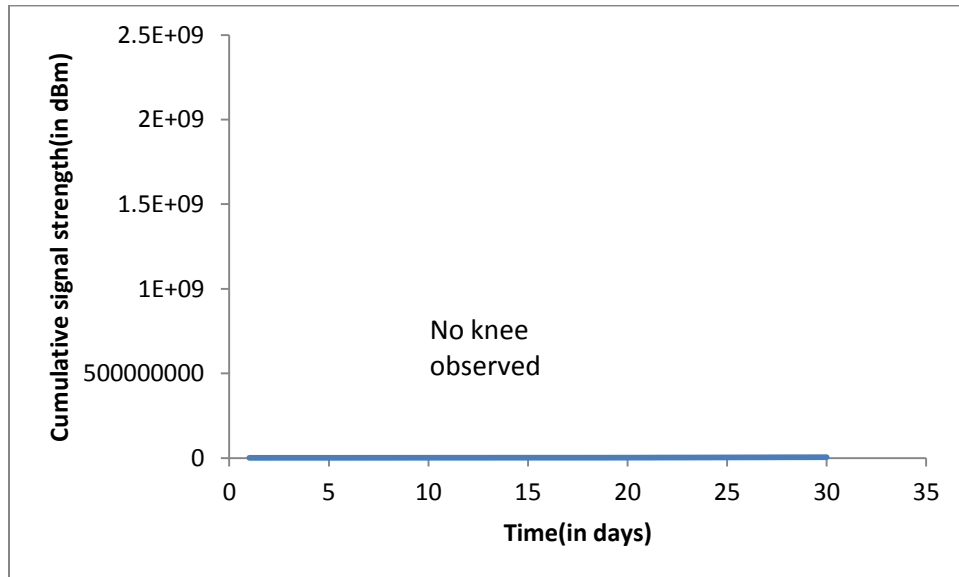


Fig.4.26: Variation of CSS of Specimen B2

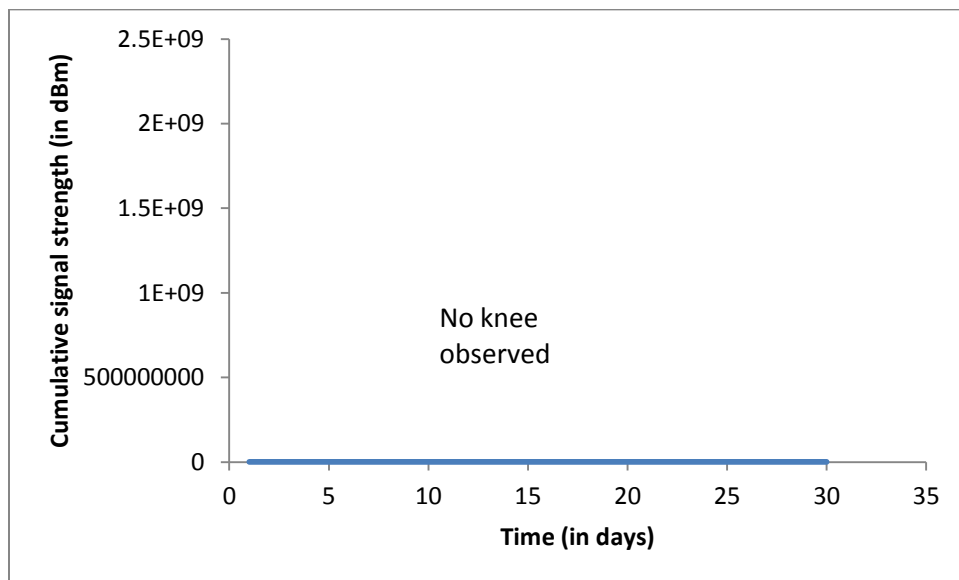


Fig.4.27: Variation of CSS of Specimen B3

(c) Beam B4

- Two spikes are observed in the CSS v/s time plot (**Fig.4.28**).
- The first spike which is relatively of shorter height corresponds to the initiation of corrosion i.e., the development of micro-cracks inside the concrete. However, it can be observed that the first spike was observed at the 15th day of corrosion exposure.
- This further signifies the delay in the initiation of corrosion activity and therefore, the corrosion inhibitor proves to be effective in delaying the onset of corrosion activity.
- The second spike was observed at 25th day of corrosion exposure indicating severe macro damage due to the development of macro cracks in concrete. This is further confirmed by higher values of recorded AE amplitude ranging between 45 to 100 dB. This further indicates that maximum damage has occurred during this period.
- Hence, corrosion inhibitor is very effective in delaying the whole process of corrosion to greater extent.

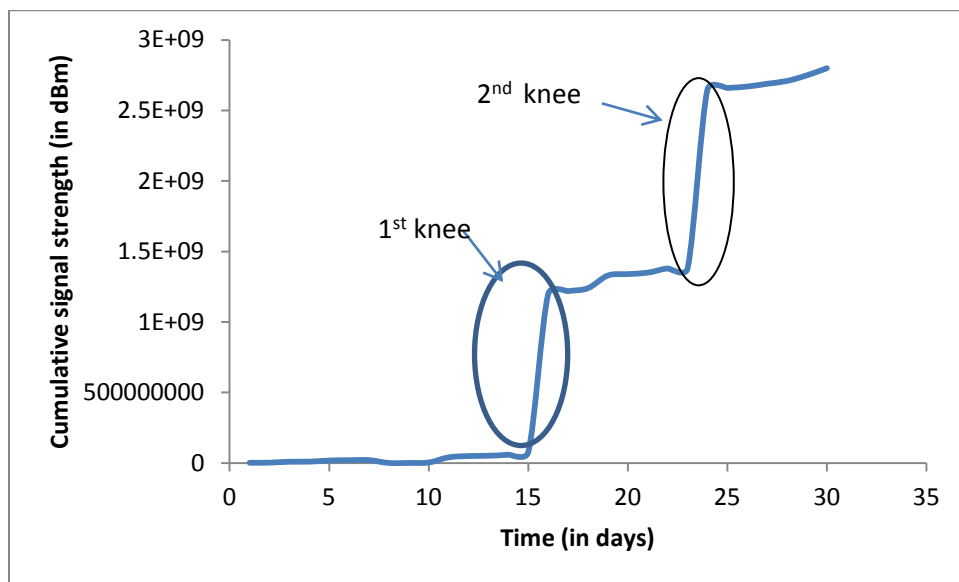


Fig.4.28: Variation of CSS of Specimen B4

Hence, it can be concluded that AET is extremely efficient in detecting the onset of corrosion and its progression in RC beam specimens using the AE parameters, AE hits. However, Amplitude of AE hits and CSS effectively evaluates the intensity of damage in terms of extent (micro and macro).

CONCLUSIONS AND FUTURE SCOPE

5.1 CONCLUSIONS

The focus of this study is to investigate the effectiveness of various corrosion protection methods using a combination of Ultrasonic Guided Wave Technique and Acoustic Emission Technique. The efficacy of the corrosion impeding agents which are Epoxy (rebar coated with epoxy before casting), Paint (rebar coated with paint before casting) and Corrosion Inhibitor (which was mixed in concrete during casting) was evaluated. The conclusions of the study are given below:

- 1) A crack of 200mm length in inhibitor treated specimen as compared to full length crack in control specimen indicates lesser damage due to corrosion in inhibitor admixed specimen. Epoxy treated specimen appears healthy itself showing no corrosion after the experiments. Paint treated specimen also appears healthy but small amount of corrosion occurs on the part which is not embedded in the concrete.
- 2) The cell current values are very less initially and peak value obtained is also very less in inhibitor admixed specimen as compared to control specimen, indicating a delay in the corrosion onset and progression. And cell current values are negligible in case of epoxy treated and paint treated specimens indicating no corrosion occurrence.
- 3) The delay in the delamination and pitting in case of inhibitor admixed specimen as compared to control specimen is identified with the change in signatures using surface seeking and core seeking mode of UGW monitoring. No signatures change occurs in case of epoxy and paint treated specimen, which means no corrosion initiation and progression in these two specimens.
- 4) Very less number of AE hits are recorded up to 15 days in case of specimen prepared using admixed inhibitor as compared to control specimen, which shows a delay in the corrosion initiation. Overall AE hits recorded are extremely less in case of epoxy treated and paint treated specimens which indicate no corrosion at all in these two specimens.
- 5) The range of amplitude in initial 15 days is very less (45-55dB) in inhibitor admixed specimen in comparison to control specimen in which the range reaches up to 75db till 15 days. This indicates the delay in onset of corrosion using inhibitor as preventive measure.

In epoxy treated and paint treated specimens the range of amplitude lies between 45-55dB throughout the experiments which indicates that no corrosion activity occurs in these two beams.

- 6) Instead of 3 spikes in the plot of cumulative signal strength v/s time for control specimen, only 2 spikes are observed for inhibitor admixed specimen. And the strength of signal is very less initially which shows that the onset of corrosion is delayed. No spikes are observed in case of epoxy and paint protected specimens and the signal strength is extremely low which shows no initiation of corrosion in these two specimens..

5.2 FUTURE SCOPE OF WORK

The present study focuses on the effectiveness of various corrosion protection methods for the RC beams, with the help of two non-destructive techniques (Ultrasonic Guided Waves Technique and Acoustic Emission Technique). As far as this study is concerned, all the methods have proven to be very effective in protection against corrosion.

Lot of work in the area is required to be done before adopting these protection methods in actual structures.

- Epoxy coated and painted rebars are effective in corrosion impediment but their application in actual structures requires the study of their effect on bond between steel and concrete.
- Only Amine-ester based corrosion inhibitor is used, effect of various other inhibitors on corrosion impediment needs to be studied.
- Effect of Dosage level on corrosion inhibition needs to be studied.

CHAPTER 6

REFERENCES

1. <http://www.wikipedia.com>
2. Ahmad S. Reinforcement corrosion in concrete structures, its monitoring and service life prediction - A review. *Cem Concr Compos.* 2003;25(4):459–71.
3. Jamil HE, Shrirri A, Boulif R, Montemor MF, Ferreira MGS. Corrosion behaviour of reinforcing steel exposed to an amino alcohol based corrosion inhibitor. *Cem Concr Compos.* 2005;27(6):671–8.
4. Berke NS, Hicks MC. Predicting long-term durability of steel reinforced concrete with calcium nitrite corrosion inhibitor. *Cem Concr Compos.* 2004;26(3):191–8.
5. Söylev TA, Richardson MG. Corrosion inhibitors for steel in concrete: State-of-the-art report. *Constr Build Mater.* 2008;22(4):609–22.
6. Ormellese M, Berra M, Bolzoni F, Pastore T. Corrosion inhibitors for chlorides induced corrosion in reinforced concrete structures. 2006;(6):536–47.
7. Söylev TA, McNally C, Richardson MG. The effect of a new generation surface-applied organic inhibitor on concrete properties. *Cem Concr Compos.* 2007;29(5):357–64.
8. Vaysburd AM, Emmons PH. Corrosion inhibitors and other protective systems in concrete repair: Concepts or misconcepts. *Cem Concr Compos.* 2004;26(3):255–63.
9. Soeda K, Ichimura T. Present state of corrosion inhibitors in Japan. *Cem Concr Compos.* 2003;25(1):117–22.
10. Gaidis JM. Chemistry of corrosion inhibitors. *Cem Concr Compos.* 2004;26(3):181–9.
11. Tritthart J. Transport of a surface-applied corrosion inhibitor in cement paste and concrete. *Cem Concr Res.* 2003;33(6):829–34.
12. Nmai CK. Multi-functional organic corrosion inhibitor. *Cem Concr Compos.* 2004;26(3):199–207.

13. Wombacher F, Maeder U, Marazzani B. Aminoalcohol based mixed corrosion inhibitors. *Cem Concr Compos.* 2004;20(9):209–16.
14. Kundu T. *Ultrasonic Nondestructive Evaluation: Engineering and Biological Material Characterization.* Pub. CRC Press, USA.(2004).
15. <http://www.wins-ndt.com>
16. <http://www.msheiksirajuddin.blogspot.in>
17. He C. Health Monitoring of Rock Bolts Using Ultrasonic Guided Waves. *AIP Conf Proc.* 2006;(5):195–201.
18. Behnia A, Chai HK, Shiotani T. Advanced structural health monitoring of concrete structures with the aid of acoustic emission. *Constr Build Mater.* 2014; 29(5):282-302.
19. Ono K. Application Of Acoustic Emission For Structure Diagnosis. *Diagnostics Struct Heal Monit.* 2011;58(2):3–18.
20. Elbatanouny M, Mangual J, Larosche A, Barrios F, Ziehl P, Matta F. Acoustic Emission and Cyclic Load Test Criteria Development for Prestressed Girders. 2008;(July).
21. Pavlakovic BN, Lowe MJS, Cawley P. High-Frequency Low-Loss Ultrasonic Modes in Imbedded Bars. *J Appl Mech.* 2001;68(1):67.
22. Na W, Kundu T, Ehsani MR. Ultrasonic guided waves for steel bar concrete interface testing. *ARIEL.* 2002;12(9):31-248.
23. Beard MD, Lowe MJS, Cawley P. Ultrasonic Guided Waves for Inspection of Grouted Tendons and Bolts. *J Mater Civ Eng.* 2003;15(6):212–8.
24. Cawley P. Practical guided wave inspection and applications to structural health monitoring. *Proc Australas Congr Appl Mech.* 2007;51(12):412-23.
25. Mahmoud AM, Ammar HH, Mukdadi OM, Ray I, Imani FS, Chen A, et al. Non-destructive ultrasonic evaluation of CFRPconcrete specimens subjected to accelerated aging conditions. *NDT E Int.* 2010;43(7):635–41.
26. Raiutis R, Kays R, Ukauskas E, Maeika L, Vladiuskas A. Application of ultrasonic guided waves for non-destructive testing of defective CFRP rods with multiple delaminations. *NDT E Int.* 2010;43(5):416–24.

27. Sharma S, Mukherjee a. Longitudinal Guided Waves for Monitoring Chloride Corrosion in Reinforcing Bars in Concrete. *Struct Heal Monit.* 2010;9(6):555–67.
28. Sharma S, Mukherjee A. Monitoring corrosion in oxide and chloride environments using ultrasonic guided waves. *J Mater Civ Eng.* 2011;23(2):207–11.
29. Sharma S, Mukherjee A. Nondestructive Evaluation of Corrosion in Varying Environments Using Guided Waves. *Res Nondestruct Eval.* 2013;24(2):63–88.
30. Sharma A, Sharma S, Sharma S, Mukherjee A. Ultrasonic guided waves for monitoring corrosion of FRP wrapped concrete structures. *Constr Build Mater.* 2015;15(96):690-702.
31. Yoon DJ, Weiss WJ, Shah SP. Assessing damage in corroded reinforced concrete using acoustic emission. *J Eng Mecha.* 2000;126(3):273-83.
32. Ohtsu M, Tomoda Y. Corrosion Monitoring in Reinforced Concrete By Acoustic Emission. 2003;21(7):157–65.
33. Ohtsu M, Tomoda Y, Suzuki T. Damage evaluation and corrosion detection in concrete by acoustic emission. *Carpint A al.* 2007;12(1):981–9.
34. Ohtsu M, Tomoda Y. Phenomenological model of corrosion process in reinforced concrete identified by acoustic emission. *ACI Mater J.* 2008;105(2):194–9.
35. Kawasaki Y, Wakuda T, Kobarai T, Ohtsu M. Corrosion mechanisms in reinforced concrete by acoustic emission. *Constr Build Mater.* 2013;(48):1240–7.
36. Kondratova IL, Montes P, Bremner TW. Natural marine exposure results for reinforced concrete slabs with corrosion inhibitors. *Cem Concr Compos.* 2003;25(5):483–90.
37. Dhouibi L. Studies on corrosion inhibition of steel reinforcement by phosphate and nitrite. *Mater Struct.* 2003;36(2):530–40.
38. Chaussadent T, Nobel-Pujol V, Farcas F, Mabilie I, Fiaud C. Effectiveness conditions of sodium monofluorophosphate as a corrosion inhibitor for concrete reinforcements. *Cem Concr Res.* 2006;36(3):556–61

39. Loto CA, Popoola API, Fayomi OS, Loto RT. Corrosion polarization behaviour of type 316 stainless steel in strong acids and acid chlorides. *Int J Electrochem Sci.* 2012;7(4):3787–97.
40. Sancak E, Çoban Ö. The Corrosion Inhibition Effect of Forsterite (Mg_2SiO_4) Mine Tailings for Steel Rebar in Reinforced Concrete. *Int. J. Electrochem. Sci.* 2015;(10):5770-86.
41. Melchers RE, Li CQ. Phenomenological modeling of reinforcement corrosion in marine environments. *ACI Mater J.* 2006;103(1):25-32